POLYTECHNIC UNIVERSITY OF BUCHAREST
Doctoral School of Industrial Engineering and Robotics

DOCTORAL THESIS

-abstract-

Increasing the performance of mobile robots and autonomously guided vehicles serving industrial environments

Increasing the performance of mobile robots and autonomously guided vehicles serving the industrial environment

Author, Ing. Iosif-Adrian MAROȘAN

PhD supervisor, Prof. PhD. eng. George CONSTANTIN

Bucharest, 2023

CONTENTS

GLOSSARY OF TERMS

ADC - analog-to-digital converter;
AGV - Automated Guided Vehicles;
AHP - Analytic Hierarchy Process;
CAD - computer aided design;
CAE - Computer-aided engineering;
CAM - Computer-aided manufacturing;
CAN - serial bus used in the automotive industry (Controller Area Network));
CCD - charged-coupled device (CCD);
CG - centre of gravity of the vehicle;
CMOS - Complementary metal-oxide-semiconductor sensor;
DBS - Digital Block Simulation;
DC - direct current;
GPS - Global Positioning System;
I2C - master-slave serial data bus (The Inter-Integrated Circuit);
IoT - Internet of Things;
KF - Kalman filter;
LAN - Local Area Network;
LiDAR - Laser imaging, detection, and ranging (LiDAR) system;
MCL - Monte Carlo localization;
MPC - Model Predictive Control;
OM - major objective;
OS - secondary objective;
PID - Proportional-integral-derivative controller;
PLA - Polylactic Acid Polymer;
PLC - Programmable Logic Controller;
PWM - pulse-width modulation;
RGS - Rigid Body Simulation;
RMA - autonomous mobile robots;
ROS - Robot Operating System;
SC - configuration space;
SFD - dedicated manufacturing system;
SFF - flexible manufacturing system;
SFR - reconfigurable manufacturing system;
SLAM - Simultaneous Localization and Mapping system;
WLAN - Wireless Local Area Network.

CHAPTER. 1. INTRODUCTION

Today, robotics is one of the fastest growing areas of scientific research. Thanks to their abilities, mobile robots can replace the human factor in many fields [1]. In general, mobile robots are those robots that can move from one place to another to perform complex tasks and reach the desired results in a much shorter time. They also perform repetitive or dangerous actions replacing humans performing indoor or outdoor activities in many fields, such as: industry, military, hospital operations, sports, agriculture, etc. Depending on the destination, they can have different configurations, and different locomotion systems, being equipped with multiple sensors (infrared, ultrasonic, cameras, GPS, etc.) or different command and control algorithms, being locally or remotely supervised [2]. In the paper [3] mobile robots are presented that are controlled in real time via the Internet using a protected *web* page or with *Internet of Things* (IoT) technology. All these platforms are based on a *Raspberry Pi* computer that allows online viewing of the working environment via a *webcam* [4]. Mobile robotic platforms are increasingly used in industry to transport materials, semi-finished products, sub-assemblies or machined parts between phases of the technological flow, to handle, load or unload products. Mobile platforms can be found in various industries, such as the automotive, pharmaceutical, chemical, food, plastics and paper industries. Platforms can also serve logistics centres, transport different parts, and generally perform any transport operation between two or more phases of a technological flow.[5]. Mobile robots can move autonomously, i.e. without assistance from external human operators. A mobile robot can be called autonomous when it has the ability to determine actions to be taken to perform a task, using a perception system to help detect obstacles and a control system to coordinate all subsystems belonging to the robot [1].

Mobile robotic platforms are often referred to as Automated *Guided* Vehicles (AGVs). They range in size from centimetres to tens of metres.

The use of mobile robotic platforms increases the flexibility and productivity of manufacturing systems where handling and palletising operations take up a large volume of activity. Automated guided vehicles help reduce costs and increase efficiency in a production system. Mobile platforms can transport objects, equipped with different towing or transport systems, such as container or tipper systems to move materials directly to the production line or forklift systems to lift or lower objects into storage areas.

CHAPTER. 2. THE CURRENT STATE OF RESEARCH IN MOBILE ROBOTS AND AUTONOMOUS GUIDED VEHICLES

Mobile robotic platforms are undergoing a major development in recent times, and in their hardware structure we find a variety of mechatronic systems that have in their component sensors, actuators and microprocessors of the latest performance. The fields of activity where mobile robotic platforms are found are varied [6]Mobile robots are found in various industrial sectors, in education and research, in agriculture as well as in social care, helping people with disabilities.

2.1. THE EVOLUTION OF AUTONOMOUS MOBILE ROBOTS

Next-generation autonomous mobile robots (AMRs) have a range of features that help them move safely in crowded environments, interpret voice commands, recognise real objects, plan routes or navigate autonomously. The design of RMA platforms uses intelligent control methodologies and technologies based on high-performance computing units and highly flexible hardware architectures. [7].

The field of RMA navigation and control has evolved over time to reach a high level today, both in theory and in practice. A significant number of books and scientific papers have been published internationally. **Table 0.1** shows briefly in chronological order the evolution in the field in terms of the most important publications [8].

Table 0.1. Books dealing with autonomous mobile robots, navigation and control (1991-2022) [8]**.**

Author	Publication year	Summary
A.M. Meystel [9]	1991	Intelligent motion control. Evolution of autonomous mobile robots (AMR). Autonomous mobility. Cognitive control of RM.A Intelligent modules (planning, navigation).
J.C. Latombe [10]	1991	The configuration space (CS) of the rigid object. Obstacles in the SC. road map methods. Robotic cell composition. Potential field methods. Dealing with uncertainty. Moving objects.
J.L. Leonard [11]	1992	The navigation problem. Sonar sensor model based on location models. Simultaneous construction of location map. Directed detection strategies.

J.L. Jones [12]	1995	TuteBot. Design and prototyping. Sensors. Mechanics. Motors. Robot programming. Robot applications. Robot design principles. Unsolved problems.
H.R. Everett [13]	1995	Design considerations. Odometry sensors. Doppler and inertial navigation. Typical mobility configurations. Tactile and proximity sensors. Triangulation variation. Positioning and location sensors. Ultrasonic and optical sensors for localisation systems.
J. Borenstein [14]	1996	Sensors for positioning the mobile robot. Direction control sensors. Active beacons. Map positioning sensors. Active navigation systems with beacons.
R.C. Arkin [15]	1998	Robot behaviour. Behavior-based architectures. Representation issues. Adaptive behaviour. Social behaviour.
J. Canny [16]	1998	Robot motion planning issues. Motion constraints. Elimination theory. Lower bounds for motion planning. Motion planning with uncertainty.
X.Zhu [17]	2001	Mobile outdoor robots. Motion control. Cooperative motion control and architecture. Kinematic motion control.
U.Nehmzow [18]	2003	Robot hardware systems. Robot learning. Simulation. Modelling the robotic environment. Analysis of robot behaviour. Locomotion. Mobile robot kinematics. Perception. Mobile robot localization. Planning and navigation.
R. Siegwart [19]	2005	Locomotion. Mobile robot kinematics. Perception. Mobile robot localization. Planning and navigation.
F. Cuesta [20]	2005	Fuzzy systems. Stability analysis. Takagi-Sugeno fuzzy systems. Intelligent control of mobile robots with fuzzy logic. Stability of mobile robots with feedback loop fuzzy navigation. Intelligent parallel machine parking system.
K. Berns [21]	2009	History of autonomous ground vehicles. Robot kinematics. Sensory systems. Location problem. Map construction. Navigation strategies.
G. Dudek [22]	2010	Fundamental issues. Hardware systems for mobile robots. Non-visual sensors and algorithms. Visual sensors and algorithms. Representation and reasoning about space. System control. Robots in practice. The future of mobile robots.
G. Cook [23]	2011	Mobile robot control. Robot attitude. Robot navigation. Application of Kalman filtering. Remote sensing. Obstacle mapping and its application to robot navigation. Kinematics.
C.A. Berry [24]	2012	Introduction. Hardware. Control. Feedback control. Representation. Control architectures. Software.

		Navigation. Location. Mapping. Simultaneous localization and mapping.
R. Tiwari [25]	2012	Graph-based route planning. Common planning techniques. Evolutionary robotics. Behavioural path planning. Hybrid graph-based methods. Hybrid behavioural methods. Multi-robot systems.
A. Kelley [26]	2013	Introduction. Mathematical foundations. Numerical methods. Dynamics. Optimal estimation. Control. Perception. Localization and mapping. Movement planning.
S.G. Tzafestas [27]	2014	Mobile robots. Kinematics of mobile robots. Dynamics of mobile robots. Sensors for mobile robots. Mobile robot control. Adaptive and robust methods. Fuzzy and neural methods. Mobile robot localization and mapping. Experimental studies. Mobile robots at work.
L. Jaulin [28]	2017	Three-dimensional modelling. Feedback linearization. Model-free control. Guidance. Instant localization. Identification. Kalman filter.
N. Martins [29]	2022	Use of software computing techniques such as fuzzy logic and artificial neural networks. Stability analysis for both kinematic and dynamic controllers based on Lyapunov's stability theory.

2.1.1. Analysis of the latest literature

The field of robotics is vast and constantly changing. Researchers' interest in the field is growing, as is the number of publications that appear each year. This section presents a review of some bibliographic references, showing the current state of the art in the field of mobile robotics. The analysis is made on the basis of several topics that will be found in this article. The first section 1.1 presents a selection of papers presenting applications in which mobile robots are integrated and their general aspects. The following section 1.2 presents aspects related to sensors used in mobile robotics, presenting in detail aspects of the hall current sensor. Section 1.3 is dedicated to modular robotics, in which the latest news and research on modularity and re-configurability of mobile robots is presented. The fourth section 1.4 highlights the use of Matlab Simulink in robot design and development. The last section 1.5 presents the latest news on the energy consumption of mobile robots, and selected references deal with topics on the energy efficiency of mobile robots depending on the path they travel or the locomotion systems they use. Selected references are presented in **Table 0.2** grouped by each section. The relevance of the references is quantified by evaluating the searches and the number of citations using specialised search engines for scientific references such as Google Scholar or Web of Science. [30].

Table 0.2 References by section

Title [source]	Document type	Number of references cited	Number of citations in all databases	An	Categories
General aspects of mobile robots					
Mobile robot locomotion [31]	Review	73	3	2022	Engineering, Mechanical
Mobile robots with wheels [32]	Review	118	2	2021	Disciplines, Multidisciplinary
Omnidirectional mobile robots [33]	Article	354	21	2020	Engineering, Mechanical
Mobile robot navigation [34]	Review	208	220	2019	Engineering, Multidisciplinary
Mobile robots reviews [1]	Review	188	120	2019	Robotics
Hall sensors					
Hall current sensors [35]	Article	103	6	2022	Engineering, Applied
Hall effect induced [36]	Article	34	3	2021	Engineering, Electrical
Current sensors [37]	Article	21	15	2019	Engineering, Electrical
Wireless current monitoring [38]	Conf.	8	0	2019	Engineering, Electrical
MagFET- current sensors [39]	Article	23	14	2013	Engineering, Electrical
Modular and reconfigurable mobile robots					
Reconfigurable mobile robots [40]	Article	23	8	2020	Artificial Intelligence; Robotics
Modularity and ROS [41]	Conf.	31	1	2020	Engineering, Robotics
Modular mobile platforms [42]	Conf.	16	3	2019	Automation & Control Systems
Reconfigurable robots [43]	Conf.	16	25	2010	Automation & Control Robotics
iMobot Design [44]	Conf.	12	51	2010	Automation & Control Robotics
Modeling with Matlab Simulink					
Holonic mobile robots [45]	Article	40	4	2022	Multidisciplinary; Engineering
Controlling wheeled robots [46]	Article	66	5	2021	Automation & Control Systems
Mobile robot trajectories [47]	Conf.	27	1	2021	Engineering, Industrial
Autonomous 4-wheeled robots [48]	Article	29	30	2019	Engineering, Electrical
Mobile robots and Simscape [49]	Conf.	14	5	2019	Engineering, Multidisciplinary
Energy consumption of mobile robots					
Differential drive [50]	Article	30	12	2020	Engineering, Electrical
Estimated robot consumption [51]	Article	23	11	2020	Robotics
Consumer robot modelling [52]	Article	30	27	2019	Energy & Fuels
Power consumed by robots [53]	Article	25	18	2019	Computer Science, Robotics
Trajectory-influenced energy consumption [54]	Article	21	17	2019	Robotics

All searches were conducted in February 2023

2.2. RESEARCH OBJECTIVES

The literature review identified a large number of studies addressing topics related to the planning and navigation of autonomous mobile robots. The main performances highlighted in most of the works are: the degree of autonomy of the robot in terms of navigation in an unknown environment, the possibility to avoid obstacles and positioning accuracy. In terms of modularity and the possibility of reconfiguration, a smaller number of studies on wheeled mobile robots were found. Most of these studies have been conducted on cellular mobile robots of the "snake" type. The energy consumption of mobile robots is another aspect less addressed in the literature. Most of the existing studies analyse energy consumption in terms of the robot's navigation strategy along a given trajectory. Less addressed is the influence of the locomotion system on the total energy consumption for traversing a trajectory. Based on these considerations, which emerge from the analysis of the current state of research, the objectives of the research, the results of which are original, are as follows:

1. Analysis of the evolution of autonomous mobile robots.
2. Study on modularity and reconfiguration of mobile robots.
3. Analysis of wheeled mobile robots in terms of energy consumption.
4. Study on the locomotion of mobile robots and autonomous guided vehicles in industrial environments.
5. Study on the types of sensors used in the construction of mobile robots.
6. Analysis of autonomous mobile robot localization systems.
7. Kinematic modeling of modular mobile robots with differential drive and classic wheels.
8. Kinematic modelling of modular mobile robots with omnidirectional drive and 90° castor wheels.
9. Kinematic modelling of modular mobile robots with omnidirectional traction and 45° arranged mecanum wheels.
10. Methods of choosing and checking the electric motor for driving the modular mobile platform.
11. 3D modelling and construction of the modular mobile platform.
12. Development of a functional model for a mobile robotic platform for measuring absorbed current using a Hall current sensor.
13. Omnidirectional and differential kinematic modelling.
14. Making the dynamic model of the robot using Matlab Simulik.
15. Determination of the currents absorbed by wheel motors, both by simulation and experimental measurement.
16. Analysis of the structure and characteristics of the modular mobile platform.
17. Dynamic modelling of 5 mobile robot configurations using Matlab Simulink.
18. Determination of currents through wheel motors by simulation for 5 mobile robot configurations.
19. Conduct experimental tests to validate simulated models.
20. Calculation of energy consumed and comparison of simulated and measured results for the 5 mobile robot configurations.

Table 0.3 presents the main and secondary objectives of the scientific research, and **Fig. 0.1** concept map of these objectives with the specification of the sections where they are realised.

Table 0.3 Major and secondary objectives of the PhD thesis

MAJOR RESEARCH OBJECTIVES	SECONDARY OBJECTIVES OF THE RESEARCH
OM1. Objectives referring to the fundamentals of the field of study and the required performance of mobile robots	
OM2. Review of the state-of-the-art literature related to the chosen research topic	**SO2.1** Analysis of the evolution of autonomous mobile robots
	SO2.2 Study on modularity and reconfiguration of mobile robots
	OS2.3 Analysis of wheeled mobile robots in terms of energy consumption
	SO2.4 Study on the locomotion of mobile robots and autonomous guided vehicles in industrial environments
	SO2.5 Study on types of sensors used in the construction of mobile robots
	OS2.6 Analysis of autonomous mobile robot localization systems
OM3. Theoretical contributions on kinematic and dynamic modelling of a modular mobile platform	**OS3.1** Kinematic modelling of modular mobile robots with differential drive and classic wheels
	OS3.2 Kinematic modelling of modular mobile robots with omnidirectional drive and 90° castor wheels
	OS3.3 Kinematic modelling of modular mobile robots with omnidirectional drive and 45° arranged mecanum wheels
	OS3.4 Methods of choosing and checking the electric motor for driving the modular mobile platform
OM4. Theoretical contributions on the development of a modular mobile platform using CAD-CAM-CAE techniques	**OS4.1** 3D modelling and construction of the modular mobile platform
	OS4.2 Develop a functional model for a mobile robotic platform for measuring absorbed current using a Hall current sensor.
OM5. Preliminary research on an omnidirectional mobile platform with mecanum wheels	**OS5.1** Omnidirectional and differential kinematic modelling
	OS5.2 Making the dynamic model of the robot using Matlab Simulik
	OS5.3 Determine the currents absorbed by wheel motors, both by simulation and experimental measurements
OM6. Original contributions on simulations and experimental research on mobile robot designs	**SO6.1** Analysis of the structure and characteristics of the modular mobile platform
	OS6.2 Dynamic modelling of 5 mobile robot configurations using Matlab Simulink.
	OS6.3 Determination of currents absorbed by wheel motors by simulation for 5 mobile robot configurations
	SO6.4 Conduct experimental tests to validate simulated models

	OS6.5 Calculation of energy consumption and comparison of simulated and measured results for the 5 mobile robot configurations
OM6. General discussions and conclusions	

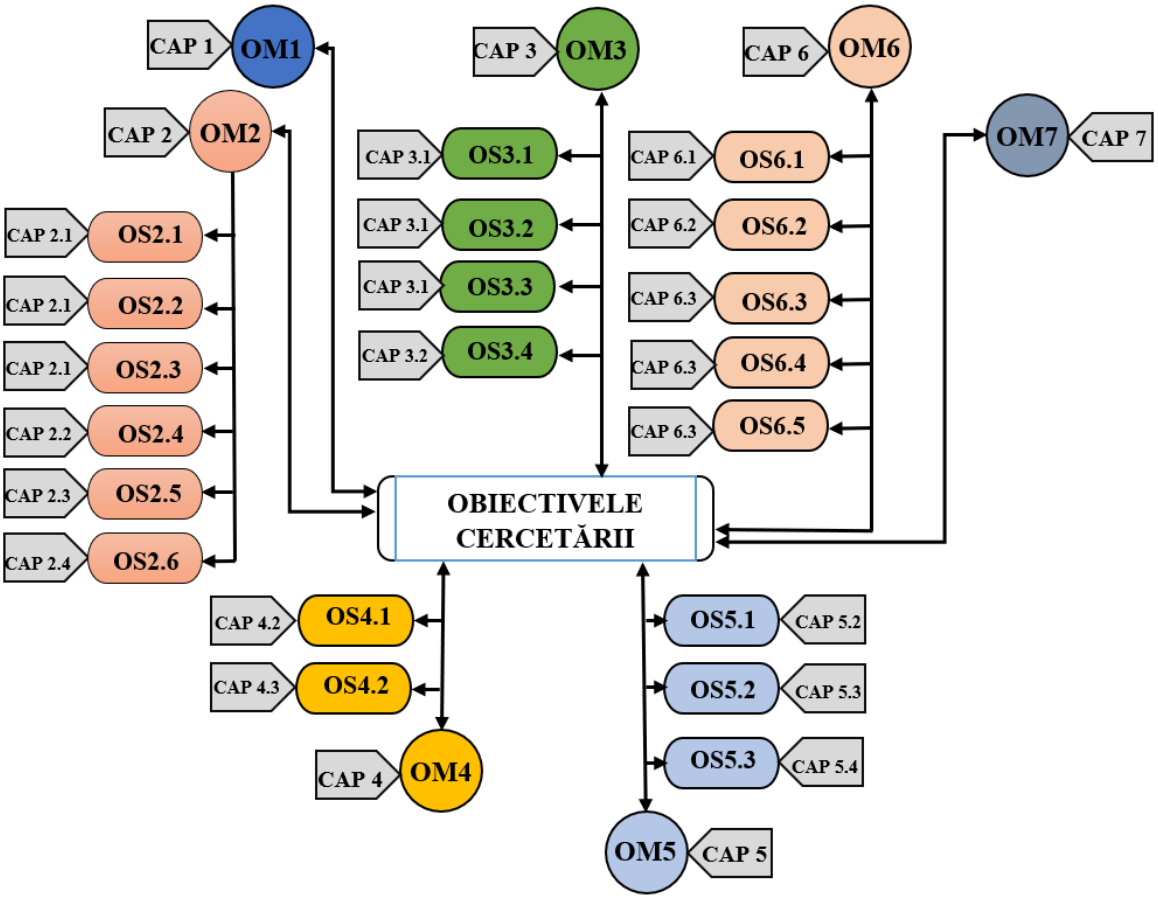

Fig. 0.1. Concept map with main and secondary objectives.

CHAPTER. 3. KINEMATIC AND DYNAMIC MODELING OF THE MODULAR MOBILE PLATFORM

3.1. MATHEMATICAL MODELLING OF THE LOCOMOTION SYSTEM OF A MODULAR MOBILE ROBOT

An efficient locomotion system for a mobile robot in an industrial environment must facilitate its operation in different environments, such as production areas, or logistics areas that are constantly developing and changing. In most cases, a single type of locomotion system is not sufficient to cope with the situations encountered, as environments can present complex obstacles such as steep slopes, ditches and obstacles of different sizes. [55]. The main advantage of a modular mobile robot is that it can have different locomotion systems by adding new modules with different types of wheels. In this way, the modular mobile robot can be configured with a locomotion system suitable for its environment. In **Fig. 0.2** shows the possible configurations of a modular mobile platform considering the locomotion system. The figure shows 5 different locomotion systems. **Fig. 0.2a** shows a robotic configuration with two conventional wheels and two ball-bearing elements **and Fig. 0.2b** shows a configuration with four conventional wheels, both platforms using differential drive**. Fig. 0.2c and d** show two robotic configurations with 3 and 4 omni-directional wheels with rollers arranged at 90°. **Fig. 0.2e** shows a robotic configuration with omnidirectional drive and four Mecanum wheels with rollers arranged at 45°.

The following shows the kinematic patterns and movement possibilities for all 5 configurations.

3.1.1. Kinematic model for modular mobile robots with differential drive and classic wheels

The kinematics of conventional four- and two-wheeled modular mobile robots are based on mathematical equations of motion specific to differential traction. This solution is based on the Mobile Robotics Simulation Toolbox [56] from the Matlab software package (The MathWorks Inc., Natick, MA, USA), and is adapted to the configurations of the developed modular mobile robots. According to **Fig. 0.3.**

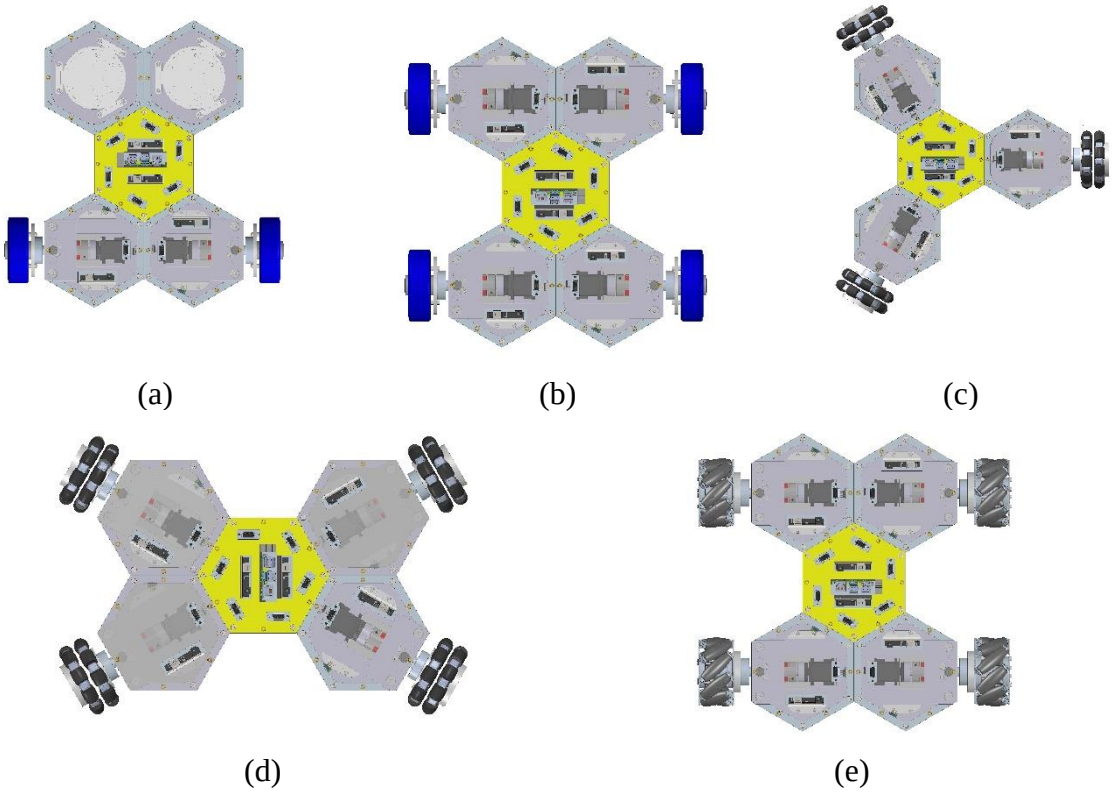

(a) (b) (c)

(d) (e)

Fig. 0.2 Possible configurations of the locomotion system of a modular mobile platform: (**a**) conventional two-wheel locomotion system; (**b**) conventional four-wheel locomotion system; (**c**) omnidirectional three-wheel locomotion system; (**d**) omnidirectional four-wheel locomotion system; (**e**) mechanum four-wheel locomotion system .

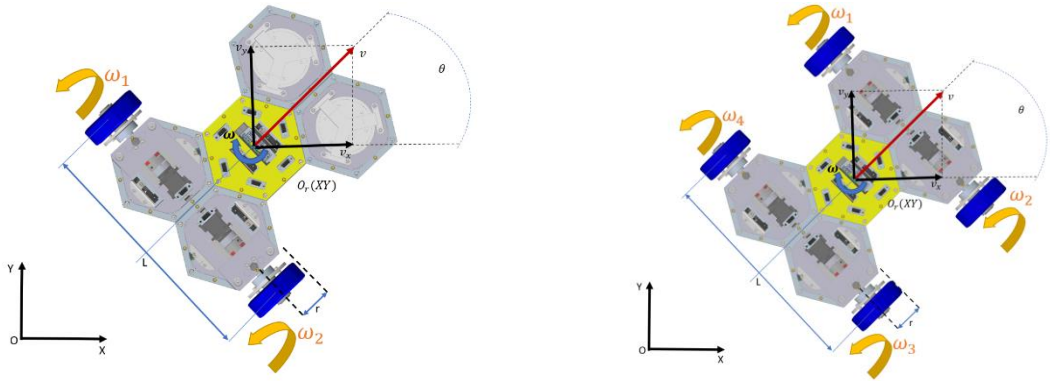

(a) (b)

Fig. 0.3. Kinematic model of the modular mobile platform with differential traction: (**a**) conventional two-wheel locomotion system; (**b**) conventional four-wheel locomotion system.

The inputs to the kinematic model are as follows:

v - linear speed of the robot;

ω - robot angular velocity;

θ - rotation angle of the robot;

ω_1 - angular velocity of the wheel driven by the M1 motor;

ω_2 - angular velocity of the wheel driven by the M2 motor;

ω_3 - angular velocity of the wheel driven by the M3 engine;

ω_4 - angular velocity of the wheel driven by the M4 motor;

L - distance between wheel centres;

r - wheel radius.

The following mathematical relations describe the direct kinematics:

$$v = \frac{r}{2}(\omega_2 + \omega_1),\ \omega = \frac{r}{L}(\omega_2 - \omega_1), \tag{0.1}$$

$$v = \frac{r}{2}(\omega_4 + \omega_3),\ \omega = \frac{r}{L}(\omega_4 - \omega_1), \tag{0.2}$$

The following mathematical relations describe the inverse kinematics:

$$\omega_1 = \frac{1}{r}(v - \frac{\omega \cdot L}{2}),\ \omega_2 = \frac{1}{r}(v + \frac{\omega \cdot L}{2}), \tag{0.3}$$

$$\omega_3 = \frac{1}{r}(v - \frac{\omega \cdot L}{2}),\ \omega_4 = \frac{1}{r}(v + \frac{\omega \cdot L}{2}). \tag{0.4}$$

3.1.2. Kinematic model for modular mobile robots with omnidirectional traction and 90° castor wheels

One of the most common types of mobile robots used in services or industry is the three or four-wheeled robot with 90° casters, known as an omnidirectional mobile robot. [57]. This type of robot has many advantages, such as flexibility of movement patterns, also having the ability to move freely in both directions compared to the conventional two-wheel and four-wheel drive robot [135, 136]. Having the same speed and acceleration, the omnidirectional wheeled robot can move in either direction, which is very useful if the robot is working, for example, in a logistics warehouse. The omnidirectional construction with three wheels, each wheel mounted at 120°, has high mobility and manoeuvrability, allowing the robot to move through the narrowest of areas. In this configuration, the wheels are designed to rotate either perpendicular or parallel to the direction of movement. [60].

The kinematics of the three- and four-wheel omnidirectional modular mobile robot are based on the Mobile Robotics Simulation Toolbox solution [56] from the Matlab software package (The MathWorks Inc., Natick, MA, USA), being adapted to the configuration of the developed modular mobile robot. According t**o Fig. 0.4**, the input variables of the kinematic model are as follows:

v_x - linear velocity decomposed on the X axis;

v_y - linear velocity decomposed on the Y-axis;

ω - angular velocity;

ω_1 - the angular velocity of the wheel driven by the M1 motor;

ω_2 - the angular velocity of the wheel driven by the M2 motor;

ω_3 - the angular velocity of the wheel driven by the M3 engine;

L - robot's range;

r - wheel radius;

θ - the angle of rotation of the robot;

α_1- wheel angle 1;

α_2- wheel angle 2;

α_3- wheel angle 3.

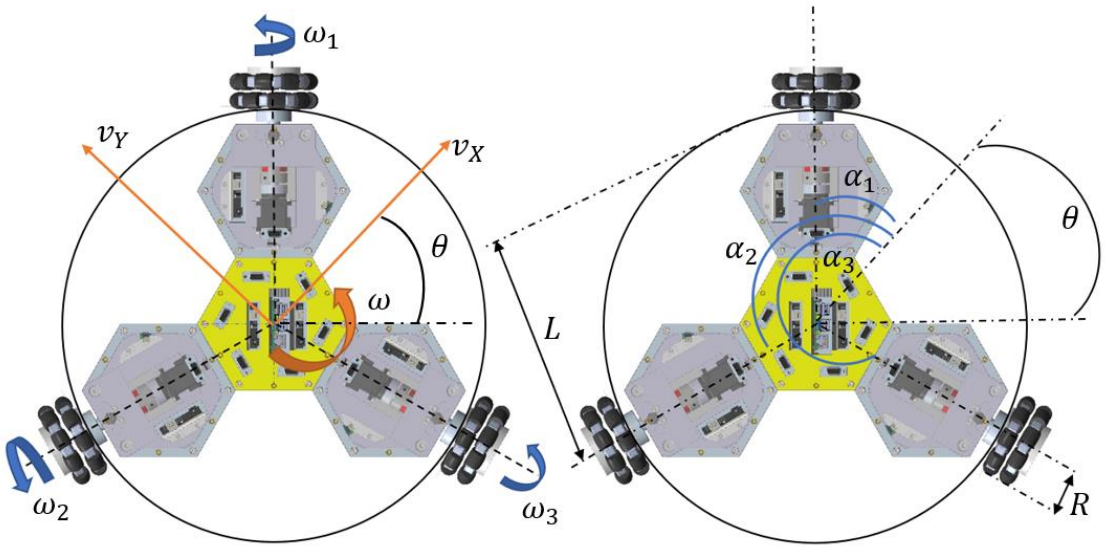

(a) (b)

Fig. 0.4 Kinematic model of the modular mobile platform with 3 omnidirectional wheels: (**a**) representation of the angular velocity of the robot and the 3 omnidirectional wheels; (**b**) representation of the 3 wheel angles and the rotation angle of the robot.

This configuration represents a mobile robot with 3 omnidirectional wheels placed radially around a circular body. Because there are 3 independently driven wheels, the vehicle has full motion control in all degrees of freedom with unique solutions.

Direct kinematics can be expressed in matrix form as follows:

$$\begin{bmatrix} v_X \\ v_Y \\ \omega \end{bmatrix} = \frac{R}{3} \begin{bmatrix} sin\,(\alpha_1) & sin\,(\alpha_2) & sin\,(\alpha_3) \\ -cos\,(\alpha_1) & -cos\,(\alpha_2) & -cos\,(\alpha_3) \\ -1/L & -1/L & -1/L \end{bmatrix} \begin{bmatrix} \omega_1 \\ \omega_2 \\ \omega_3 \end{bmatrix} = \boldsymbol{M} \begin{bmatrix} \omega_1 \\ \omega_2 \\ \omega_3 \end{bmatrix}. \tag{3.5}$$

Inverse kinematics is described by the following relationship:

$$\begin{bmatrix} \omega_1 \\ \omega_2 \\ \omega_3 \end{bmatrix} = \boldsymbol{M}^{-1} \begin{bmatrix} v_X \\ v_Y \\ \omega \end{bmatrix}. \tag{3.6}$$

For the four-wheel omnidirectional robot configuration, the kinematic model inputs are as follows:

v_x - *X-axis* component of linear velocity;

v_y - *Y-axis* component of linear velocity;

ω - angular velocity;

ω_1 - the angular velocity of the wheel driven by the M1 motor;

ω_2 - the angular velocity of the wheel driven by the M2 motor;

ω_3 - the angular velocity of the wheel driven by the M3 engine;

ω_4 - angular velocity of the wheel driven by the M4 motor;

L - robot's range;

R - wheel radius;

θ - the angle of rotation of the robot;

L_{xi}- the distance from the centre of gravity to the centre of the wheel on the *X-axis*;

L_{yi}- the distance from the centre of gravity to the centre of the wheel on the *Y-axis*.

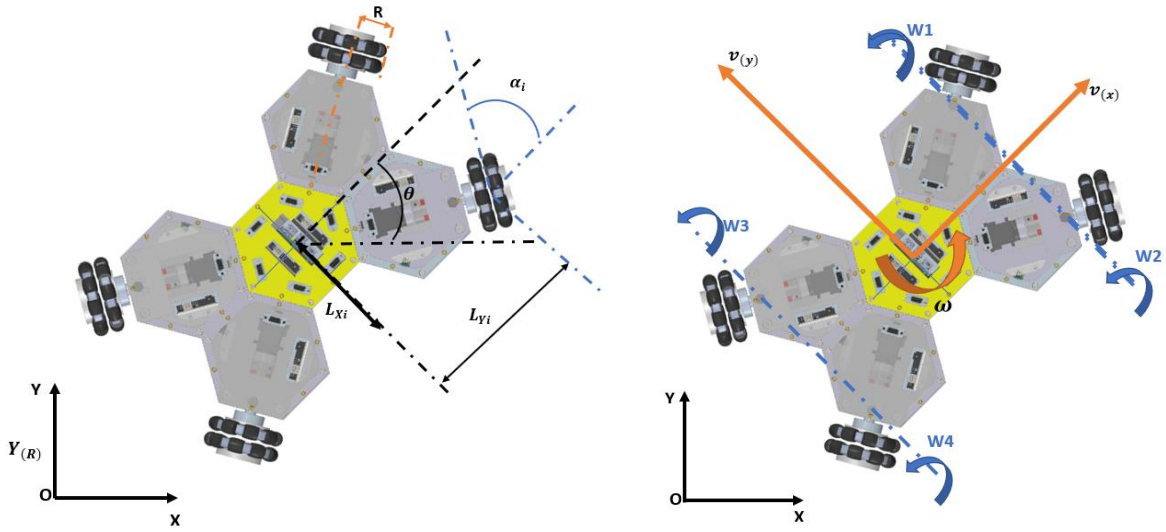

(a) (b)

Fig. 0.5 Kinematic model of the modular mobile platform with 4 omnidirectional wheels: (**a**) representation of the distances from the centre of the robot to the centre of the wheel on the two axes *X* and *Y*; (**b**) representation of the angular velocity of the robot and the 4 omnidirectional wheels.

Fig. 0.5 shows the configuration of the robot with four omnidirectional wheels, positioned and oriented relative to the vehicle's centre of gravity (CG). Configurations with 3 or more independently driven omnidirectional wheels have full motion control for all degrees of freedom.

Direct kinematics can be expressed by the following equation:

$$\begin{bmatrix} v_X \\ v_Y \\ \omega \end{bmatrix} = \frac{R}{N} \begin{bmatrix} cos\,(\alpha_1) & cos\,(\alpha_2) & \dots & cos\,(\alpha_N) \\ sin\,(\alpha_1) & sin\,(\alpha_2) & \dots & sin\,(\alpha_N) \\ \frac{1}{D_1} & \frac{1}{D_2} & \dots & \frac{1}{D_N} \end{bmatrix} \begin{bmatrix} \omega_1 \\ \omega_2 \\ \vdots \\ \omega_N \end{bmatrix} = \boldsymbol{M} \begin{bmatrix} \omega_1 \\ \omega_2 \\ \vdots \\ \omega_N \end{bmatrix}. \tag{0.7}$$

where: D_i - the perpendicular distance from the axis of rotation of the wheel to the centre of gravity of the robot.

Inverse kinematics can be obtained by inverting the matrix $\boldsymbol{M}$ of the direct kinematics. However since the matrix $\boldsymbol{M}$ is of order 3 it can only be inverted for $N = 3$. Therefore, this model uses the pseudoinverse matrix $\boldsymbol{M}^+$:

$$\begin{bmatrix} \omega_1 \\ \omega_2 \\ \vdots \\ \omega_N \end{bmatrix} = \boldsymbol{M}^+ \begin{bmatrix} v_X \\ v_Y \\ \omega \end{bmatrix}. \tag{0.8}$$

3.1.3. Kinematic model for modular mobile robots with omnidirectional traction and 45° arranged mecanum castors

The mecanum type mobile robot with omnidirectional wheels is the best known and most widely used mobile robot with omnidirectional drive. The mecanum wheel with passive rollers arranged at 45° allows the robot to move freely without any room for manoeuvre. Although it has a number of important advantages, finding an efficient control algorithm for tracking a trajectory is a complex task, covered in many articles in the literature. [61]. The kinematics of the modular four-wheel omnidirectional mechanum mobile robot is based on the Mobile Robotics Simulation Toolbox solution [56] from the Matlab software package (The

MathWorks Inc., Natick, MA, USA), being adapted to the configuration of the developed modular mobile robot. According t**o Fig. 0.6** the input variables of the kinematic model are as follows:

v_x - *X-axis* component of linear velocity;
v_y - *Y-axis* component of linear velocity;
ω - angular velocity;
ω_1 - the angular velocity of the wheel driven by the M1 motor;
ω_2 - the angular velocity of the wheel driven by the M2 motor;
ω_3 - the angular velocity of the wheel driven by the M3 engine;
ω_4 - angular velocity of the wheel driven by the M4 motor;
R - wheel radius;
θ - the angle of rotation of the robot;
L_x- the distance between the wheels in the direction of the *X-axis*;
L_y- the distance between the wheels in the direction of the *Y-axis*.

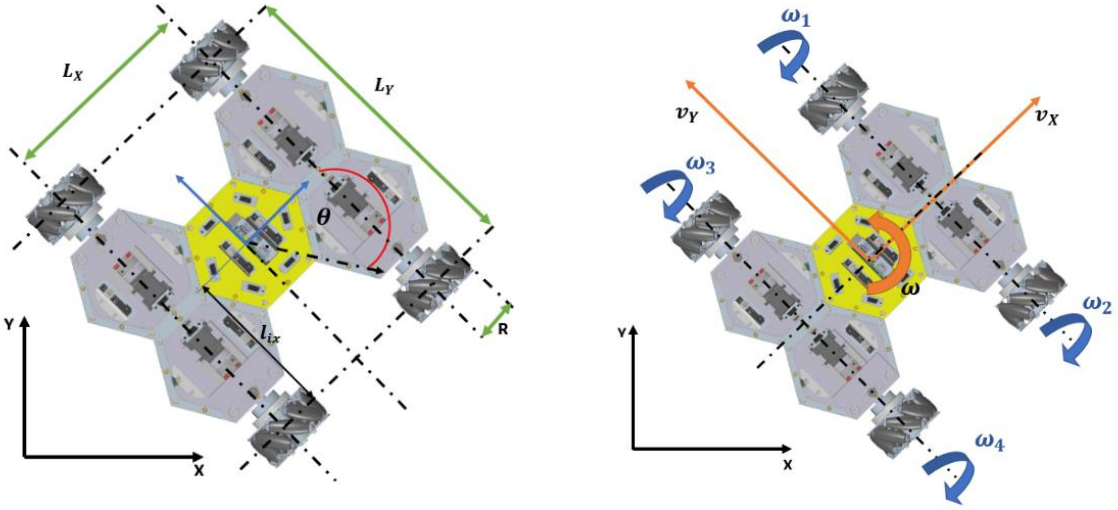

(a) (b)

Fig. 0.6 Kinematic model of the modular mobile platform with 4 omnidirectional mecanum wheels: (**a**) representation of the distances between the wheels on the two directions *X* and *Y* and the radius of the drive wheel; (**b**) representation of the angular velocity of the robot and the 4 mecanum wheels.

Direct kinematics can be expressed by the following equation:

$$\begin{bmatrix} v_X \\ v_Y \\ \omega \end{bmatrix} = \frac{R}{4} \begin{bmatrix} 1 & 1 & 1 & 1 \\ -1 & 1 & 1 & -1 \\ -2/(L_X + L_Y) & 2/(L_X + L_Y) & -2/(L_X + L_Y) & 2/(L_X + L_Y) \end{bmatrix} \begin{bmatrix} \omega_1 \\ \omega_2 \\ \omega_3 \\ \omega_4 \end{bmatrix}. \quad (0.9)$$

Inverse kinematics is described by the following relationship:

$$\begin{bmatrix} \omega_1 \\ \omega_2 \\ \omega_3 \\ \omega_4 \end{bmatrix} = \begin{bmatrix} 1 & -1 & -(L_X + L_Y)/2 \\ 1 & 1 & (L_X + L_Y)/2 \\ 1 & 1 & -(L_X + L_Y)/2 \\ 1 & -1 & (L_X + L_Y)/2 \end{bmatrix} \begin{bmatrix} v_X \\ v_Y \\ \omega \end{bmatrix}. \quad (0.10)$$

The direction and speed of the diagonal wheels are set independently. Using the same speed on each wheel at the same time during operation results in eight directions for the robot's movement without changing its orientation.

3.2. CONCLUSIONS

Chapter 3 presents theoretical contributions on the kinematic and dynamic modelling of a reconfigurable modular mobile platform. In the first part of this chapter, kinematic modelling for possible mobile robot configurations resulting from the reconfiguration of the modular platform was performed. Thus the kinematic model for the following robotic structures was presented:

- Mobile robot with differential drive, with four or two conventional wheels;
- Omnidirectional mobile robot with three or four omnidirectional wheels with rollers arranged at 90°;
- Omnidirectional four-wheel drive mobile robot mechanum.

The equations defining the kinematic models were further used to achieve dynamic models and control of each individual robot configuration. In order to be able to use independent drive modules, a series of calculations were performed to choose the electric motor. For these calculations the robotic configuration with differential drive and two conventional wheels was considered. For this configuration the distributed mass on one module had the highest value. Following these calculations the required torque and speed were determined and the electric motor was chosen. Knowing the motor parameters required to drive a module, different robotic structures with two or more driving wheels were created depending on the industrial application in which the modular mobile robot will be integrated.

CHAPTER. 4. DEVELOPMENT OF A MODULAR MOBILE PLATFORM USING CAD-CAM-CAE TECHNIQUES

4.1. 3D MODELLING OF CONSTRUCTION VARIANTS

According to chapter 2, which presents the latest developments in the field of robotics, it can be seen that the trend of mobile robots is towards mobile platforms with omni-directional wheels, due to their advantages in terms of mobility and flexibility. Today, however, we are going through continuous changes in terms of industrial processes and terms such as "Economic and environmentally friendly", "Efficiency and economy", "Industry 4.0", "Flexible solutions", "Low cost", are the main characteristics that new equipment in industry must have. Correlating these characteristics with the literature studies presented in Chapter 2, three concepts of mobile robotic platforms have been developed, and in **Fig. 0.7** shows the evolution of this concept.

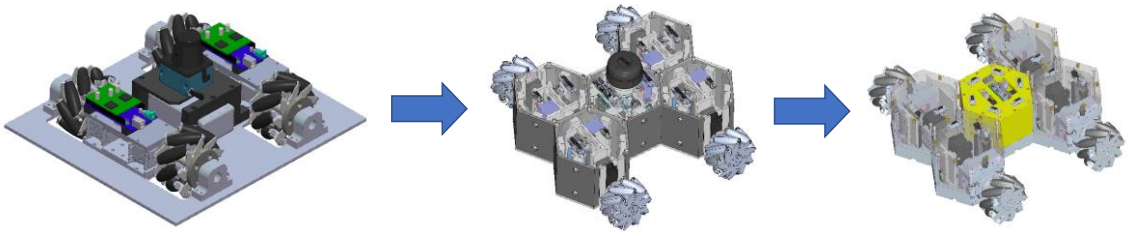

(a) (b) (c)

Fig. 0.7 Evolution of the concept of the mobile platform with four omnidirectional mecanum wheels: (**a**) Mobile platform with four omnidirectional mecanum wheels; (**b**) Modular mobile platform with four omnidirectional mecanum wheels version 1; (**c**) Modular mobile platform with four omnidirectional mecanum wheels version 2 .

4.1.1. Main module

The robot's main unit or main module is a hexagonal shaped structure with two important roles: it acts as a control unit for all the other sub modules and as a mechanical connection, which together with the other modules forms different robot structure configurations. The main feature from a mechanical point of view is the hexagonal shape of the structure which allows a quick configuration with 6 other modules of similar shape and the possibility to form different robotic structures.

The main components that make up this module can be seen in **Fig. 0.8**. The base plate was made of aluminium by precision machining on a CNC machining centre. All the other mechanical components were made by 3D printing, thus achieving a lower module manufacturing cost, excluding the electronic components. [62].

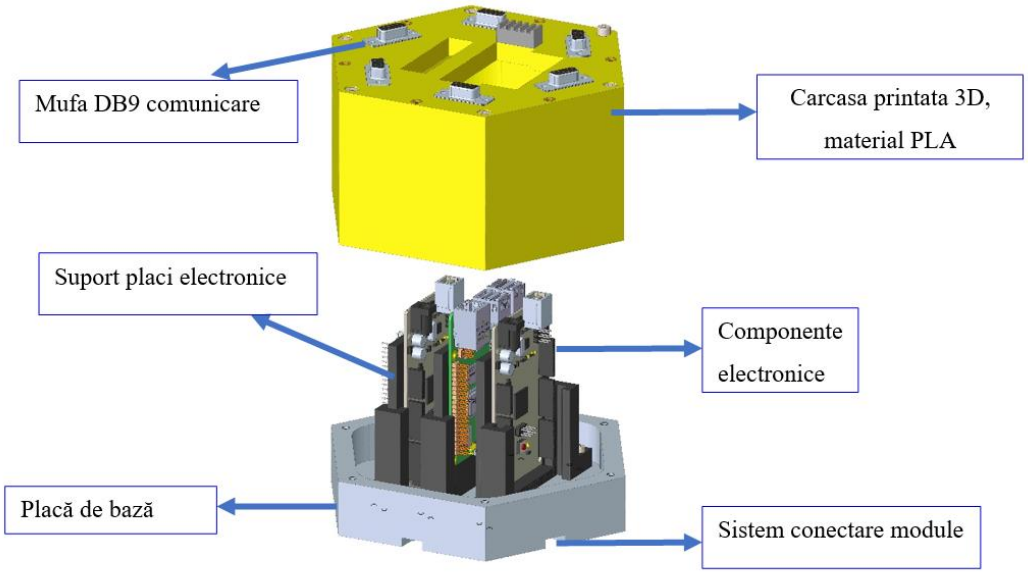

Fig. 0.8 Main module components - version 2 [62].

Compared to the original version, the connection system between modules has been modified and a simpler and more efficient system has been achieved in terms of time and complexity of module assembly. This was possible because the assembly has fewer components, thus making a direct connection between the base plates of each module and requiring only a simple connecting piece and screws for fixing, as shown in **Fig. 0.9**.

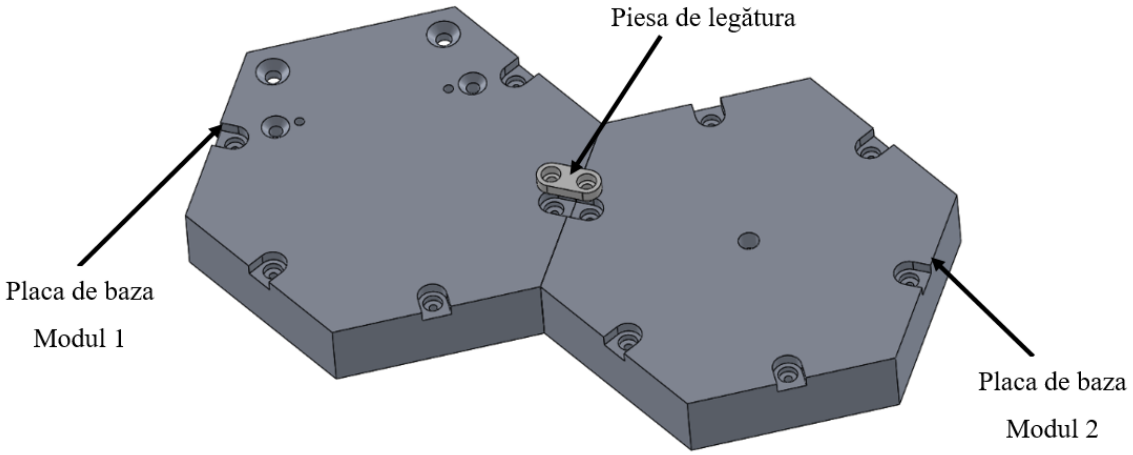

Fig. 0.9 System connection of modules .

4.1.2. Drive wheel module

The drive of the modular dolly is provided by the drive wheel module illustrated in **Fig. 0.10**where the construction and main components of the module are shown.

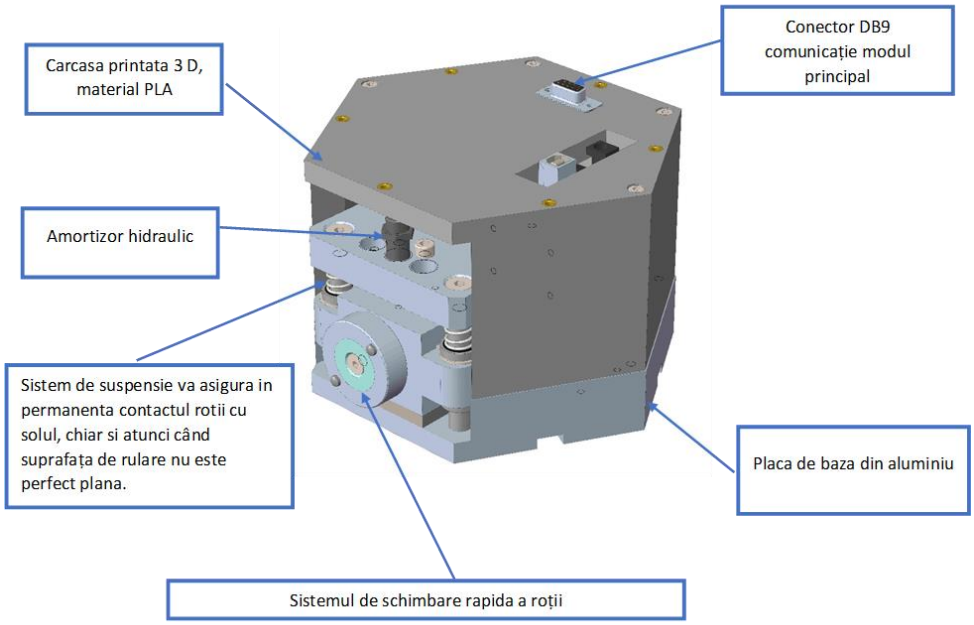

Fig. 0.10 Drive wheel module assembly.

The module is made up of several sub-systems, such as the suspension system or the wheel quick coupling system, shown in **Fig. 0.11a** and **Fig. 0.11b**. A DC servo motor drives the wheel of the modular mobile robot.

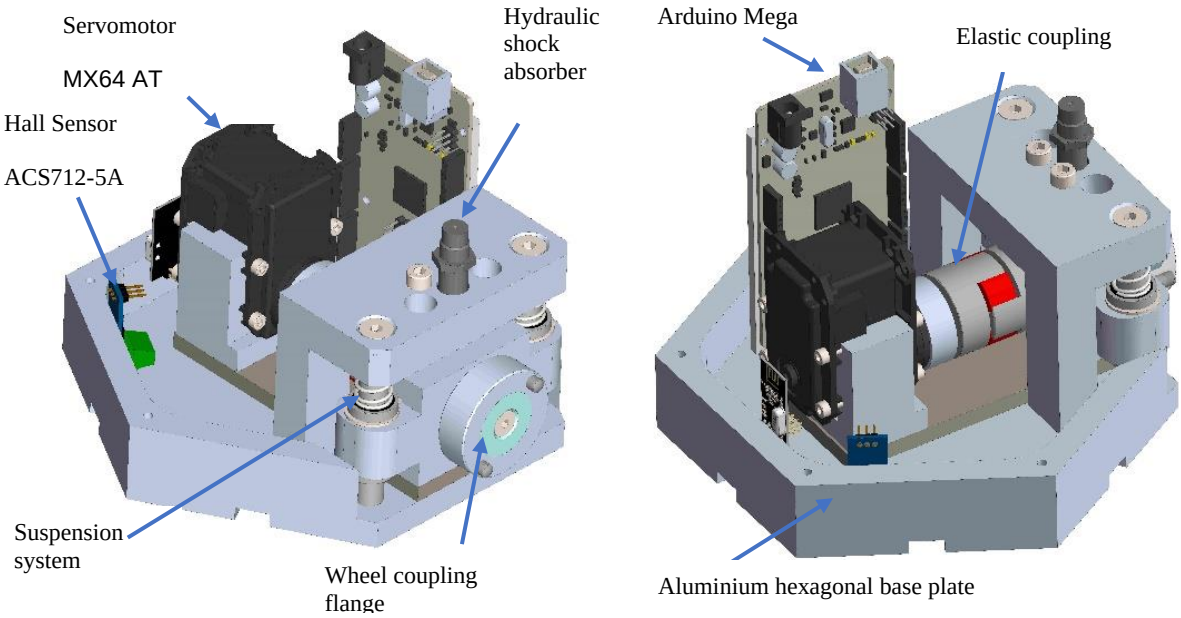

(a) (b)

Fig. 0.11 Drive wheel module (3D model): (**a**) exterior view; (**b**) interior view.

CHAPTER. 5. PRELIMINARY RESEARCH ON AN OMNIDIRECTIONAL MOBILE ROBOT WITH MECANUM WHEELS

The preliminary research chapter aims to develop a low-cost and efficient autonomous mobile robot suitable for industrial applications. Thus, the developed platform will move within a controlled environment, transferring parts between workstations. As a result, the paths are fixed and the possibility of obstacles is quite low. Thus, trajectory planning, trajectory accuracy and obstacle avoidance are not so important for the proposed autonomous mobile robot.

5.1. MOBILE ROBOT

For this research a Mecanum wheeled mobile robotic platform was developed and presented in **Fig. 0.12**.

Each wheel can be driven independently by DC motors controlled by variable-width voltage pulses using the PWM *(pulse with modulation*) method.

Maxon DCX 22 L motors (Maxon Motor AG, Sachseln, Switzerland) were used for the drive. Two Arduino Mega 2560 boards (Arduino AG, Italy) were used to manage the variable-width voltage pulse generation for the drive motors. Two VNH5019 dual motor drivers (Pololu, Las Vegas, USA) were used to control the wheel drive motors. [63].

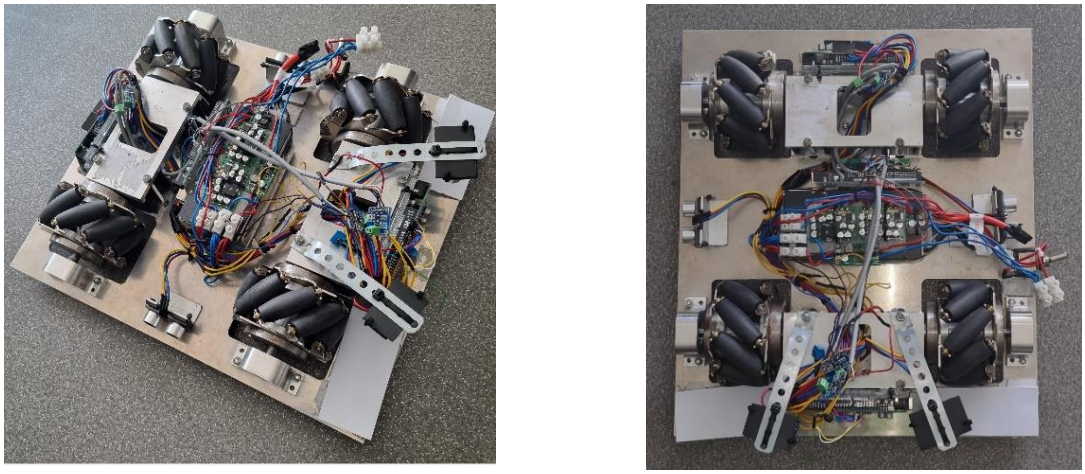

(a) (b)

Fig. 0.12 Mobile robot with mechanum wheels: (**a**) isometric view; (**b)** top view.

The platform was also equipped with various sensors, such as ultrasonic distance sensors and an infrared sensor module for obstacle avoidance, but these sensors were not used during testing.

5.2. KINEMATIC SOLUTIONS CONSIDERED

5.2.1. Kinematics of the four-wheeled mechanum

Direct kinematics can be described by the following relationship:

$$\begin{bmatrix} v_x \\ v_y \\ \omega \end{bmatrix} = \frac{R}{4}\begin{bmatrix} 1 & 1 & 1 & 1 \\ -1 & 1 & 1 & 1 \\ -2/(L_x+L_y) & 2/(L_x+L_y) & -2/(L_x+L_y) & -2/(L_x+L_y) \end{bmatrix}\begin{bmatrix} \omega_1 \\ \omega_2 \\ \omega_3 \\ \omega_4 \end{bmatrix}. \quad (0.11)$$

Inverse kinematics can be described by the following relationship:

$$\begin{bmatrix} \omega_1 \\ \omega_2 \\ \omega_3 \\ \omega_4 \end{bmatrix} = \begin{bmatrix} 1 & -1 & -(L_x+L_y)/2 \\ 1 & 1 & (L_x+L_y)/2 \\ 1 & 1 & -(L_x+L_y)/2 \\ 1 & -1 & (L_x+L_y)/2 \end{bmatrix}\begin{bmatrix} v_x \\ v_y \\ \omega \end{bmatrix}. \quad (0.12)$$

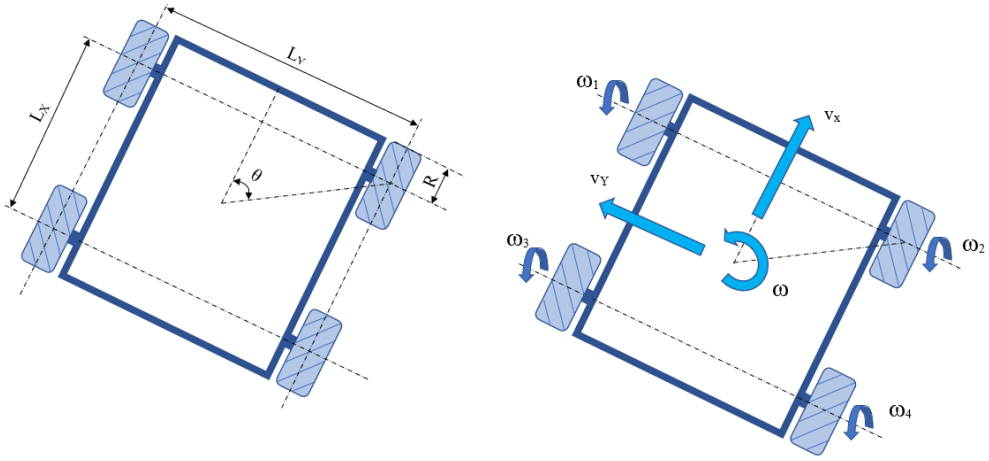

Fig. 0.13 Diagram of a four-wheeled mobile mechanum robot.

5.2.2. Differential drive kinematics

In **Fig. 0.14** shows a schematic of a mobile robot with differential drive.

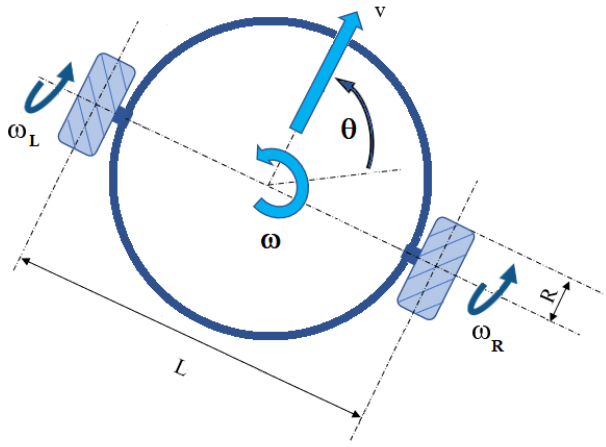

Fig. 0.14 Schematic of a mobile robot with differential drive.

According to [56], the input data of the kinematic model are the left and right wheel speeds, ω_L and ω_R (in rad/s), while the output data are the linear velocity v (in m/s) and the angular velocity ω (in rad/s).

Direct kinematics can be described by the following relationship:

$$v = \frac{R}{2}(\omega_R + \omega_L), \qquad \omega = \frac{R}{L}(\omega_R - \omega_L), \tag{0.13}$$

Inverse kinematics can be described by the following relationship:

$$\omega_L = \frac{1}{R}(v - \frac{\omega L}{2}), \omega_R = \frac{1}{R}(v + \frac{\omega L}{2}). \tag{0.14}$$

5.3. SIMULATION OF THE DYNAMIC MODEL OF THE OMNIDIRECTIONAL ROBOT

The dynamic model of the mobile robot, considering the kinematic solution of the four-wheeled mechanum, is shown in **Error! Reference source not found.**. The model also uses blocks from the Mobile Robotics Simulation Toolbox [56] within Matlab. The mechanical dependencies between the forces acting on the robot chassis and the torques acting on the wheels have been introduced in the model, also considering the harmonic gear ratio between the motor and the wheel.

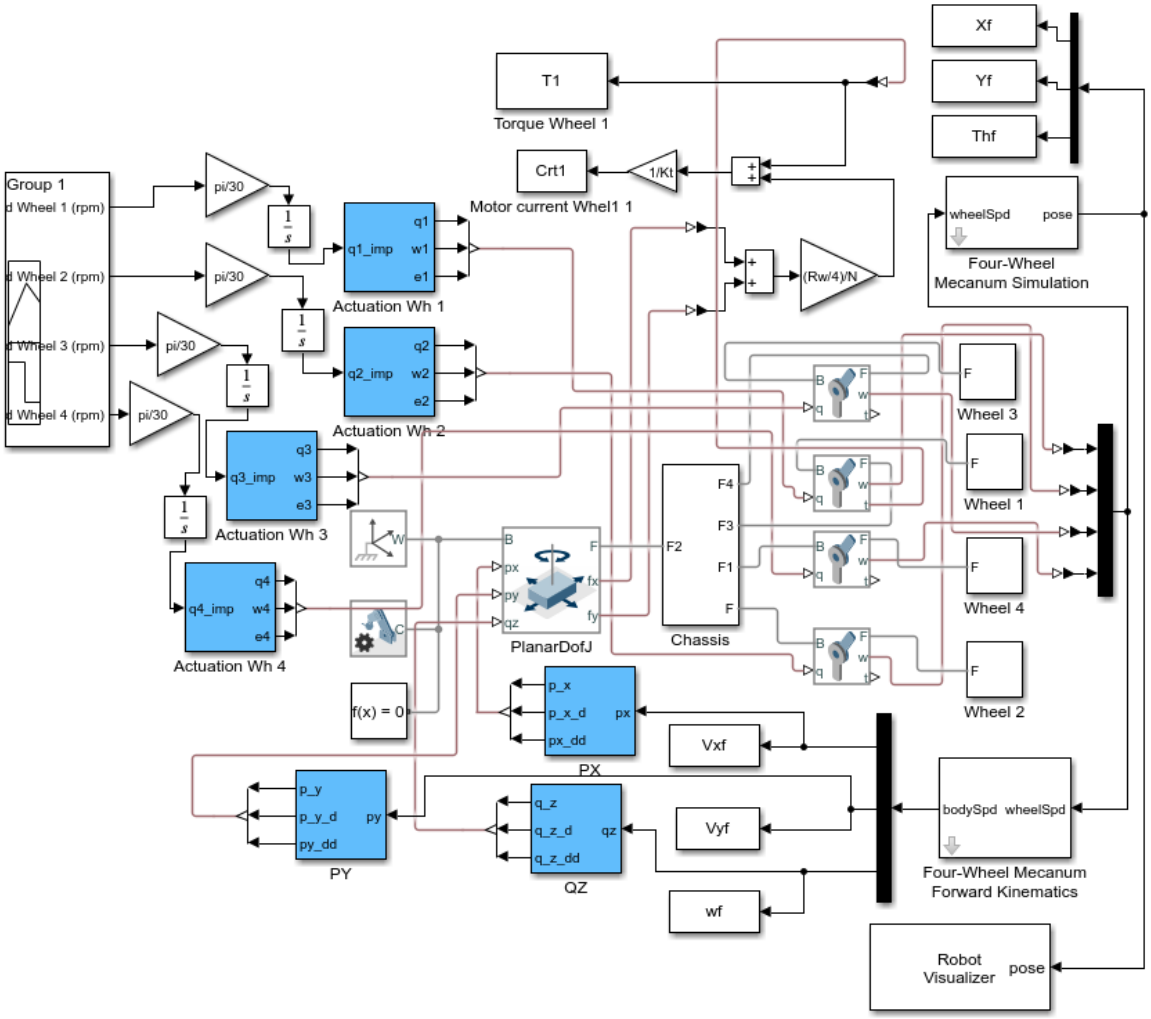

Fig. 0.15 Dynamic model for the four-wheeled mechanum kinematic solution .

In **Fig. 0.16** shows the dynamic model for the kinematic solution of the differential drive.

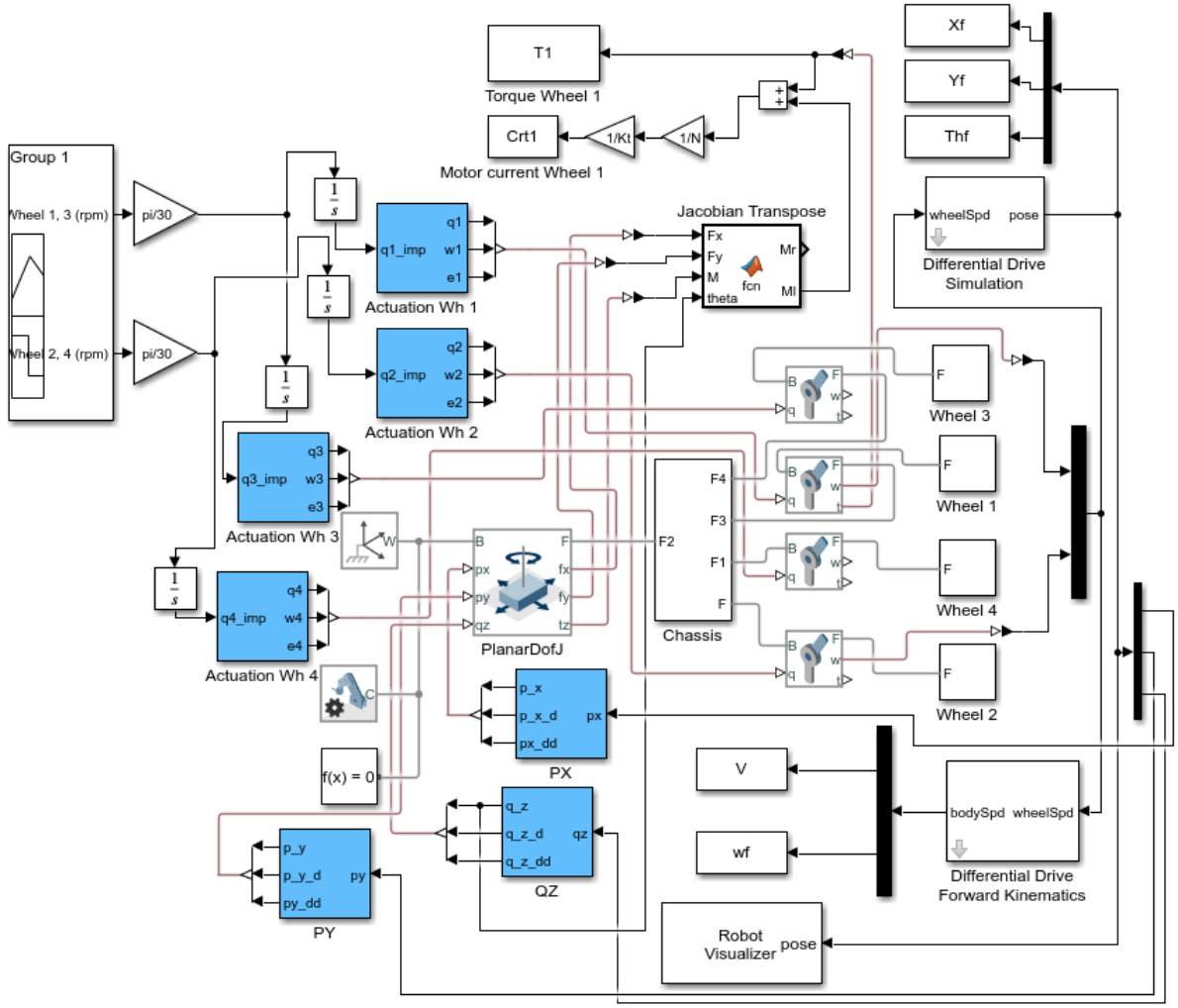

Fig. 0.16 Dynamic model of the kinematic solution with differential drive.

The simulation results (simulated trajectory) for the two cases considered are shown in **Fig. 0.17**, captures from the Robot Visualizer block in the Mobile Robotics Simulation Toolbox.

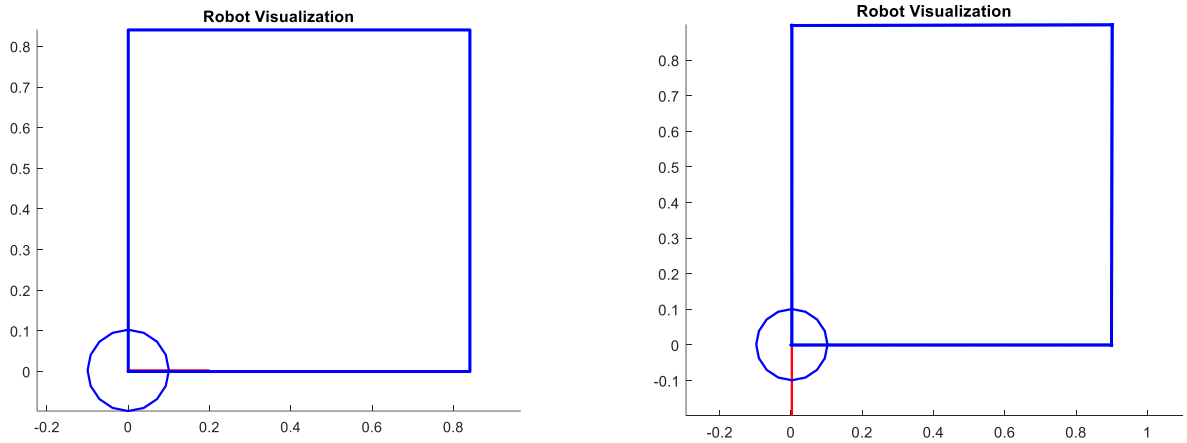

(a) (b)

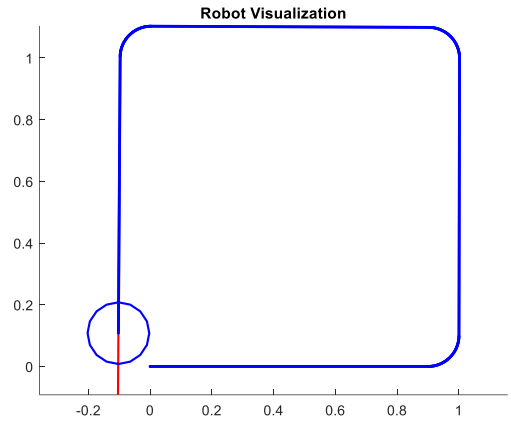

(c)

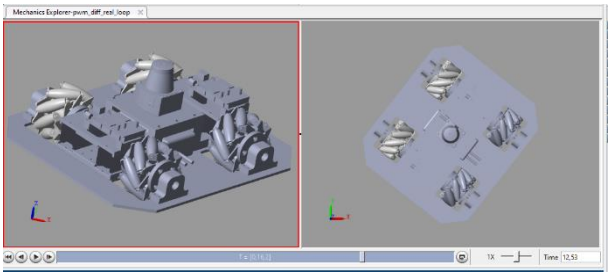

(d)

Fig. 0.17 Simulated trajectories: (**a**) trajectory for four-wheeled Mecanum; (**b**) trajectory for differential drive, without radius; (**c**) trajectory for differential drive with radius (**d**) screenshot from Mechanics Explorer - Simscape.

5.4. COMPARISON OF SIMULATED AND ACTUAL VALUES OF MOTOR CURRENTS ABSORBED

One of the main objectives of this approach was to determine the currents through the wheel motors, both by simulation and experimental measurements. Currents were measured using the CJMCU-219 INA219 sensor module (Texas Instruments, Dallas, TX, USA).

Fig. 0.18 and **Fig. 0.19** show a comparison between the simulated and measured values of these currents during the square path for all the two situations mentioned (four-wheel mechanum and differential drive).

It should be noted that friction was not taken into account in the dynamic model, while the measurements were influenced by it.

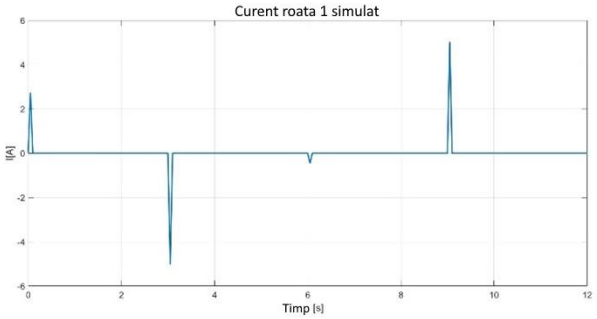

(a)

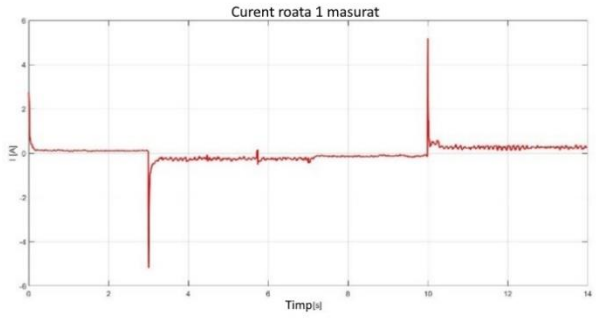

(b)

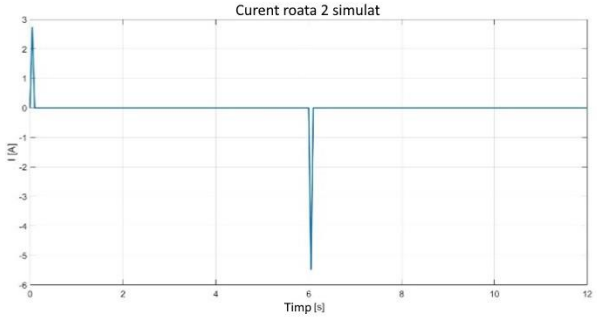

(c)

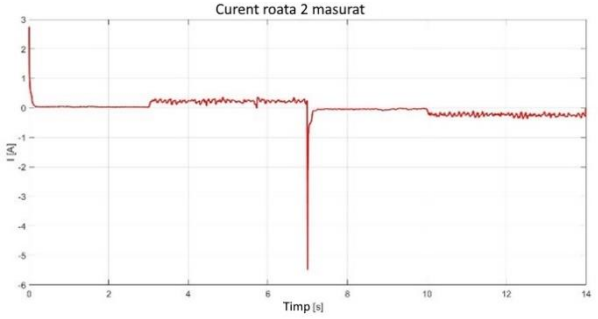

(d)

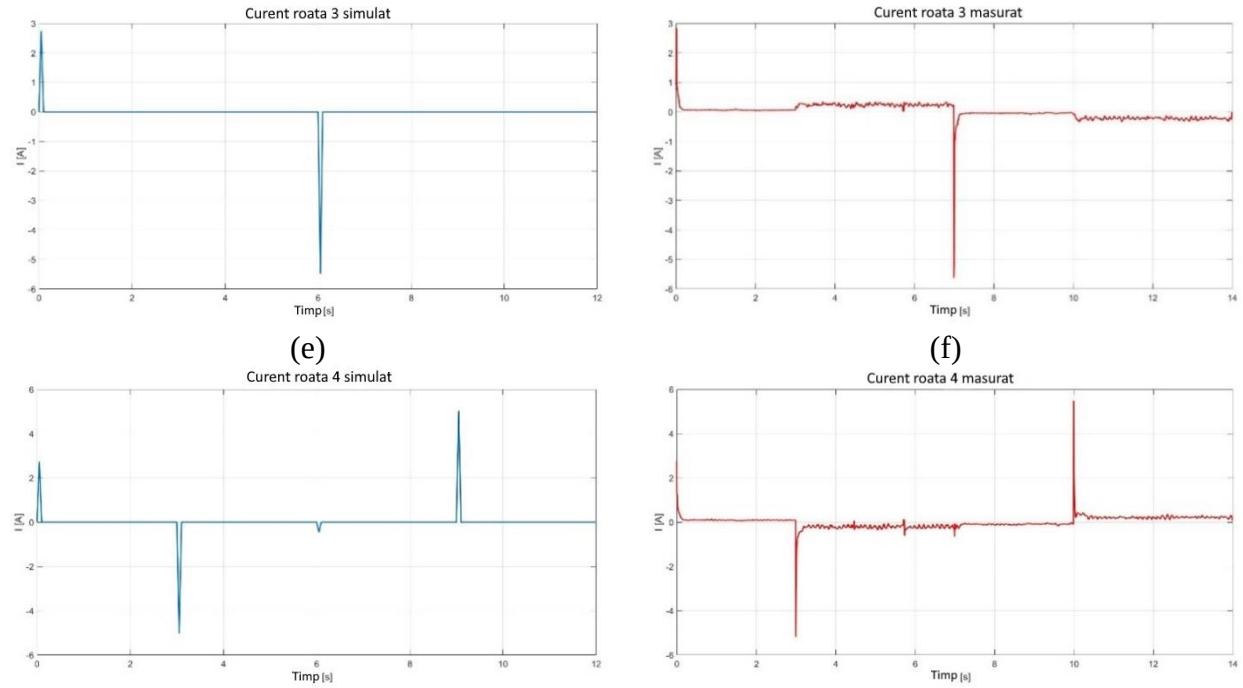

Fig. 0.18 Comparison between simulated (a, c, e, g) and measured (b, d, f, h) currents absorbed by the wheel drive motors for the four-wheel mechanum kinematic solution: (**a**, **b**) wheel 1; (**c**, **d**) wheel 2; (**e**, **f**) wheel 3; (**g**, **h**) wheel 4.

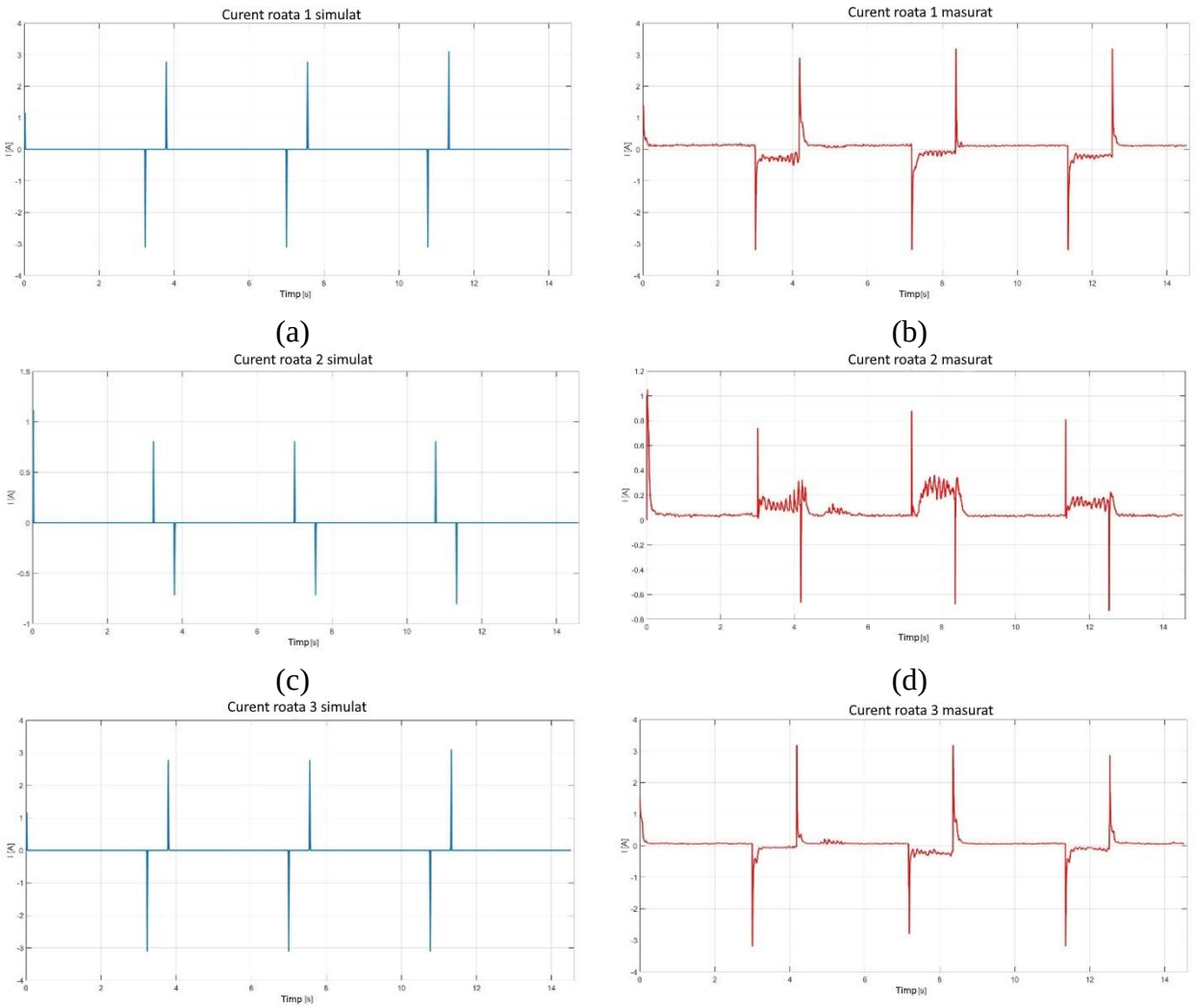

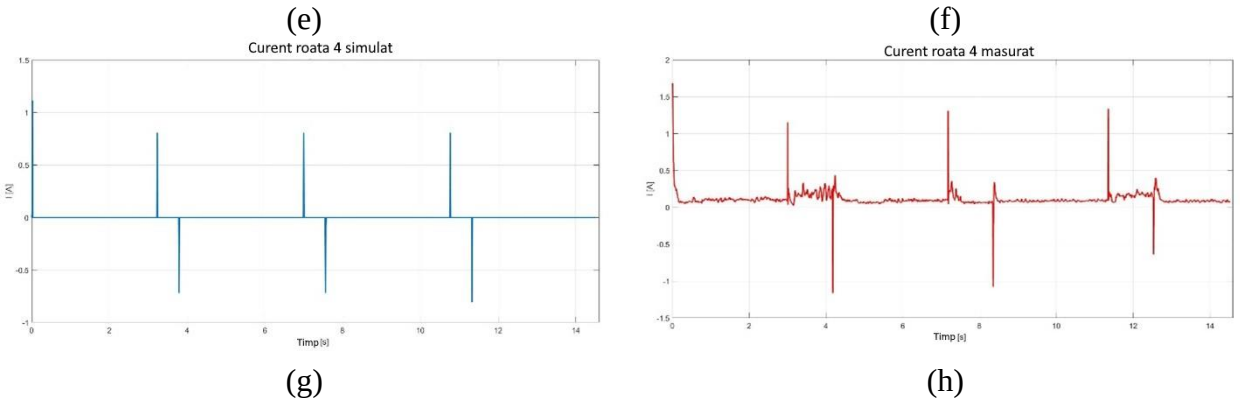

Fig. 0.19 Comparison between simulated (a, c, e, g) and measured (b, d, f, h) currents absorbed by the wheel drive motors for the kinematic solution with radius-free turning, differential drive: (**a**, **b**) wheel 1; (**c**, **d**) wheel 2; (**e**, **f**) wheel 3; (**g**, **h**) wheel 4.

5.5. CONCLUSIONS

The main objective of the preliminary research was to develop efficient dynamic digital block models to study the behaviour of autonomous mobile robotic platforms when moving along an imposed trajectory.

The models developed take into account the following:

- the geometrical and constructive characteristics of the mobile robot, by integrating its 3D model into the simulation;
- kinematics of the mobile robot, using blocks that allow the implementation of four-wheel mechanum kinematics and differential kinematics. Blocks have also been built that allow the generation of kinematic inputs for the two situations;
- robot dynamics, both through Simscape-specific blocks and user-created blocks (e.g. the block for implementing the transposed Jacobian matrix).

The models also allow 3D visualisation of the robot's movement during simulation via the Mechanics Explorer interface in Simscape.

Of course, the proposed models and some disadvantages:

- do not take friction phenomena into account;
- they do not include the control part of the drive system (for the chosen drive solution, DCPWM, this is not relevant).

Validation of the proposed models was performed by comparing the simulation results with the experimental ones. For this comparison, the currents absorbed by the motors driving the robot wheels were chosen, mainly because of the ease with which they can be measured experimentally.

The comparison between experimental and simulated values demonstrated the accuracy of the proposed simulation plots.

Using the proposed simulation schemes, the behaviour of the mobile robot when moving on square trajectories was studied. The simulations showed that the advantages of mecanum wheels come together with the disadvantage of high values of the currents absorbed by the wheel drive motors, in the variant of using the drive solution based on DC motors driven by PWM voltage pulses.

The use of differential kinematics, which does not benefit from the facilities of mecanum gears, leads to lower currents, which can be further reduced by introducing arcing instead of turning on the spot around its own vertical axis.

Comparison of the experimental test results showed that the simulated current values are close to the measured ones.

CHAPTER. 6. MODELLING, SIMULATION AND EXPERIMENTAL RESEARCH CARRIED OUT ON MOBILE ROBOT DESIGNS

6.1. STRUCTURE AND FEATURES OF THE MODULAR MOBILE PLATFORM DEVELOPED

Following preliminary research, it can be seen that the dynamic model of the omnidirectional mobile robot with roti mecanum that was developed in Matlab Simulink and experimentally validated, can estimate the energy consumption of the robot as a function of the trajectory travelled. Thus it was desired to continue this research for other types of mobile robots and to be able to determine the influence of the robotic structure and the locomotion system in the energy consumption of the robot. Based on these considerations, a modular mobile platform was developed that can be configured into 5 robotic structures with 3 different types of wheels. To demonstrate the modularity and reconfigurability of the original concept, **Fig. 0.20** shows 3D CAD models of the 5 mobile robot configurations.

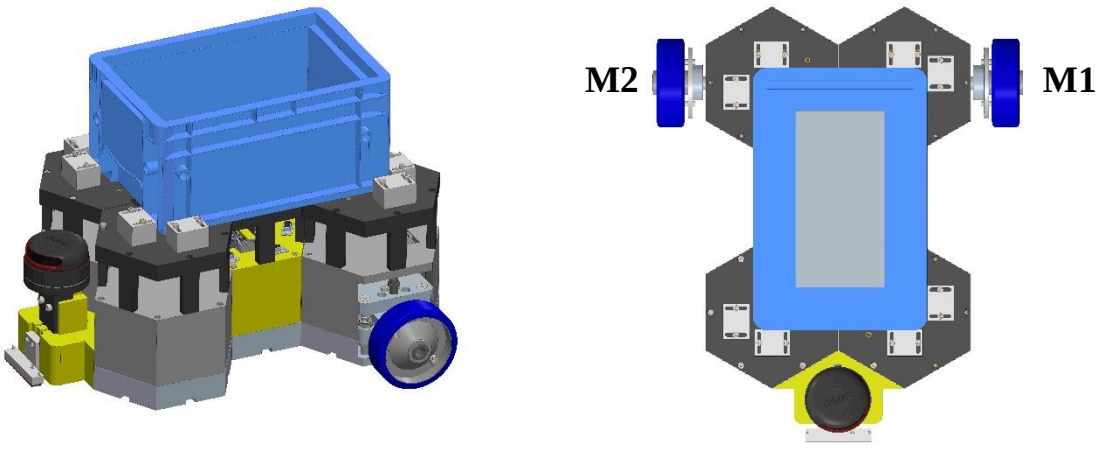

(a)

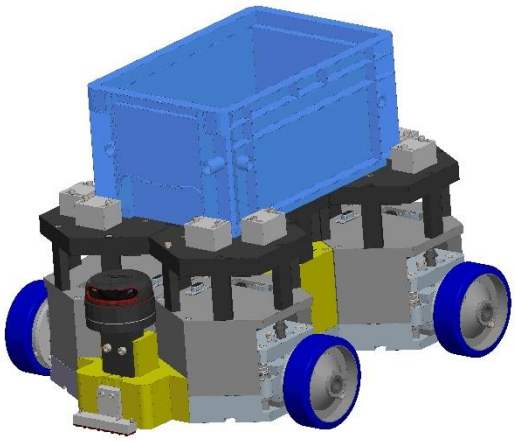

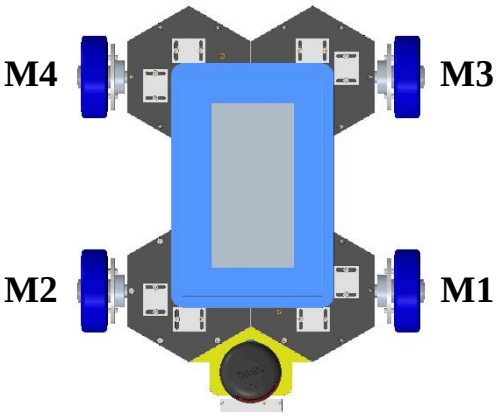

(b)

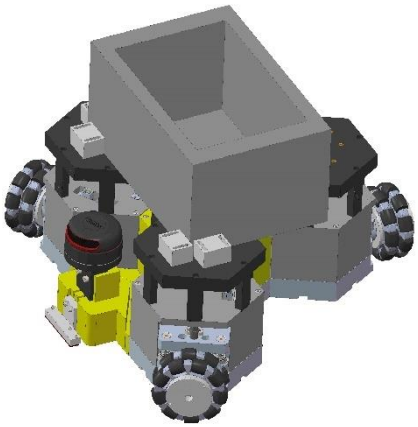

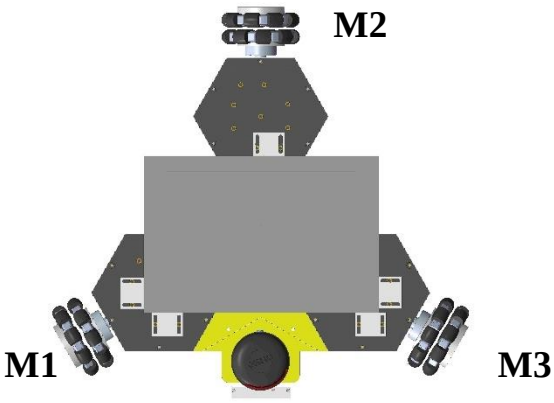

(c)

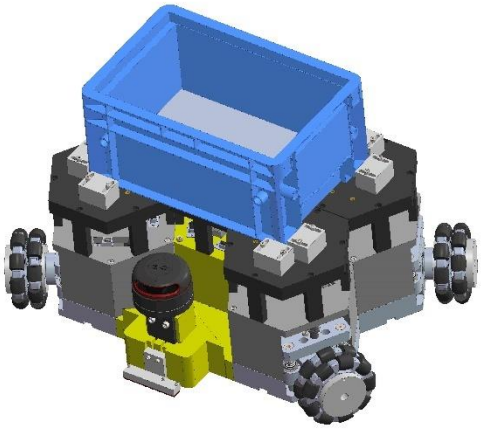

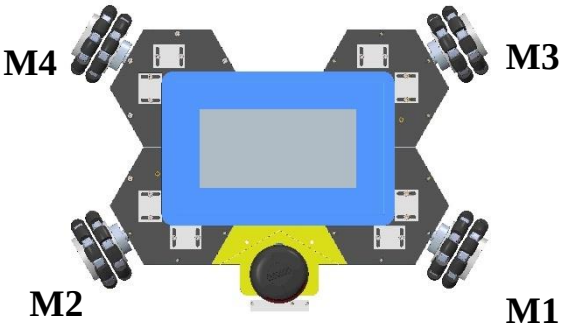

(d)

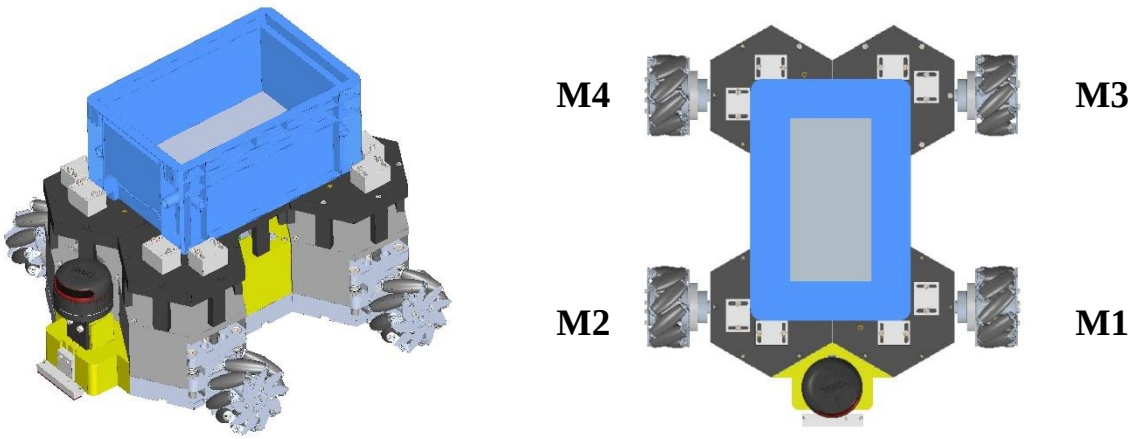

(e)

Fig. 0.20 Possible modular mobile platform configurations: (**a**) mobile robot with differential drive and two conventional wheels ; (**b**) mobile robot with differential drive and four conventional wheels; (**c**) mobile robot with omni-directional drive and three omni-directional wheels; (**d**) mobile robot with omni-directional drive and four omni-directional wheels; (**e**) mobile robot with omni-directional drive and four mechanum wheels.

The configuration of the modular mobile robot with differential locomotion and two conventional wheels is shown in **Fig. 0.20a**. The wheels are driven by two servomotors (M1, M2). **Fig. 0.21a** shows a general view of the physical assembly of the mobile robot, while **Fig. 0.21b** shows a bottom view of the robot to highlight the Ball Castor modules.

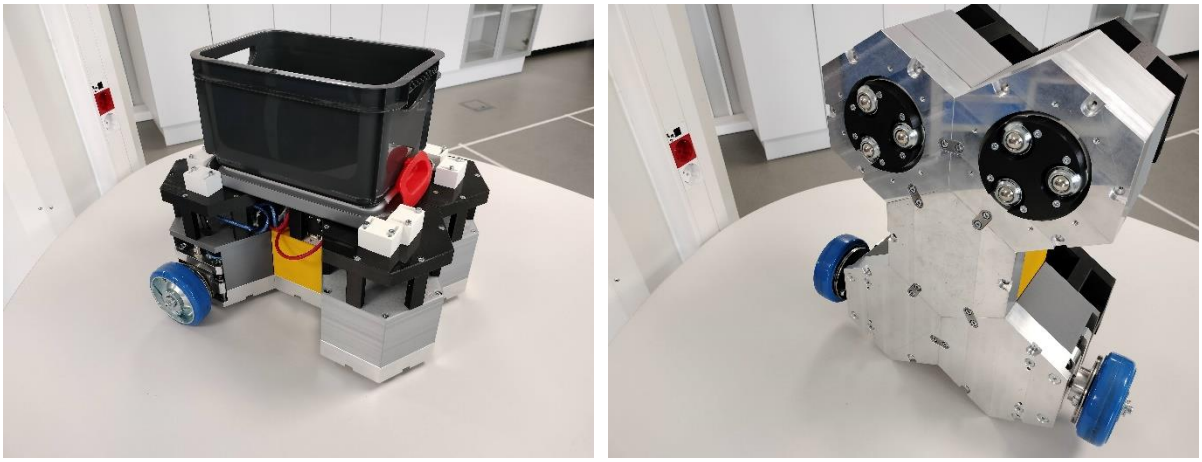

(a) (b)

Fig. 0.21 Modular mobile robot with two conventional wheels (real model): (**a**) isometric view; (**b**) bottom view.

This robot configuration includes the following modules:

- A main module, which acts as a control and link to the other modules;
- Two drive wheel modules that drive the robot;
- Two modules with support wheels.

The configuration of the modular mobile robot with differential locomotion and four conventional wheels is shown in **Fig. 0.20b**. The wheels are driven by four servomotors (M1, M2, M3, M4). **Fig. 0.22a** shows an overview of the physical assembly of the mobile robot,

while **Fig. 0.22b** shows a top view of the robot to highlight the modularity of the box attachment system for transporting parts.

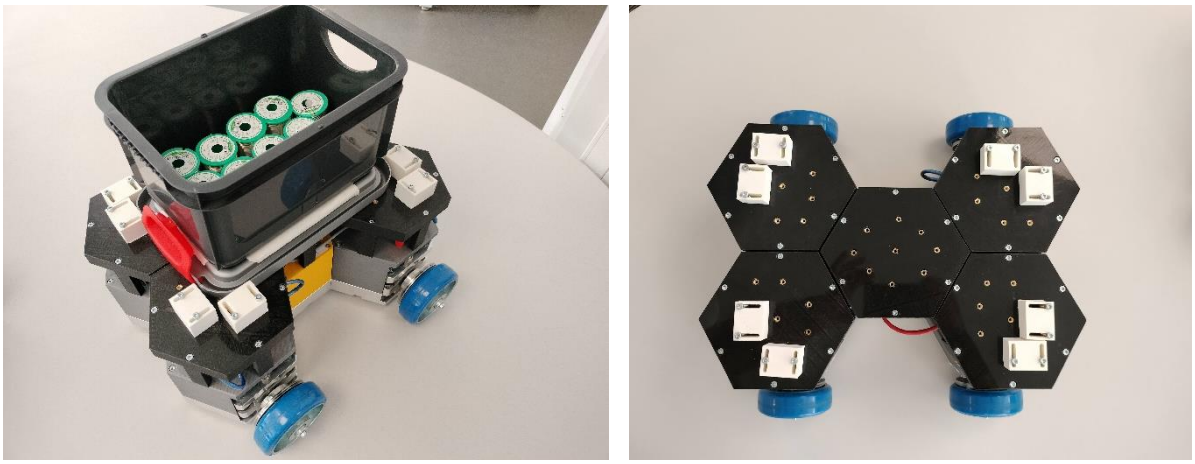

(a) (b)

Fig. 0.22 Modular mobile robot with four conventional wheels (real model): (**a**) isometric view. (**b**) top view.

This robot configuration includes the following modules:

- A main module, which acts as a control and link to the other modules;
- Four drive wheel modules that drive the robot.

The configuration of the modular mobile robot with omnidirectional locomotion and three wheels with rollers arranged at 90° is shown in **Fig. 0.20c**. The wheels are driven by three servomotors (M1, M2, M3). **Fig. 0.23a** shows an overview of the physical assembly of the mobile robot, while in **Fig. 0.23b** shows a top view of the robot to highlight the modularity of the system and the configuration possibilities.

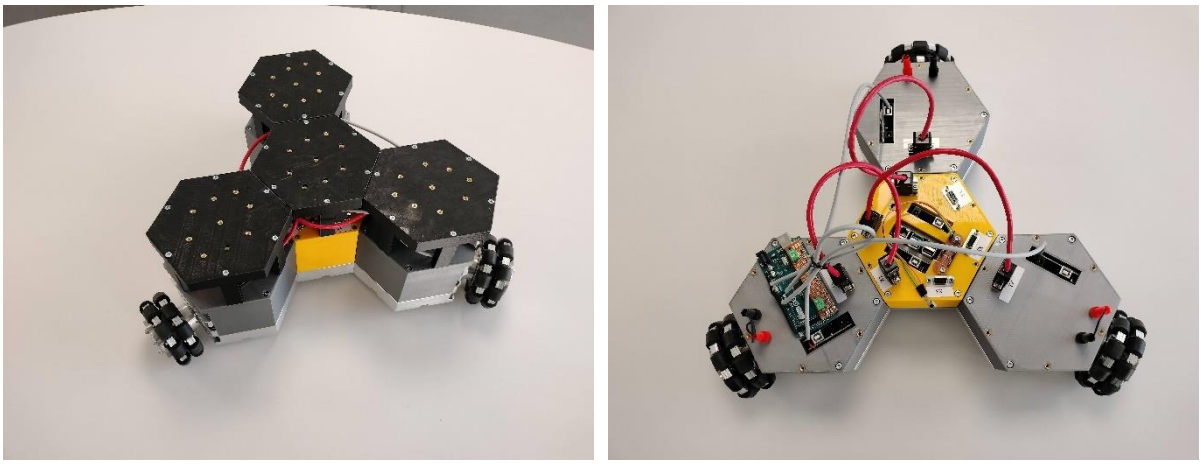

(a) (b)

Fig. 0.23 Modular mobile robot with three omnidirectional wheels (real model): (**a**) isometric view; (**b**) top view.

This robot configuration includes the following modules:

- A main module, which acts as a control and link to the other modules;
- Three drive wheel modules that drive the robot;

- Three omni-directional wheels with rollers arranged at 90°.

The configuration of the modular mobile robot with one omnidirectional locomotion and four wheels with rollers arranged at 90° is shown in **Fig. 0.20d**. The wheels are driven by four servomotors (M1, M2, M3, M4). **Fig. 0.24a** shows a general view of the physical assembly of the mobile robot, while **Fig. 0.24b** shows a top view of the robot to highlight the modularity of the system and the configuration possibilities.

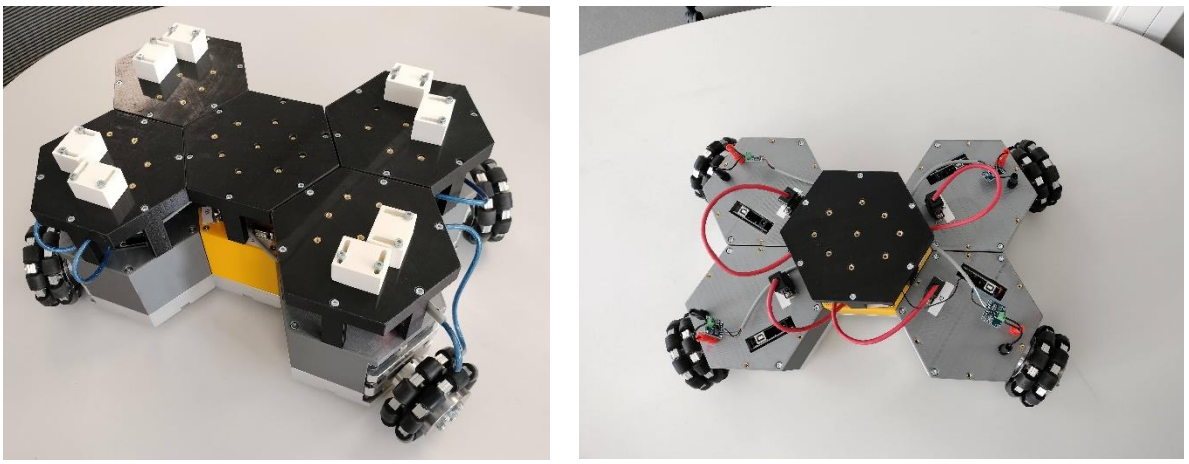

(a) (b)

Fig. 0.24 Modular mobile robot with three omnidirectional wheels (real model): (**a**) isometric view; (**b**) top view.

This robot configuration includes the following modules:

- A main module, which acts as a control and link to the other modules;
- Four drive wheel modules that drive the robot;
- Four omni-directional wheels with rollers arranged at 90°.

The main features of the robotic platform are presented in **Error! Reference source not found.**.

The configuration of the modular mobile robot with omnidirectional locomotion and four mecanum wheels is shown in **Fig. 0.20e**. The wheels are driven by four servomotors (M1, M2, M3, M4). **Fig. 0.25a** shows an overview of the physical assembly of the mobile robot, while **Fig. 0.25b** shows a top view of the robot to highlight the modularity of the system and the configuration possibilities.

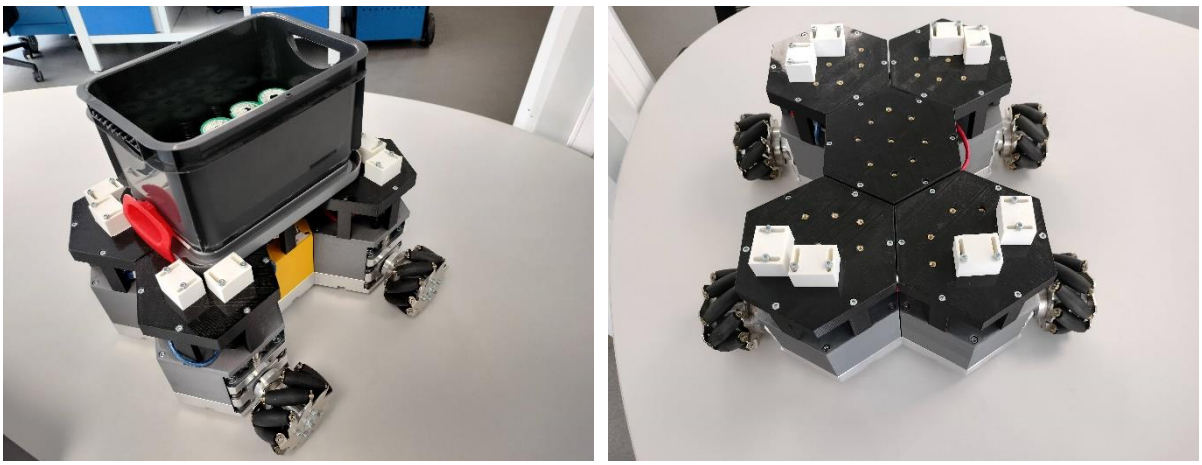

(a) (b)

Fig. 0.25 Modular mobile robot with four mecanum wheels (real model): (**a**) isometric view; (**b**) top view.

This robot configuration includes the following modules:

- A main module, which acts as a control and link to the other modules;
- Four drive wheel modules that drive the robot;
- Four omnidirectional mecanum wheels.

6.2. DYNAMIC MODELLING OF ROBOTIC CONFIGURATIONS

For modelling the mobile robot, after creating the 3D CAD model, the export to Simulink Simscape was performed. **Fig. 0.26** shows the result after import, i.e. the whole CAD model transformed into a kinematic chain consisting of several plane and rotation joints, coordinate systems and rigid bodies.

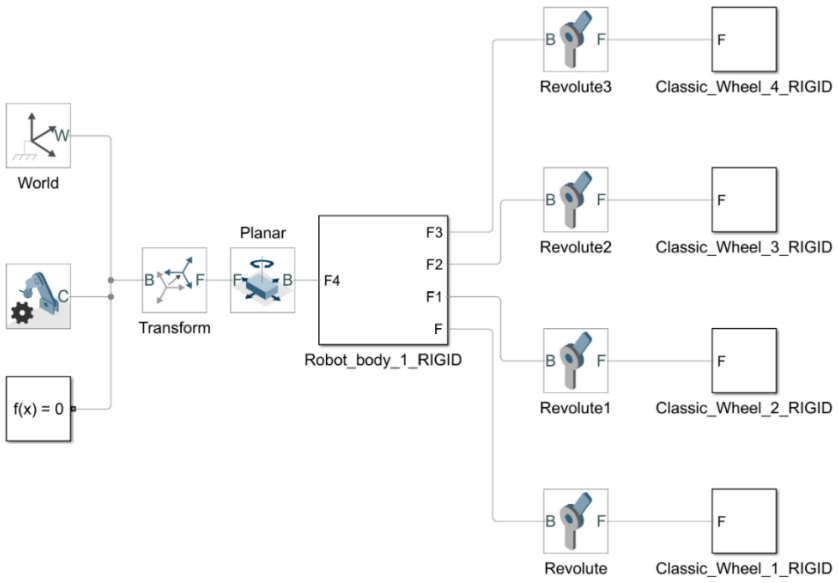

Fig. 0.26 Result of CAD model import into Simulink Simscape.

Starting from the theoretical foundations related to the kinematics of mobile robots, the relationship between kinematic torque variables and the positions of kinematic elements was established in two successive steps: the direct kinematics problem and the inverse kinematics problem. In the case of the Simulink dynamic model of the mobile robot it is not possible to model the link between the workspace and the motion of the robot wheels [64].

Inverse kinematics is required to drive the robot body along a certain trajectory, resulting in inertial forces. Direct kinematics is required for driving the wheels, from which the value of the torques acting on the wheels during movement (driving) can be derived.

In **Fig. 0.27**, **Fig. 0.28**, **Fig. 0.29**, **Fig. 0.30** and **Fig. 0.31** show the original dynamic models of the 5 mobile robot configurations as Simulink digital block models. These contain the part of blocks characteristic of the kinematic chain of the robots, blocks specific to the actuators in the joints, blocks defining the monitoring of forces and torques in the joints, and blocks for implementing the mathematical model of the robot kinematics for movement along the trajectory. At the same time, the robot dynamics models contain a computational block that also takes into account the friction between the wheels and the running surface.

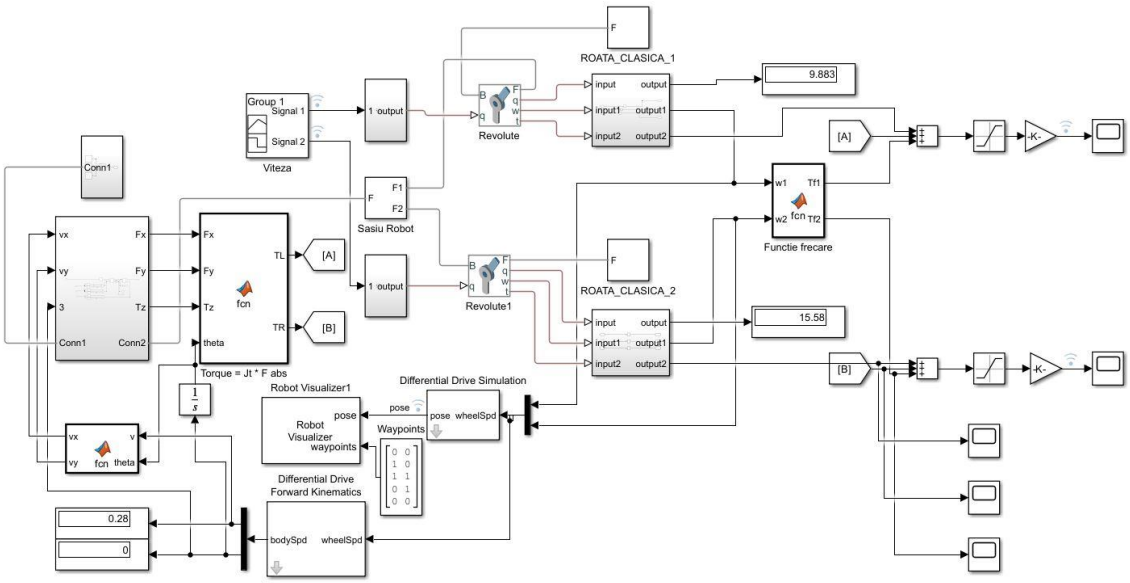

Fig. 0.27 Dynamic model of the mobile robot with differential drive and two conventional wheels.

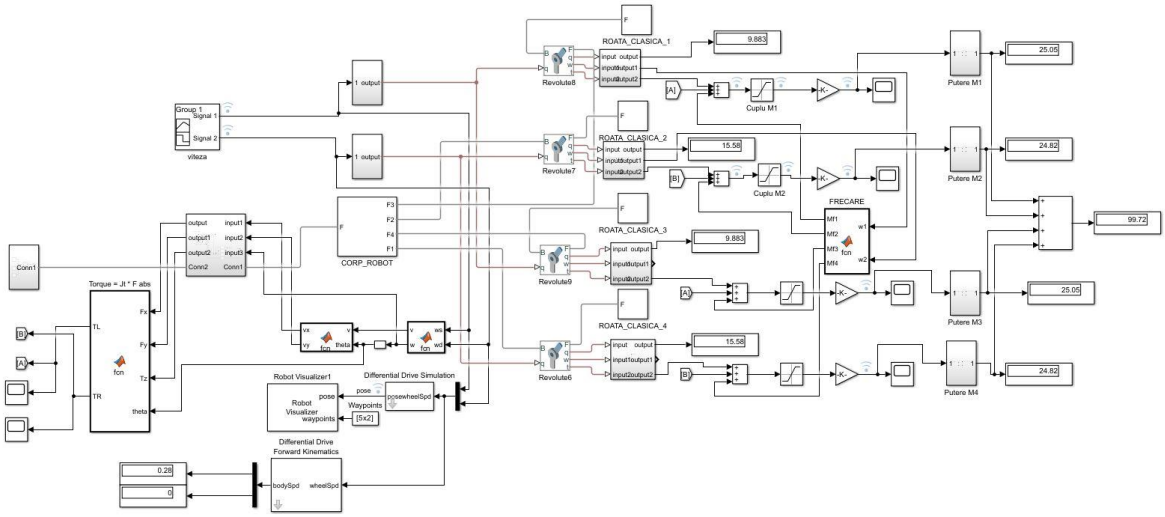

Fig. 0.28 Dynamic model of the mobile robot with differential drive and four conventional wheels.

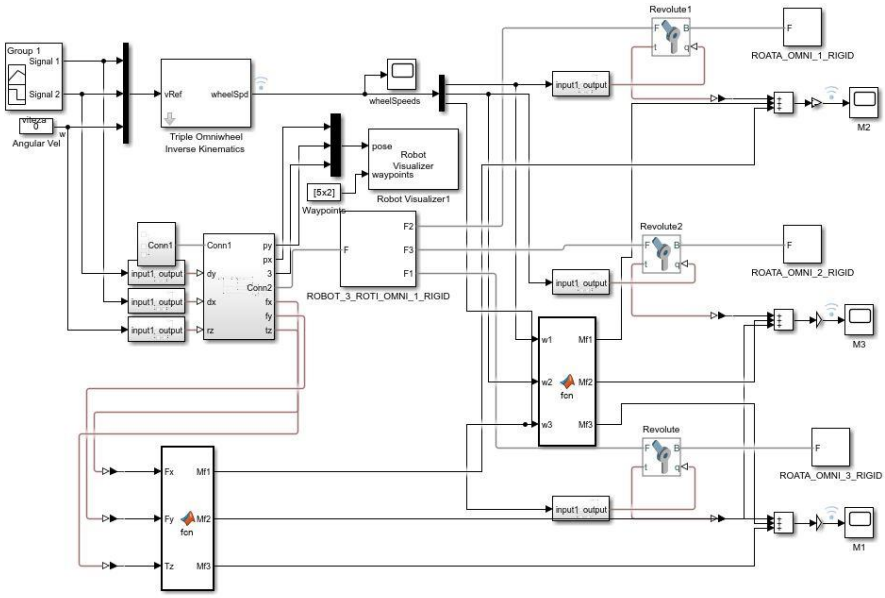

Fig. 0.29 Dynamic model of the mobile robot with omnidirectional traction and three omnidirectional wheels.

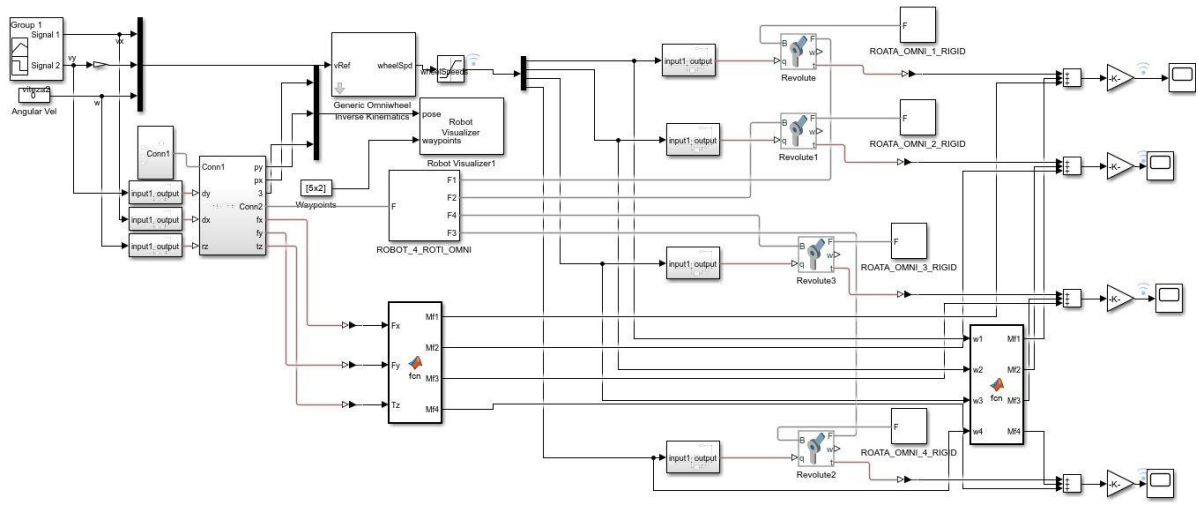

Fig. 0.30 Dynamic model of mobile robot with omnidirectional traction and four omnidirectional wheels.

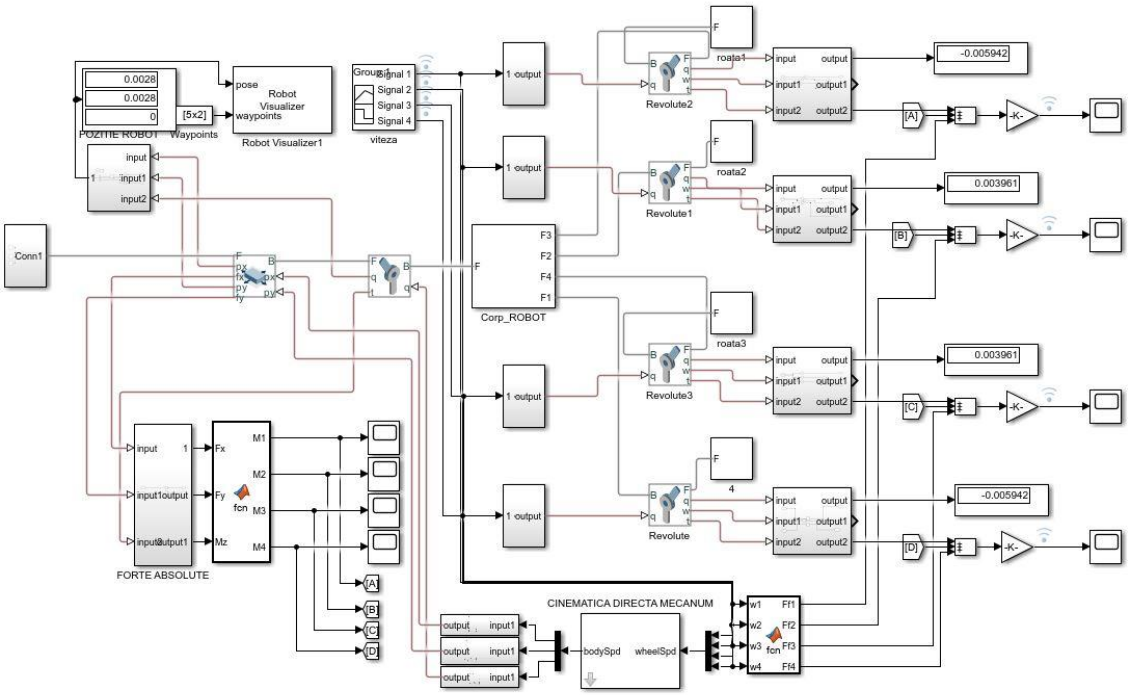

Fig. 0.31 Dynamic model of the mobile robot with omnidirectional traction and four mechanum wheels.

In **Fig. 0.32a** shows the path in the form of a square with a side of 1 m travelled by the robot during the simulation. In **Fig. 0.32b** shows when the robot completes the linear movement of 1 m and then starts to rotate around the centre of mass by 90°. In order to complete the entire trajectory, the robot must perform four linear movements and three rotations. An open-loop system was used to control the robot. A series of calibrations were performed whereby the distance travelled by the robot and the angle of rotation were physically measured. Using these calibrations, the times required to drive the robot motors for the 1 m travel and to perform a 90° rotation were determined. The programming of linear and rotational movements for the entire path was performed as a function of time using the Arduino board.

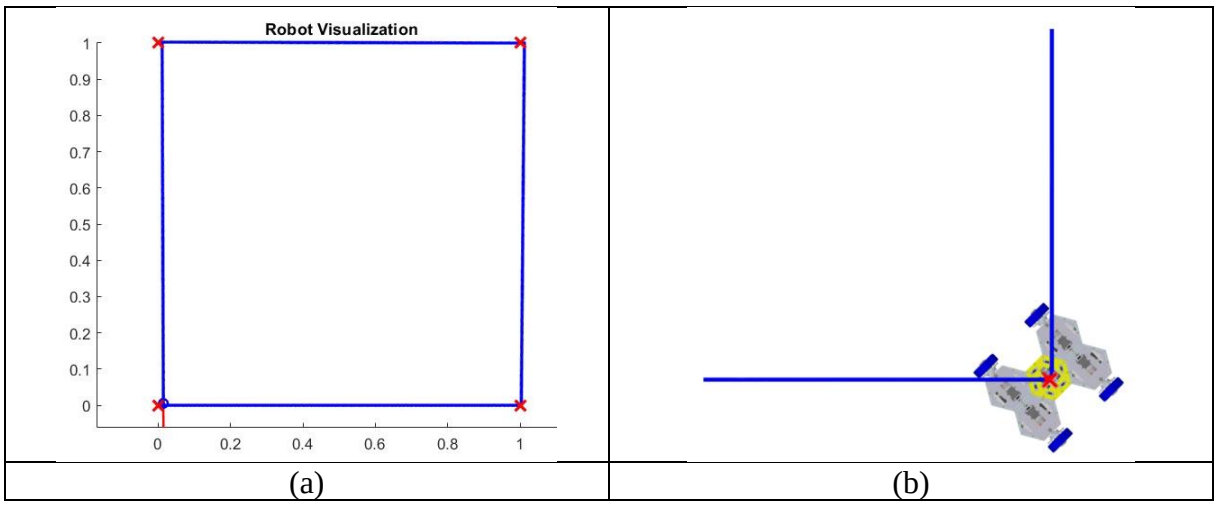

Fig. 0.32 The path taken by the robot in the simulation: (**a**) the resulting path; (**b**) the 90° turn of the robot.

6.3. RESULTS

6.3.1. Simulation of dynamic models for the five mobile robot configurations

By simulating the dynamic models in the Simulink environment, the resistive torques of the electric motors driving the wheels of the mobile robots were determined. Based on the determined resistive torques, block diagrams equivalent to the electric motor drive were created using Simulink. Using as accurate a virtual model of the DC electric motor as possible, it was possible to determine the current absorbed by the motors when the robots travel the required path.

6.3.1.1. Simulation of the dynamic model of the robot with differential drive and four conventional wheels

The variable currents absorbed by the servomotors are shown in **Fig. 0.33**. The values recorded for wheels 3 and 4 have identical variations to those of wheels 1 and 2 respectively. The four segments corresponding to the linear movements of the robot can be seen, where the current is constant, having a value of 0.15 A for all wheels. The curves have three areas for 90° rotation, where wheels 1 and 3 reverse rotation (**Fig. 0.33a**, with a maximum of -3.08 A followed by a constant part of -0.61 A), and wheels 2 and 4 accelerate (**Fig. 0.33b**, with a maximum of -2.09 A followed by a constant step of -0.60 A).

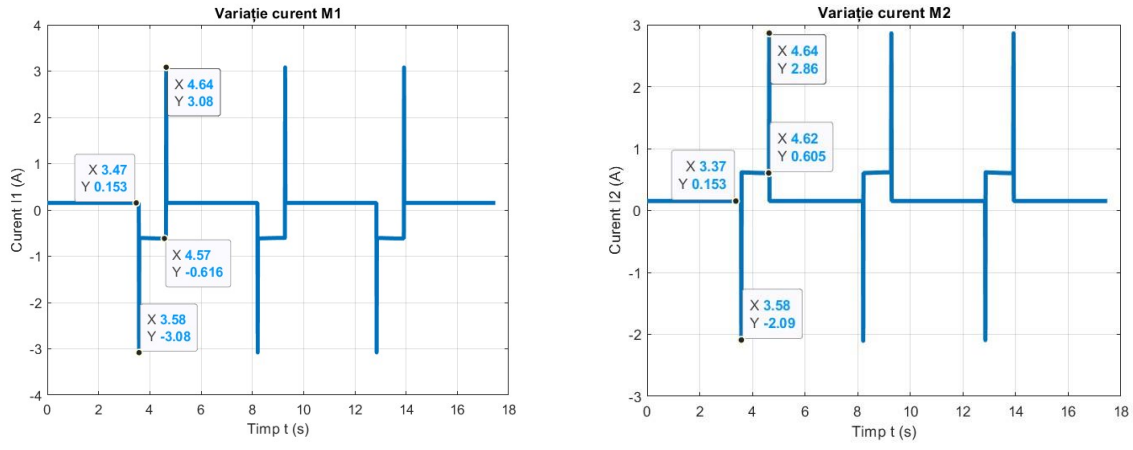

(a) (b)

Fig. 0.33 Current variation determined in the model simulation for a 1 m square path: (**a**) wheel 1 (similar to wheel 3); (**b**) wheel 2 (similar to wheel 4).

6.3.1.2. Simulation of the dynamic model of the robot with differential drive and two conventional wheels

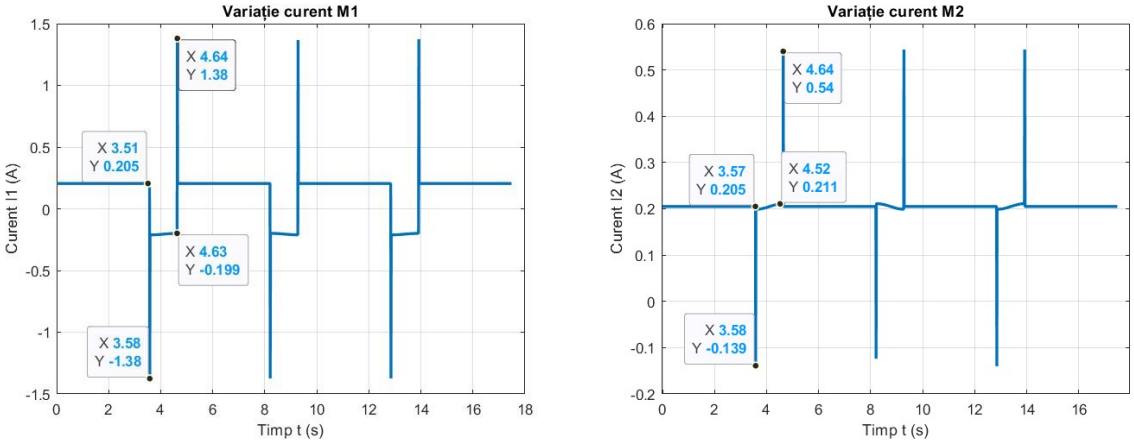

(a) (b)

Fig. 0.34 Current variation determined in the model simulation for a 1 m square trajectory: (**a**) wheel 1; (**b**) wheel 2.

The simulated current values for the wheel driven by the M1 motor are shown in **Fig. 0.34a** and the values for motor M2 are shown in **Fig. 0.34b**. One can see the four segments corresponding to the linear movements of the robot, in which the current is constant, having a value of 0.205 A for both wheels. The curves have three steps for the 90° turn, in which wheel 1 reverses its rotation having a maximum of -1.38 A, followed by a constant part of -0.19 A, and wheel 2 accelerates with a maximum of -0.13 A, followed by a constant step of 0.20 A.

6.3.1.3. Simulation of the dynamic model of the robot with omnidirectional drive and three 90° castor wheels

The variable currents absorbed by the servomotors in the simulation are shown in **Fig. 0.35**. It can be seen that when the robot starts to move in a straight line, the values recorded for gear 1 (**Fig. 0.35a**) and 3 (**Fig. 0.35b**) have identical variations, equal to 0.5 A, while wheel 2 (**Fig. 0.35c**) is stopped. After the robot has travelled 1 metre in a straight line, a sideways movement follows, at which point wheel 1 changes direction of rotation with a maximum peak current of -2.5A. Wheel 2 starts to rotate at half the speed of wheels 1 and 3, with a maximum current of -1 A, while wheel 3 will have a maximum current of -0.8 A.

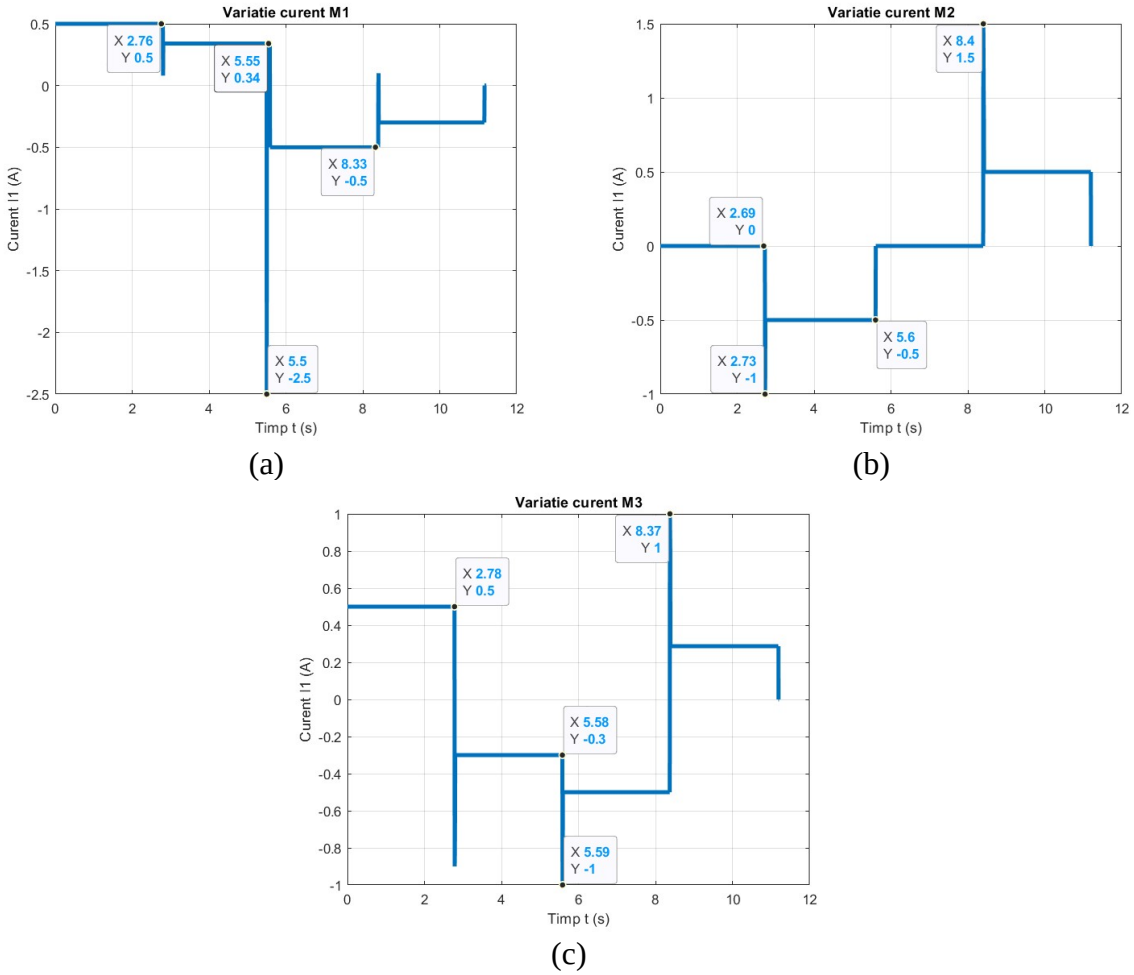

Fig. 0.35 Current variation determined in the model simulation for a 1 m square trajectory: (**a**) wheel 1; (**b**) wheel 2; (**c**) wheel 3.

6.3.1.4. Simulation of the dynamic model of the robot with omnidirectional traction and four wheels with 90° rollers.

For the 4-wheel robot with omni-directional drive, the variable currents absorbed by the servomotors are shown in **Fig. 0.36**. It can be seen that, for the first straight line motion, the values recorded by wheels 1 (**Fig. 0.36a**) and 4 (**Fig. 0.36d**) are equal to -0.45 A and 0.45 A, while wheel 2 (**Fig. 0.36b**) records a value of 0.3 A and wheel 3 (**Fig. 0.36c**) a value of -0.1A. Following the trajectory, the next displacement is a lateral one, where wheel 1 changes direction of rotation with a peak of 2.76 A, wheel 4 behaves almost similarly with a peak of -2.8 A. Wheels 2 and 3 do not change direction of rotation, having values of 0.7 A and -0.6 A respectively. Next, the robot moves backwards, and here it can be seen that large current peaks are absorbed by the motors driving wheels 2 (-1.5 A) and 3 (2.2 A), while wheels 1 and 4 have peak values of -0.5 A and -0.4 A respectively.

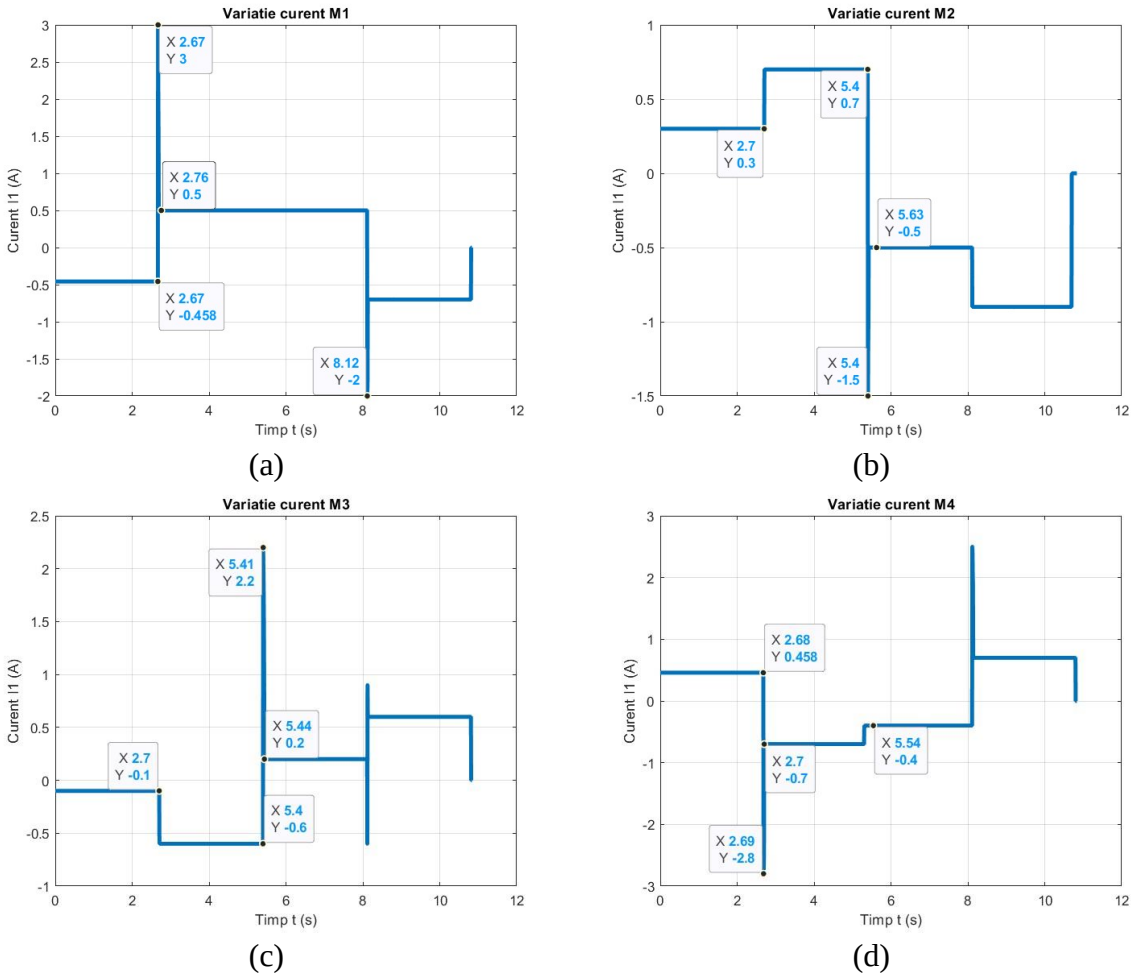

Fig. 0.36 Current variation determined in the model simulation for a 1 m square path: (**a**) wheel 1; (**b**) wheel 2; (**c**) wheel 3; (**c**) wheel 4.

6.3.1.5. Simulation of the dynamic model of the omnidirectional four-wheel drive mechanum robot

In the case of the mobile robot with differential drive and 4 mechanum wheels, the variable currents absorbed by the servomotors are shown in **Fig. 0.37**. It can be seen that for the first straight line motion, the values recorded by wheels 1 (**Fig. 0.37a**) and 4 (**Fig. 0.37d**) are equal to the values of wheels 2 (**Fig. 0.37b**) and wheel 3 (**Fig. 0.37c**) all being 0.12 A. Following the trajectory, the next displacement is a lateral one, where wheel 1 changes its direction of rotation with a peak of -2 A, wheel 4 behaves almost similarly with a peak of -1.75 A. Wheels 2 and 3 do not change their direction of rotation, both having the same value of 0.45 A. Next, the robot moves backwards, and here it can be seen that large current peaks are absorbed by the motors driving wheels 2 (-0.99 A) and 3 (-2.2 A), while wheels 1 and 4 have peak values of -0.5 A and -0.45 A respectively.

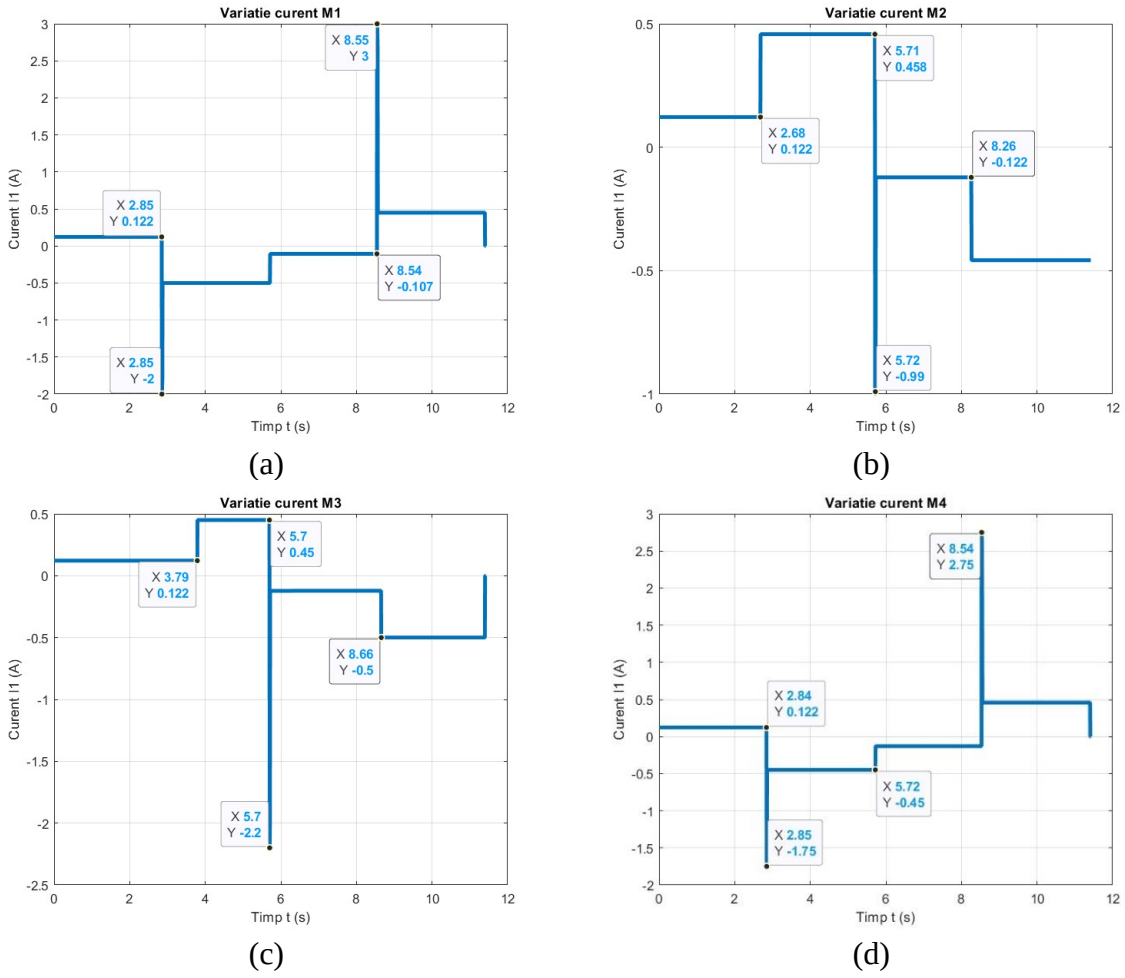

Fig. 0.37 Current variation determined in the model simulation for a 1 m square trajectory: (**a**) wheel 1 mechanum; (**b**) wheel 2 mechanum; (**c**) wheel 3 mechanum; (**c**) wheel 4 mechanum.

6.3.2. Experimental validation of simulated models

6.3.2.1. Experimental tests performed on the differential drive robot with conventional four-wheel drive

The experimental validation of the results obtained from the simulations in Matlab Simulink was performed by monitoring the current consumed by each motor driving the wheels of the real robot functional model.

The predefined physical path (one metre square) along which the robot moves is illustrated in **Fig. 0.38**. The running surface is made of a material specific to industrial environments. During the tests, the current was measured in real time using a Fluke 115 professional multimeter (**Fig. 0.39**), comparing the result with the measured current.

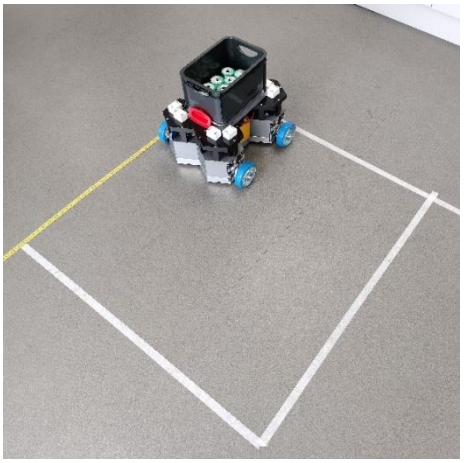

Fig. 0.38 Physical path and real mobile robot.

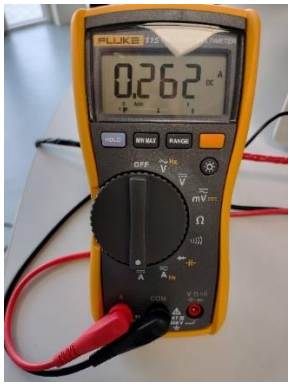

Fig. 0.39 Fluke 115 digital multimeter.

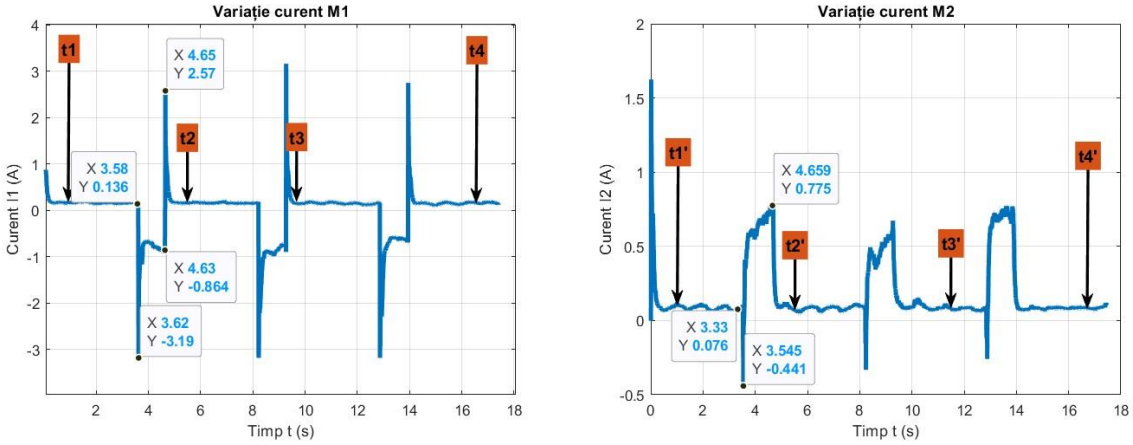

(a) (b)

Fig. 0.40 Variation of the current measured with the functional model for the redefined path: (**a**) wheel 1 (similar to wheel 3). (**b**) wheel 2 (similar to wheel 4).

Fig. 0.40 shows the variation curves of the currents detected by the sensors on the real robot moving along the path. On the four segments corresponding to the linear movements of the robot, the current has small oscillations around a constant of 0.136 A for wheels 1 and 3 (**Fig. 0.40** a) and 0.07 A for all wheels 2 and 4 (**Fig. 0.40** b). The curves have three steps for 90° rotation, where wheels 1 and 3 reverse rotation (**Fig. 0.40** a), for the first rotation there is a

maximum of -3.62 A and a peak of -0.86 A), and wheels 2 and 4 accelerate (**Fig. 0.40** b), for the first rotation there is a maximum of -0.44 A and a peak of -0.77 A).

According to the experimental results obtained by monitoring the current absorbed by the servomotors to travel the required path, a number of differences can be observed compared to the results obtained by model simulation. **Fig. 0.41** shows the difference between the variation of the simulated currents for M1 and M2 motors.

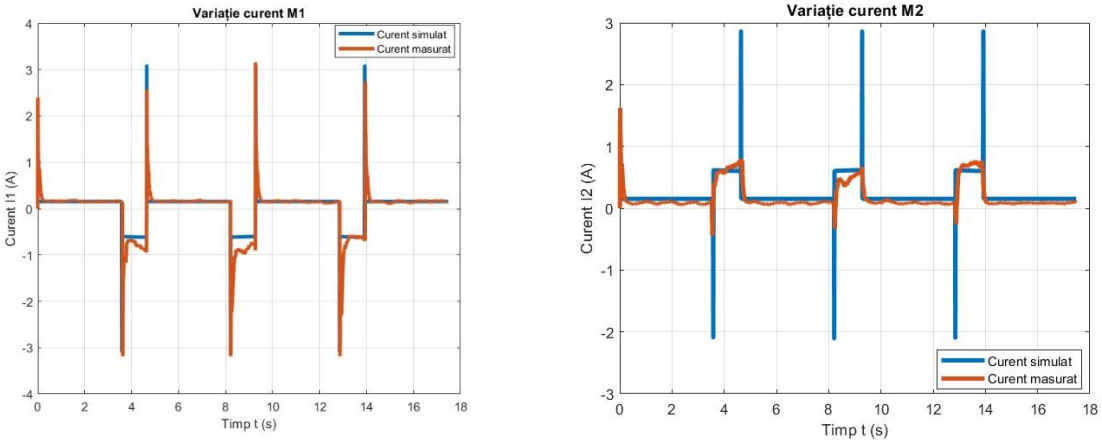

(a) (b)

Fig. 0.41 Variation of simulated and measured current: (**a**) wheel 1 (similar to wheel 3); (**b**) wheel 2 (similar to wheel 4).

In general, the measured current variation follows the shape of the simulated current curve. There are steps of constant current on the straight segments of the path for both simulated and measured currents. In the 9 0° turning regions, the current increases until it stabilizes at a constant value. The large peaks are caused by transient phenomena produced in relatively short intervals (acceleration, braking, reversal of direction of rotation).

6.3.2.2. *Experimental tests on the robot with differential drive and two conventional wheels*

The same methodology applied to the four-wheel drive mobile robot configuration was also applied to the two-wheel drive and differential drive configuration, starting from the 3D CAD model, simulation of the dynamic model of the robot and up to the tests on the physical model. The latter were easily performed and were used to validate the measurement system and the mobile robot model.

The physical path on which the robot moves is illustrated in **Fig. 0.42**. It is very important to note that the path is identical to that used in the four-wheeled configuration, the dimensions of the robot are similar, the wheels are similar, the only difference being that the mass of the two-wheeled robot is 2 kg less than that of the four-wheeled version.

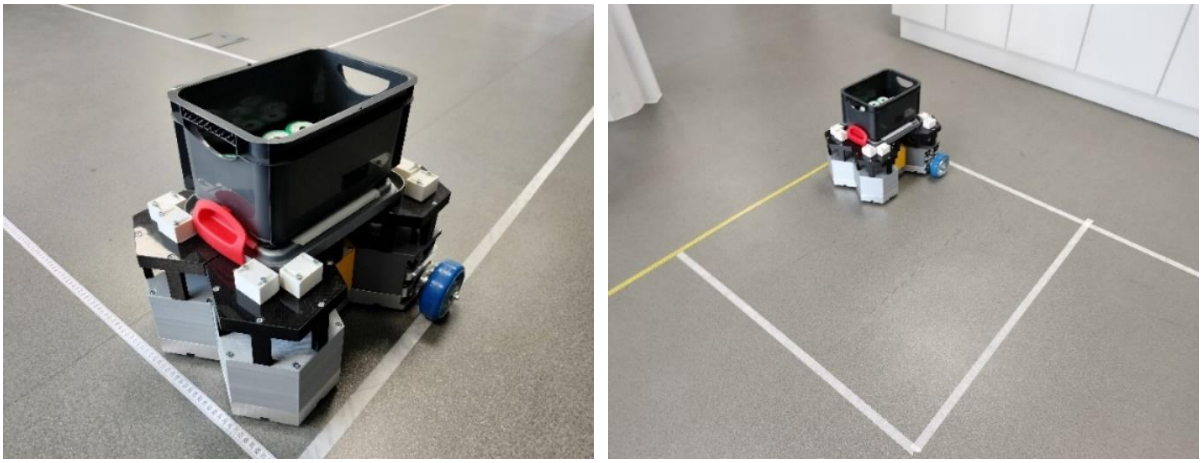

(a) (b)

Fig. 0.42 Physical trajectory and real mobile robot: (**a**) close-up view; (**b**) mobile robot on trajectory.

In **Fig. 0.43**, the current diagrams obtained from the mobile robot model simulation and experimental tests for both M1 and M2 servomotors are shown in comparison. Analysis of these plots shows a standard deviation of the simulated current from the measured one of 242.6% for the M1 motor and 24.4% for the M2 motor.

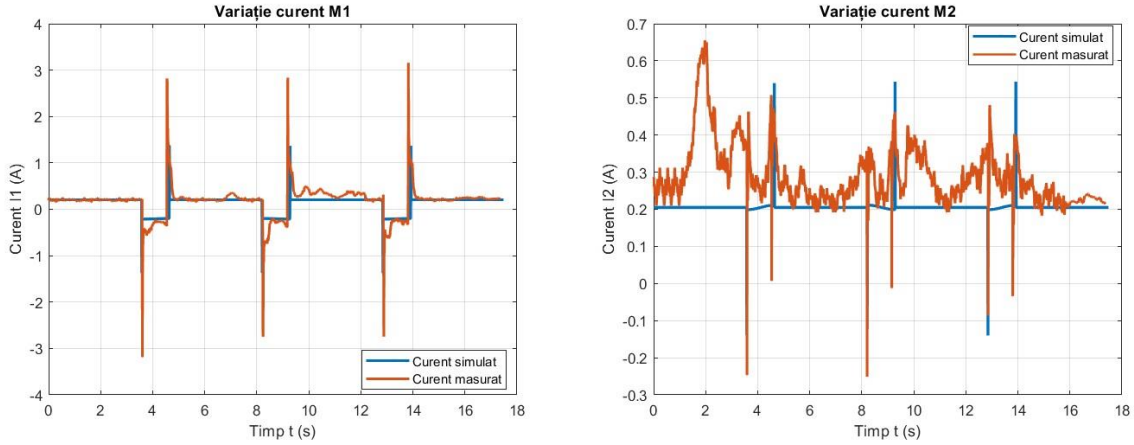

(a) (b)

Fig. 0.43 Simulated and measured current variations: (**a**) wheel 1; (**b**) wheel 2.

6.3.2.3. Experimental tests performed on the robot with omni-directional drive and three 90° roller wheels

Three drive modules and the main control module were used for the configuration of the mobile robot with three omnidirectional wheels. The same methodology was applied as for the differential drive configurations, starting from the 3D CAD model, simulation of the dynamic model of the robot and ending with tests on the physical model.

The physical path on which the robot moves is illustrated in **Fig. 0.44**. It is important to note that the path is identical to that used in conventional four- and two-wheeled configurations. The dimensions of the robot in this case change and the wheels are omnidirectional with rollers arranged at 90°, the mass of the robot is also different from the differential drive configurations, the mass carried is identical.

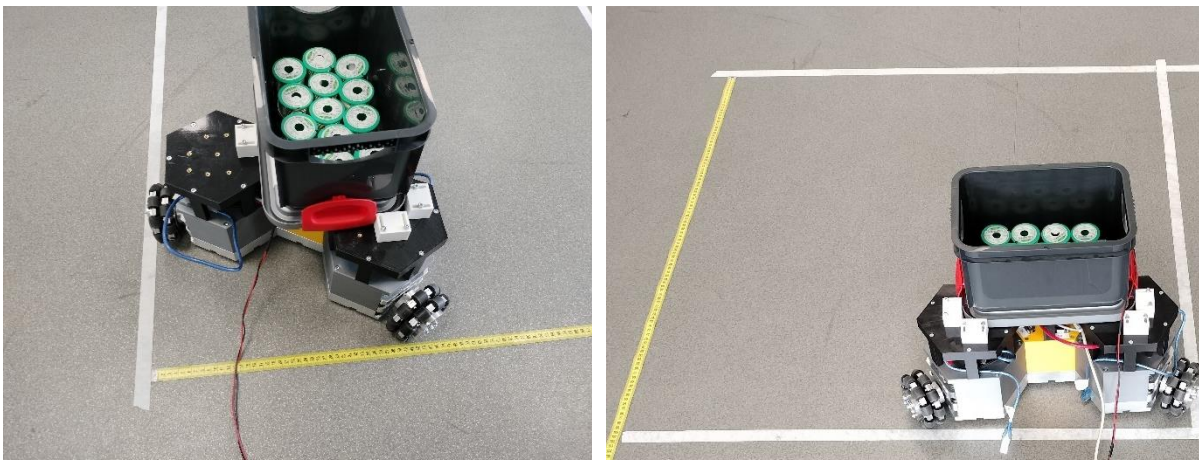

(a) (b)

Fig. 0.44 Physical trajectory and real mobile robot with three omnidirectional wheels: (**a**) close-up view; (**b**) mobile robot on trajectory.

In **Fig. 0.45** the current diagrams obtained from the simulation of the mobile robot model and validated with experimental tests for the M1, M2 and M3 servomotors, respectively, are shown in comparison.

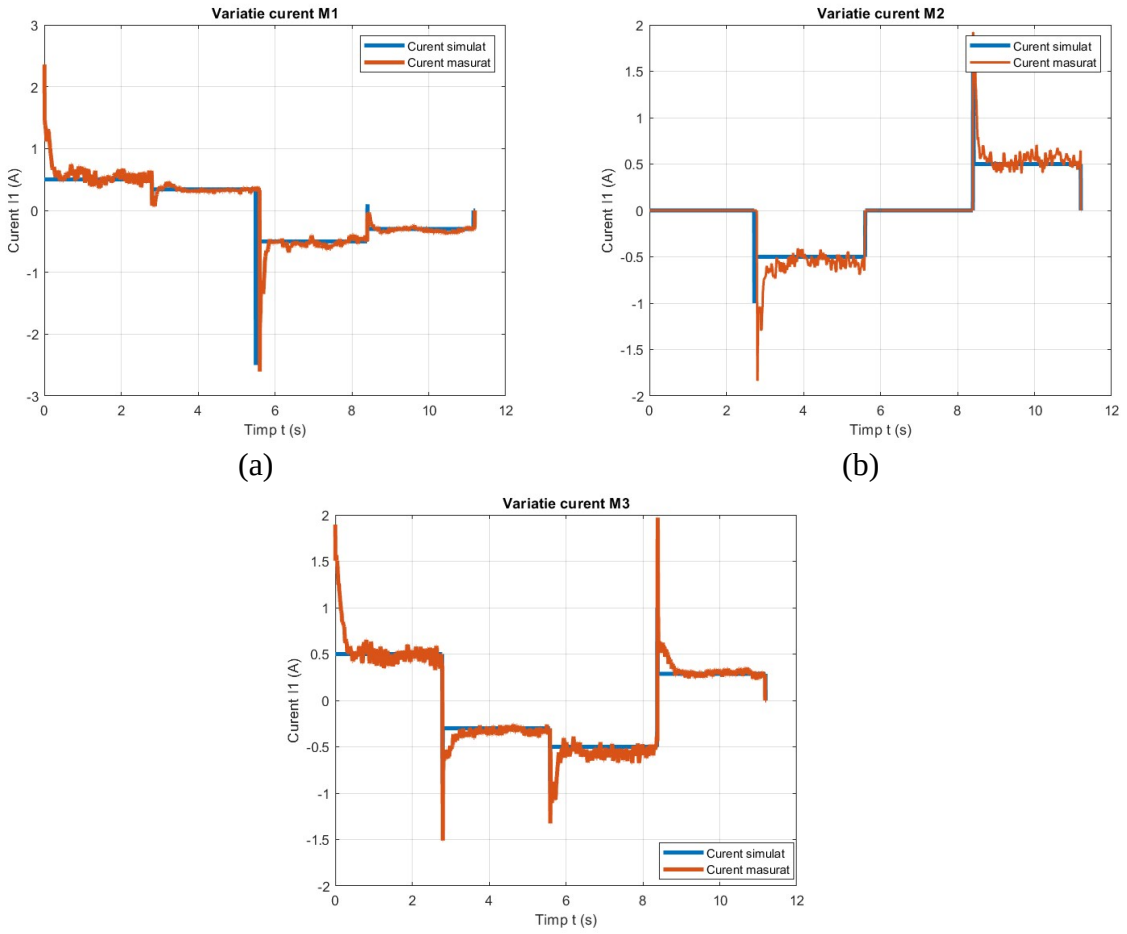

(a) (b)

(c)

Fig. 0.45 Simulated and measured current variation for the three-wheel omnidirectional configuration; (**a**) wheel 1; (**b**) wheel 2; (**b**) wheel 3.

Analysis of these graphs shows a standard deviation of the simulated current from the measured current of 14.28% for the M1 motor, 18.6% for the M2 motor and 16% for the M3 motor.

6.3.2.4. Experimental tests performed on the robot with omnidirectional traction and four 90° roller wheels

Four drive modules and one main control module were used for the configuration of the mobile robot with four omnidirectional wheels. The same methodology was applied as for the three-wheel omnidirectional configuration, i.e. 3D CAD modeling, simulation of the dynamic model of the robot and tests on the physical model. The physical path on which the robot moves is illustrated in **Fig. 0.46**with the caveat that the path is identical to the one used for the previous configurations. The dimensions of the robot in this case change and the wheels are omnidirectional with rollers arranged at 90°, the mass of the robot is also different from the configurations with differential traction, but the mass carried is identical.

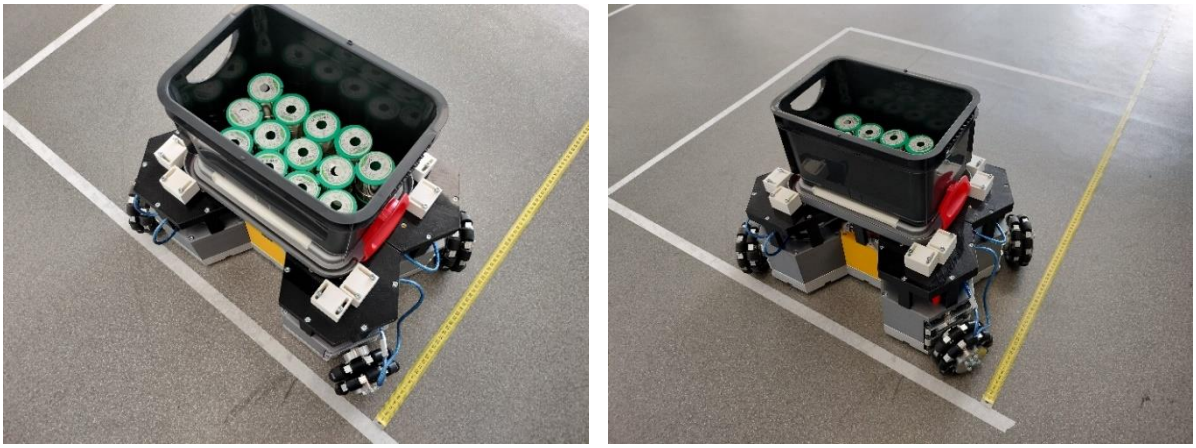

(a) (b)

Fig. 0.46 Physical trajectory and real mobile robot with four omnidirectional wheels: (**a**) close-up view; (**b**) mobile robot on trajectory.

In **Fig. 0.47** the current diagrams obtained from the simulation of the mobile robot model and validated with experimental tests for the M1, M2, M3 and M4 servomotors, respectively, are shown in comparison.

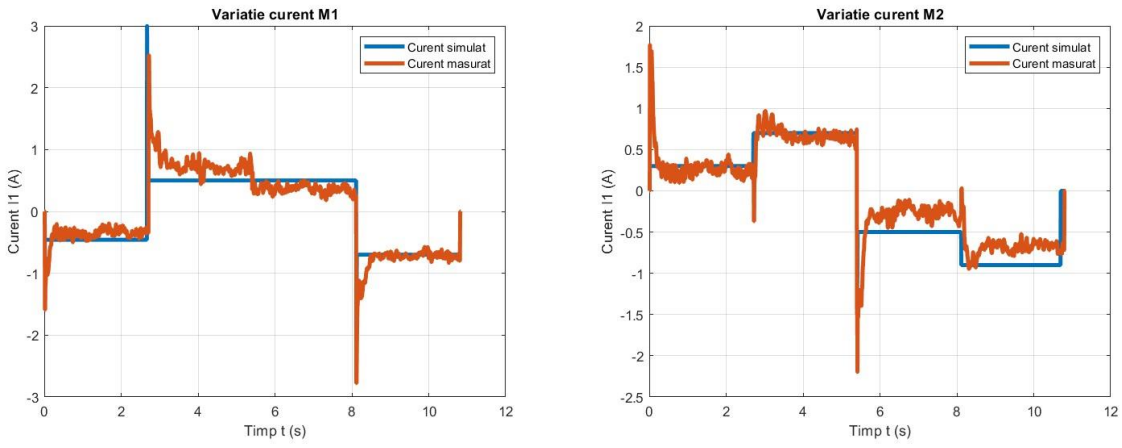

(a) (b)

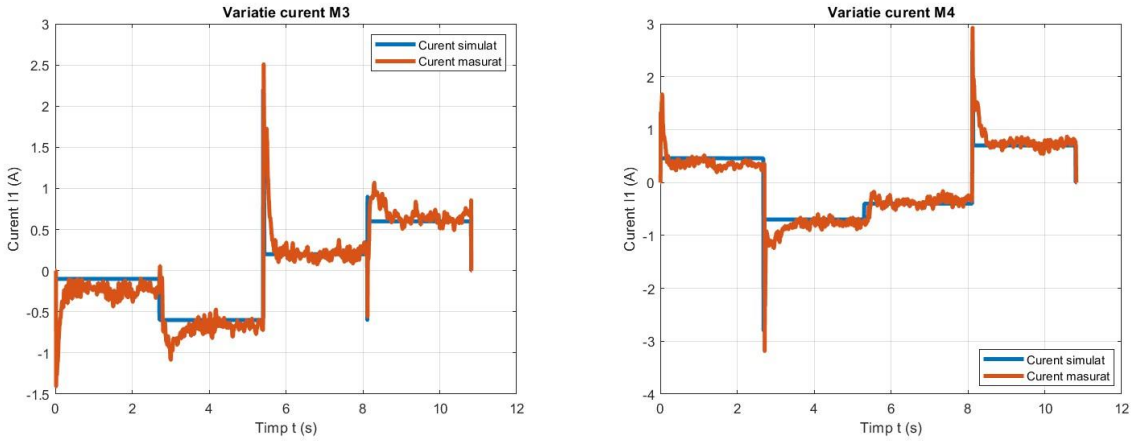

(c) (d)

Fig. 0.47 Simulated and measured current variation for the four-wheel omnidirectional configuration: (**a**) wheel 1; (**b**) wheel 2; (**b**) wheel 3; (**c**) wheel 4.

Analysis of these graphs shows a standard deviation of the simulated current from the measured current of 28.18% for the M1 motor, 9.67% for the M2 motor, 25% for the M3 motor and 11.86% for the M4 motor.

6.3.2.5. Experimental tests performed on the omnidirectional four-wheel mechanum robot

In the case of the four-wheel omnidirectional mobile robot of the mecanum type, four drive modules and one main control module were used. The same methodology was applied as for the four-wheel omnidirectional configuration, i.e. 3D CAD modelling, simulation of the dynamic model of the robot and tests on the physical model.

The physical path on which the robot moves is illustrated in **Fig. 0.48**, with the caveat that the path is identical to that used for the previous configurations. The dimensions of the robot in this case change, and the wheels are omnidirectional with rollers arranged at 45° of the mecanum type, the mass of the robot is also different from the configurations with differential traction, the mass transported is identical, it was also taken into account in the construction of the robot that the mass of each type of wheel has almost the same value.

(a) (b)

Fig. 0.48 Physical trajectory and real mobile robot with four mechanum wheels: (**a**) close-up view; (**b**) mobile robot on trajectory.

In **Fig. 0.49** the current diagrams obtained from the simulation of the mobile robot model and validated with experimental tests for the M1, M2, M3 and M4 servomotors, respectively, are shown in comparison.

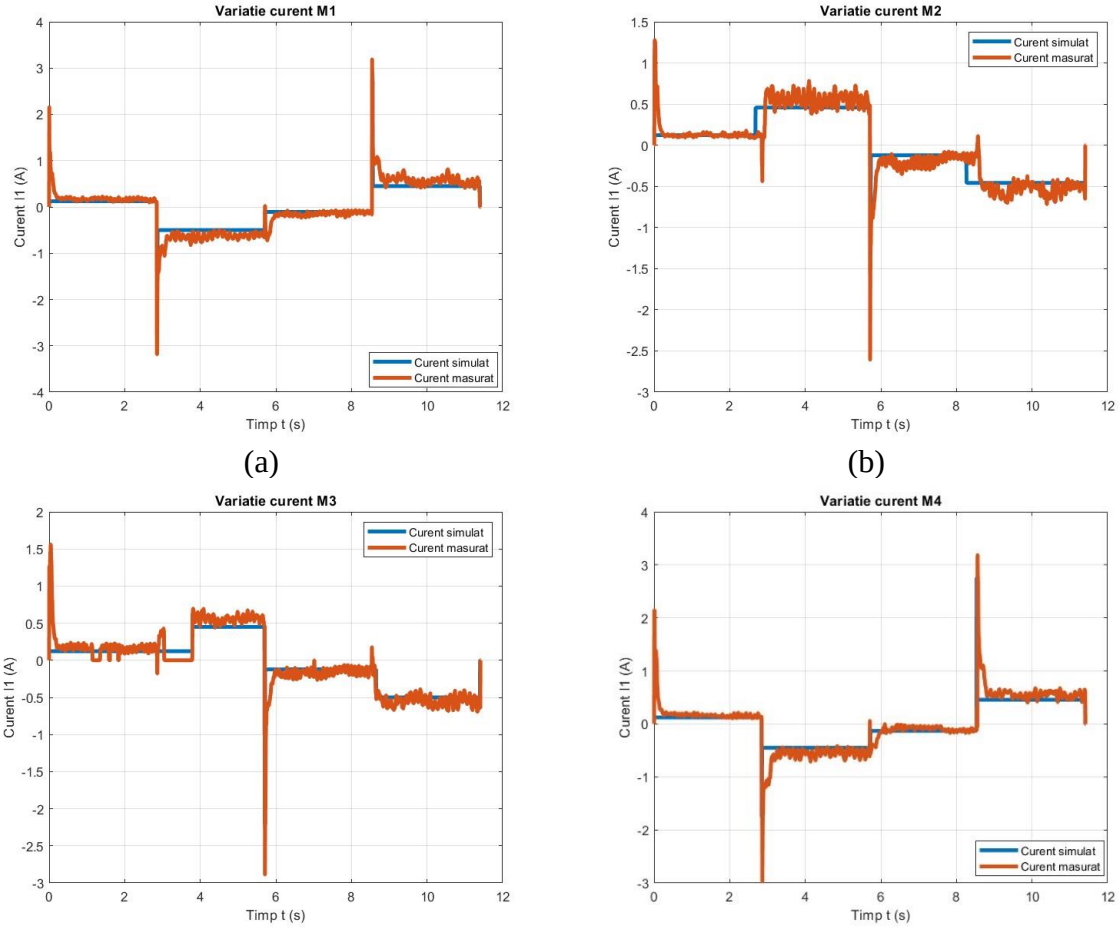

Fig. 0.49 Simulated and measured current variation for the four-wheel omnidirectional configuration: (**a**) wheel 1; (**b**) wheel 2; (**b**) wheel 3; (**c**) wheel 4.

Analysis of these graphs shows a standard deviation of the simulated current from the measured current of 35.13% for the M1 motor, 23.5% for the M2 motor, 28.12% for the M3 motor and 40% for the M4 motor.

6.3.3. Calculation of energy consumed

There are different approaches to DC energy modelling [93, 159], such as:

- the engineering method (power integration), which applies to regenerative controllers;
- energy cost method (absolute power integration);
- positive power integration method applied to non-regenerative controllers.

For the first method, the electrical energy consumed E_e is obtained by integrating the electric motor power P_{me} as a function of time:

$$E_e = \int P_{me}(t)dt. \tag{0.15}$$

In the second method, the assumption is used that the cost of the absorbed energy is proportional to the power of the source. Thus, in the equation (0.16) the power modulus of the source is used:

$$E_e = \int |P_{me}(t)|dt. \tag{0.16}$$

The third method is rarely used. Based on the relationship between energy *E*, power *P* and time *t* in direct current, *E = U-t*, for the present research and based on the equation (0.17) , the relation of energy consumed is obtained:

$$E_e = \int |UI(t)|dt. \tag{0.17}$$

The sampling time used in the Hall sensor current measurement is a characteristic of the sensor and has the value t_s = 0.005 s. The total number of measurements is *n*. In the time $t_{tot} = nt_s$ of the absorbed current measurement, when the mobile robot moves along the trajectory, the total absorbed energy is calculated using the defined integral:

$$E_e = U \int_0^{t_{tot}} |I(t)|dt. \tag{0.18}$$

If we are interested in the power consumed on, then the relationship becomes:

$$P_e = \frac{U}{t_{tot}} \int_0^{t_{tot}} |I(t)|dt. \tag{0.19}$$

Basically, the value of the defined integral is the area *A* represented schematically in **Fig. 0.50**.

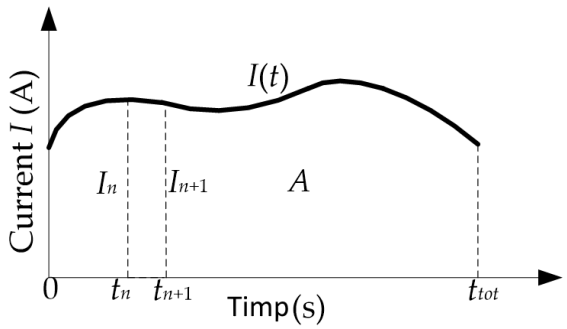

Fig. 0.50 Calculation of the definite integral.

The calculation can be done by approximation using the trapezoidal method as the sum of the areas of the component trapezoids:

$$A = \frac{1}{2} t_s \sum_{i=1}^{n} |(I_i + I_{i+1})| = t_s \sum_{i=1}^{n} |(I_i)|. \tag{0.20}$$

If the sampling time (infinitesimal step width) is taken as the ratio $t_s = t_{tot}/n$, then the power over the entire measurement range is:

$$P_e = \frac{U}{t_{tot}} \frac{t_{tot}}{n} \sum_{i=1}^{n} |(I_i)| = \frac{U}{n} \sum_{i=1}^{n} |(I_i)|, \tag{0.21}$$

which is approximated as the product of the constant voltage and the average measured current.

Methods that are more accurate involve approximating the current by a spline or polynomial curve and increasing the number of component areas by reducing the infinitesimal

step width. The Matlab program offers specialized functions for more precise calculation of the definite integral - TRAPZ, CUMTRAPZ.

6.3.3.1. Energy consumption results for the conventional two-wheeled differential drive robot

The power consumed by the mobile robot when moving along the predefined path is determined as the sum of the powers consumed by all the motors driving the robot. The procedure was applied to both the simulated and measured data sets for each actuator, and for each of the 5 mobile robot configurations. **Fig. 0.51** shows the simulated power consumption, and **Fig. 0.52** measured for the four-wheel differential drive robot.

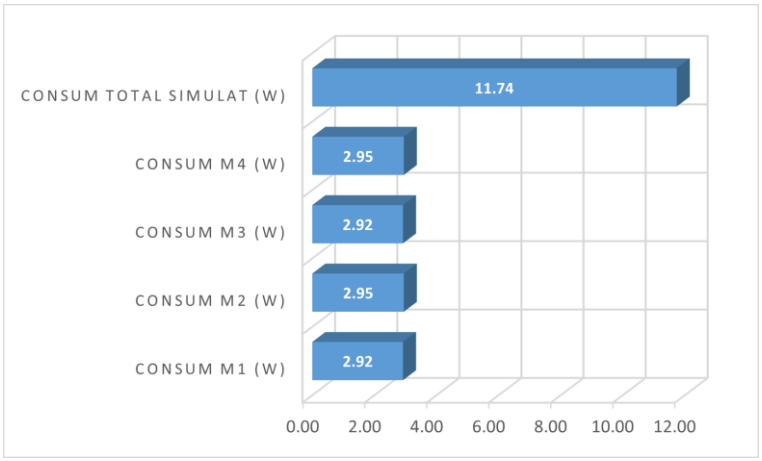

Fig. 0.51 Simulated energy consumption for the conventional four-wheeled robot.

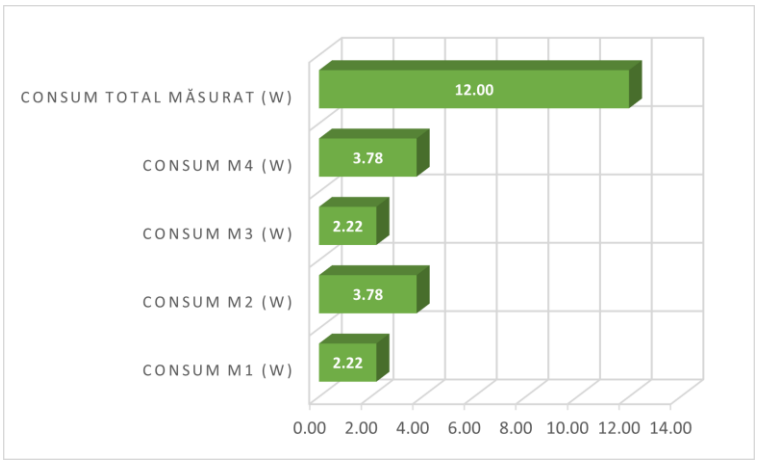

Fig. 0.52 Measured energy consumption of the conventional four-wheeled robot.

The relative error in total power consumption determined from the simulation was found to be 2.2%.

6.3.3.2. Energy consumption results for conventional four-wheel drive differential drive robot

For the conventional two-wheel drive and differential drive configuration, energy consumption is shown in **Fig. 0.53** and **Fig. 0.54** for simulated and measured power respectively. The simulated power for this configuration is estimated with an error of 29.5%.

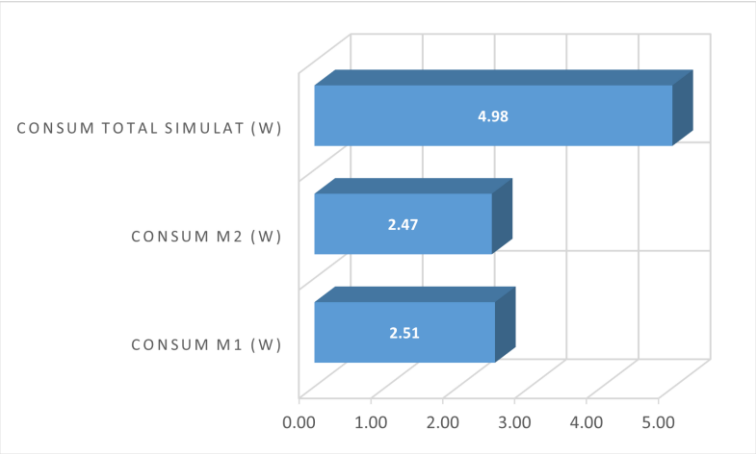

Fig. 0.53 Simulated energy consumption for the conventional two-wheeled robot.

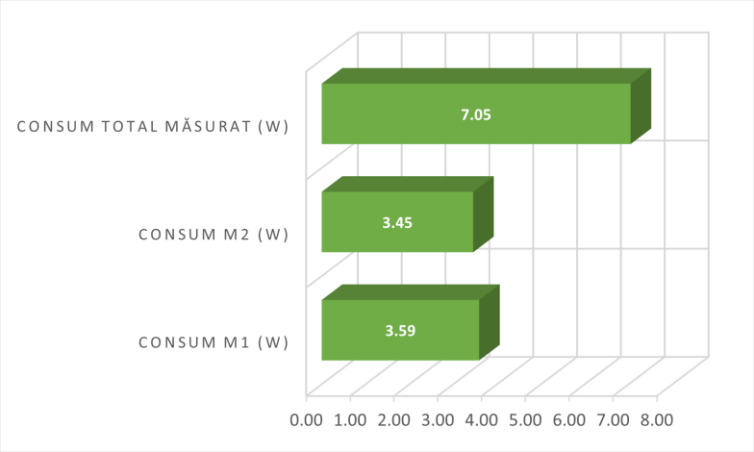

Fig. 0.54 Measured energy consumption of the conventional two-wheeled robot.

6.3.3.3. Energy consumption results for the robot with omnidirectional drive and three 90° roller wheels

In the case of the three-wheel omnidirectional configuration with rollers arranged at 90°, energy consumption is shown in **Fig. 0.55** and **Fig. 0.56** for simulated and measured power, respectively. The simulated power for this configuration is estimated with an error of 11.85%.

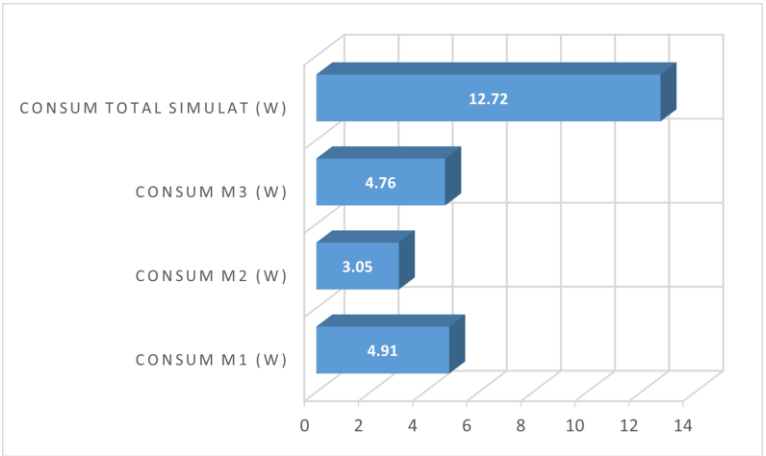

Fig. 0.55 Simulated energy consumption for the three-wheeled omnidirectional robot.

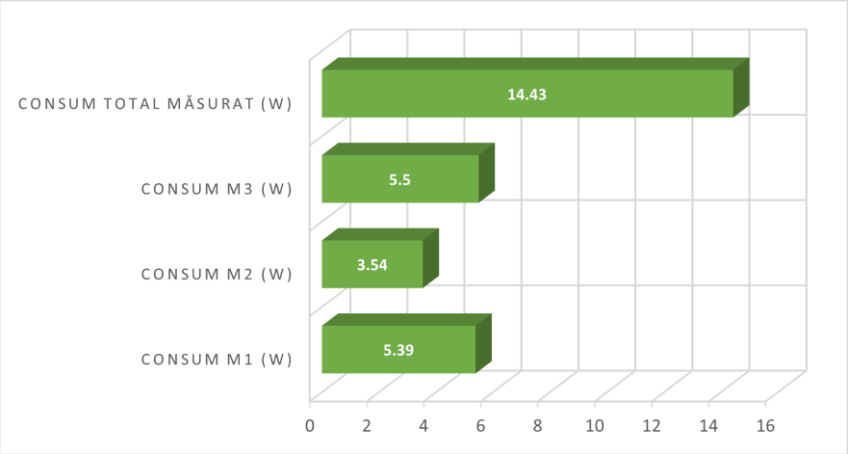

Fig. 0.56 Measured energy consumption of the three-wheeled omnidirectional robot.

6.3.3.4. Energy consumption results for the robot with omnidirectional drive and four 90° castor wheels

In the case of the four-wheel omnidirectional configuration with rollers arranged at 90°, energy consumption is shown in **Fig. 0.57** and **Fig. 0.58** for simulated and measured power respectively. The simulated power for this configuration is estimated with an error of 2.58%.

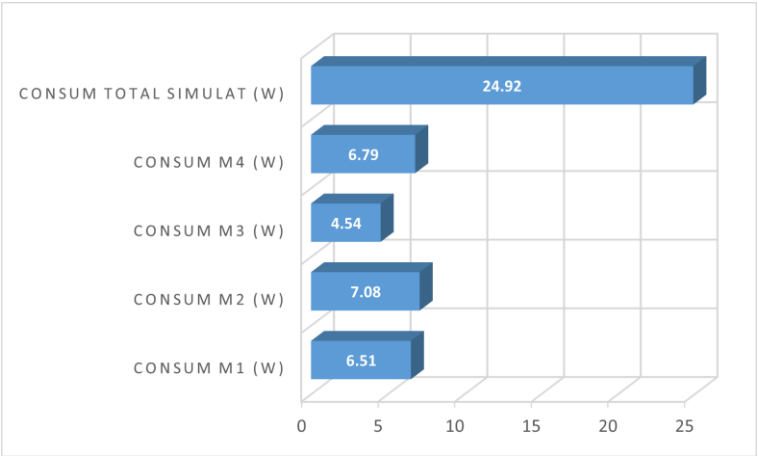

Fig. 0.57 Simulated energy consumption for the four-wheeled omnidirectional robot.

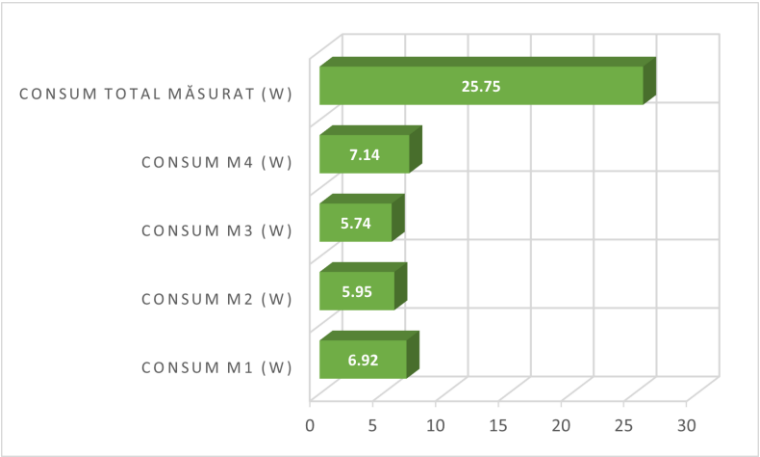

Fig. 0.58 Measured energy consumption of the four-wheel omnidirectional robot.

6.3.3.5. Energy consumption results for the omnidirectional four-wheel mechanum robot

For the four-wheel omnidirectional mecanum configuration, energy consumption is shown in **Fig. 0.59** and **Fig. 0.60** for simulated and measured power respectively. The simulated power for this configuration is estimated with an error of 20.87%.

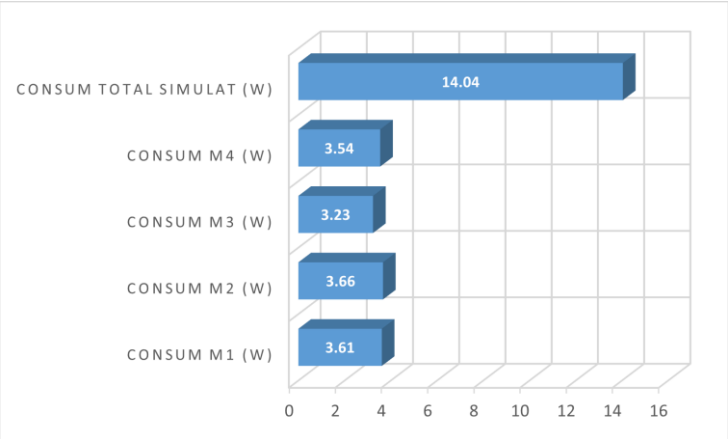

Fig. 0.59 Simulated energy consumption for the four-wheeled omnidirectional mecanum robot.

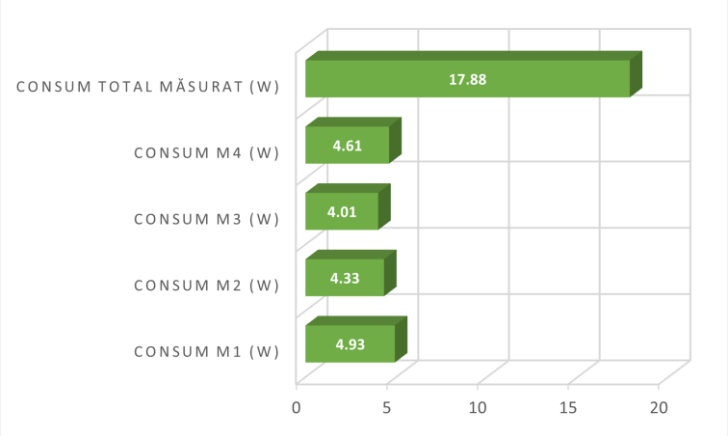

Fig. 0.60 Measured energy consumption of the four-wheeled omnidirectional mecanum robot.

6.4. DISCUSSIONS

For a better interpretation of the results, the following was done **Table 0.4** showing a shorter notation for the names of the five modular mobile robot configurations. This is useful for the graphical presentation of the results as well as their textual description.

Table 0.4 Modular mobile robot configuration notations

Configuration name	Notation
Mobile robot with differential drive and two conventional wheels	Mobile robot config.1
Mobile robot with differential drive and four conventional wheels	Mobile robot config.2
Mobile robot with omnidirectional drive and three omnidirectional wheels	Mobile robot config.3
Mobile robot with omni-directional drive and four omni-directional wheels	Mobile robot config.4
Mobile robot with omnidirectional drive and four mechanum wheels	Mobile robot config.5

It is important to note that the methodology for creating dynamic models in Matlab Simulink for all 5 configurations presented is almost identical, using the same constants and input data.

Comparison of the results obtained when measuring the current absorbed by the electric motors in the four-wheel configuration using the Hall sensor and the multimeter shows close values for the measurements taken at the same time. The errors for the M1 motor range from 0.38% to 2.48%, with an average of 1.88%, and for M2 from 4.58% to 13.75%, with an average of 9.56%. Thus, the physical current measurement system is validated.

From the analysis of the variation between simulated and measured current for the five configurations of the modular mobile platform, the following conclusions can be drawn:

For the four-wheel configuration, the simulated mean errors compared to the measured ones for M1 and M3 are less than 1%, and for M2 and M4, 41.6%. The maximum and minimum values show larger differences. In general, there are larger differences between simulated and measured currents for M2 and M4 engines.

For the two-wheel configuration, a similar behaviour is observed as for the four-wheel configuration, the average error is 1.4% for the M1 engine and 24.6% for the M2 engine. In the case of this version, there are larger differences between the simulated and measured currents for the M2 engine.

In the case of the configuration with 3 omnidirectional wheels and rollers arranged at 90°, the average error values between simulated and measured current for the M1 motor are 5.4%, 6% for M2 and 11.13% for M3. For this configuration with omni-directional traction the largest error between simulated and measured current is for the M3 motor. The errors between simulated and measured currents for the configuration with 4 omnidirectional wheels and rollers arranged at 90° are: The error with the value of 13.9% is the highest and is that of the M4 motor. For the M3 motor the error value is 4.71%, for M2 11.17% and for M1 2.97%. The differences between the simulated and measured values of the current absorbed by the four servomotors for the configuration with omnidirectional drive and four mecanum wheels, are : The error with the value of 12.6% is the highest and is that of the M2 motor. For the M1 motor the error value is 9.51%, for M3 0.19% and for M4 4.59%.

If we compare the simulated current curves for all five configurations of the mobile platform, some observations can be made.

It was found that there are very small differences in the areas of linear motion for all configurations. In general, the differences definitely come from the approximation of the wheel-ground friction coefficient in the model, especially for omnidirectional configurations being quite difficult to determine. Larger differences exist only in turning areas, where the measured current shows variations (large peak followed by oscillations) . By comparison, during turns, the simulated current curve consists of a peak and a constant area. These large variations are instantaneous current spikes lasting several milliseconds. The total energy consumption of the robot to travel the trajectory will not be significantly influenced by these spikes which have an extremely short duration. They usually occur when the direction of rotation of the drive motor changes, or when the robot accelerates or decelerates suddenly.

Differences between simulated and measured currents may have the following possible causes:

- Approximation of moments of inertia on the Simulink model. Can be related to the moment of inertia value or the position of the centre of mass of the robot model.

- Approximation of the coefficient of friction between the robot wheel and the running surface.
- Variations of the simulated current in the transient acceleration or braking phases may be caused by the modeling of friction phenomena when changing the robot's direction of motion or by speed variations in the case of wheel slip on the ground.
- Larger variations (spikes) for the simulated current could be produced by block settings in the Simulink model.
- Possible differences between physical and simulated trajectories can be attributed to the lack of position control in the functional model.

6.5. CONCLUSIONS

Analysis of the obtained results shows that the largest difference between simulated and measured currents is about 24.6% for the configuration with differential drive and two conventional wheels. The smallest difference is recorded for the four-wheel mecanum configuration, with a value of 0.19%. It was found that there are very small differences in the areas of linear motion for all configurations. In general, the differences clearly come from the approximation of the wheel-ground friction coefficient in the dynamic model, which is quite difficult to determine for omnidirectional configurations. Larger differences exist only in the turning areas, where the measured current shows variations (large peak followed by oscillations). Thus, the dynamic model is experimentally validated, with the possibility of calculating the energy consumed for the imposed trajectory which is similar to that used in the preliminary research.

The proposed dynamic model is an accurate tool that provides information for determining the most energy efficient configuration among the 5 configurations presented to travel a required trajectory.

CHAPTER. 7. GENERAL CONCLUSIONS, ORIGINAL CONTRIBUTIONS AND RESEARCH DIRECTIONS FUTURE

7.1. GENERAL CONCLUSIONS

The PhD thesis entitled "Increasing the performance of mobile robots and autonomously guided vehicles serving the industrial environment" aims to increase the performance of mobile robots and autonomously guided vehicles serving the industrial environment. The analysis of the state-of-the-art in the field has identified the main characteristics and performance parameters of mobile robots. The thesis aimed to address an important feature, namely modularity. The feature of modularity has enabled the realization of several mobile robot structures with low cost. This has enabled research aimed at reducing the energy consumption of mobile robots. In order to achieve these objectives, theoretical and experimental research has been carried out, from which the following conclusions can be drawn:

- Mobile robots and autonomously guided vehicles are constantly evolving and there are a large number of recent publications in this field. The most significant publications from 2019-2023 have been presented in the current research status in tabular form.
- Following kinematic and dynamic modelling of the locomotion system of the modular mobile platform, kinematic and dynamic models were determined for a series of five mobile robot configurations.
- Based on the results obtained from the calculations for the choice of the electric drive motor for the modular platform, a high performance servo motor was chosen that can be used in several configurations of robotic structures.
- The 3D modelling of the modular platform was carried out using Solidworks software, producing two concepts. The first concept was developed after some analysis in terms of physical realization, thus concept number 2 was developed.
- The second CAD model concept presents a series of 4 modules, which have the possibility to form a series of robotic configurations.
- The Arduino Mega development board integrated into the mobile robot's drive wheel modules is based on an Atmega328 microcontroller and an integrated analog-to-digital converter (ADC) with 10-bit resolution. Preliminary experimental investigations have shown that this development board has a number of hardware limitations. Attempts were made to circumvent these with software algorithms. The results were not effective, so an external ADNS 1115 module with 16-bit resolution was integrated to replace the internal ADC of the development board.

- Based on the experimental results, the proposed real-time current measurement method was validated, which is necessary for several stages of the research and also for the use of the robot and for future research.
- Following preliminary research on a mobile robot with omnidirectional traction and four mechanum wheels, the main objective was to develop efficient dynamic digital block models to study the behaviour of autonomous mobile robotic platforms when moving on the imposed trajectory.
- Validation of the proposed models was performed by comparing the simulation results with the experimental ones. For this comparison, the currents absorbed by the motors driving the robot wheels were chosen, mainly because of the ease with which they can be measured experimentally.
- The comparison between experimental and simulated values demonstrated the accuracy of the simulation plots obtained.
- Using the proposed simulation schemes, the behaviour of the mobile robot when moving on square trajectories was studied. The simulations showed that the advantages of mecanum wheels come together with the disadvantage of high values of the currents absorbed by the wheel drive motors, in the variant of using the drive solution based on DC motors driven by PWM voltage pulses.
- From preliminary research, it can be seen that the dynamic model of the omnidirectional mobile robot with mechanum wheels developed in Matlab Simulink and experimentally validated can estimate the energy consumption of the robot as a function of the trajectory travelled. Thus, further research for other types of mobile robots and to determine the influence of the robotic structure and locomotion system on the energy consumption of the robot was pursued.
- The Simulink-Simscape-Multibody environment was used to create the dynamic model of the robot. The model allows to determine the values of the resistive torques at the kinematic torque level of the mobile robot when it travels along a predefined trajectory.
- Knowing the torque evolution at the motor axis, it is possible to determine the electric current absorbed by each servomotor in the robot structure when travelling the required path. Thus, based on the current determined as accurately as possible, specific optimisation algorithms can be used for different ways of travelling a trajectory, so that power consumption is minimised.
- By simulating the dynamic models in the Simulink environment, the resistive torques of the electric motors driving the wheels of the mobile robots were determined. Based on the determined resistive torques, block diagrams equivalent to the electric motor drive were created using Simulink.
- The experimental validation of the results obtained from the simulations in Matlab Simulink was performed by monitoring the current consumed by each motor driving the wheels of the real robot functional model. This was achieved by integrating the ACS712-05 sensor and the ADNS 1115 module into the drive system. The data obtained after acquisition was interpreted and analysed.
- After analysing the results obtained, it can be seen that the largest difference between the simulated and measured currents is about 24.6% for the configuration with

differential drive and two conventional wheels. The smallest difference being for the configuration with four mechanum wheels having a value of 0.19%.

- These analyses show that modularity offers high flexibility and also contributes to reducing energy consumption by up to 70% depending on the configuration chosen for the required trajectory. The proposed dynamic model can be a tool that through simulations and comparison leads to the most energy efficient solution among the 5 configurations presented for the required trajectory.

The PhD thesis solves all the objectives initially formulated, through original approaches both at the conceptual and modelling level, and at the practical level, through the realisation of functional physical models, achieving a good correlation between modelling and simulation and experimental tests. The results obtained are specific to the robotic systems studied, but are also of a general nature, creating the premises for some developments in the field through future research.

7.2. ORIGINAL CONTRIBUTIONS

Current status study

- The evolution of autonomous mobile robots has been briefly presented in chronological order through the most important publications between 1991-2022.
- Literature review from 2018-2023, presenting issues related to: mobile robot navigation, differential locomotion, omnidirectional locomotion, general characteristics of autonomous mobile robots.
- Review of literature from 2018-2023 presenting methods for monitoring the energy consumption of mobile robots using Hall current sensors.
- Review of the literature from 2018-2023, presenting issues related to modular and reconfigurable mobile robots.
- Literature review from 2018-2023, presenting dynamic modeling and control of mobile robots using Matlab Simulink.
- Review of the literature from 2018-2023, presenting issues related to modelling and estimating energy consumption of mobile robots.

Preliminary research

- Determination of the mobile platform drive solution using AHP-based multi-criteria decision making method.
- Kinematic modelling of a mobile platform using blocks that allow the implementation of four-wheel mechanum kinematics and differential kinematics.
- Dynamic model building in Matlab Simulink, using Simscape-specific blocks as well as user-created blocks.
- Validation of the proposed models by comparing the simulation results with the experimental ones.
- Comparison between simulated and experimental values of the currents absorbed by electric motors.

The original concept of a modular mobile platform with applications for a range of 5 configurations used in research:

- Concept and design of hexagonal modules for control, drive, locomotion and power supply.

- Making modules by additive manufacturing or machining.
- Selection and verification of electric motors for the drive module
- Integration of Hall current sensors and Arduino acquisition boards.
- Assembly and functional verification for 5 mobile robot configurations.
- Mobile robot with differential drive and two conventional wheels.
- Mobile robot with differential drive and four conventional wheels.
- Mobile robot with omni-directional drive and three omni-directional wheels.
- Mobile robot with omni-directional drive and four omni-directional wheels.
- Mobile robot with omnidirectional drive and four mecanum wheels.
- Thanks to modularity, low-cost mobile robot structures can be created by reusing modules from other configurations.

Dynamic modeling using Matlab Simulink to determine the energy consumption of a modular mobile platform with a series of 5 modular mobile robot configurations:

- Dynamic modeling in Matlab Simulink for each configuration.
- Use of dynamic model to determine resistive torques in kinematic joints when moving along a square path with a side of 1 m.
- During the trajectory movement, the simulated values of the currents absorbed by each motor are recorded.

Experimental tests on the physical functional model to validate Simulink models:

- Development of an electrical system to drive the robot wheels and monitor the current drawn at low cost.
- Using an experimental method to monitor the current supplied by a Hall sensor integrated in the drive module of the robotic setup. The system is based on an ACS712-05Hall bidirectional Hall current sensor and data acquisition from the sensor using an Arduino Mega 2560 board.
- In order to monitor and interpret the data in real time, a digital Simulink model of the current supplied by the sensor was created, which was adjusted and improved after experimental validation using a state-of-the-art digital multimeter.

Comparison of simulated and experimental results obtained for the 5 configurations:

- Models created in Simulink were simulated to travel the same route under the same conditions for all 5 configurations.
- Experimental measurements were performed on functional models under the same conditions.
- The power consumption was determined based on the simulated current and measured with the Hall sensor, respectively, when moving along the predetermined path.
- Methods of calculating energy and power consumption have been established and used.
- Determine the energy consumption for all configurations of modular mobile robots and interpret the results.

Interpretation of the results using AHP-based multi-criteria decision making:

- In terms of reconfigurability, integrability and modularity, these performances are identical for all 5 modular mobile robot configurations.
- In terms of mobility, the best-performing configuration is the omni-directional drive and three-wheel omni-directional configuration, followed by the two-wheel conventional

and four-wheel omni-directional configurations, and the least mobile configuration is the mobile robot with differential drive and four conventional wheels.

- In terms of energy consumption, the most efficient configuration is the differential drive configuration with two conventional wheels, followed by the conventional four-wheel configuration. The least energy-efficient configuration is the configuration with omni-directional traction and four omni-directional wheels.

7.3. RESEARCH DIRECTIONS FUTURE

The modular robotic platform described and used in this research is a concept that highlights modularity, i.e. the possibility of forming multiple robotic structures using the same hardware components but with different configurations of the locomotion system. Due to modularity, the performance of mobile robots can be increased in terms of autonomy and flexibility for integration into various applications.

Further research can be carried out along the following lines:

- The validated models can be used for analysis and studies to predict and optimise energy consumption for several types of modular platform configurations.
- Validated models can be developed for other types of trajectories, looking at energy consumption for several types of modular platform configurations.
- A LiDAR sensor, or position sensors can be integrated on the functional model and controlled using digital block simulation software.
- The presented modular mobile platform can be further used for analysis and optimisation procedures using more accurate energy consumption models.
- The errors detected and their causes can be taken into account further for the refinement of modular mobile robot designs.
- The functional model can be equipped with sensors for trajectory displacement control for research purposes.

BIBLIOGRAPHY

Rubio, F.; Valero, F.; Llopis-Albert, C. A Review of Mobile Robots: Concepts, Methods, Theoretical Framework, and Applications. *International Journal of Advanced Robotic Systems* **2019**, *16*, 1-22, doi:10.1177/1729881419839596.

2. Oltean, S.E. Mobile Robot Platform with Arduino Uno and Raspberry Pi for Autonomous Navigation *Procedia Manufacturing* **2019**, *32*, 572-577, doi:10.1016/j.promfg.2019.02.254.
Kadim, N.; Al-Sahib, A.; Zuhair Azeez, M. Build and Interface Internet Mobile Robot Using Raspberry Pi and Arduino. *Innovative Systems Design and Engineering* **2015**, *6*, 106-114.
4. **Maroșan, I.-A**.; Constantin, G. Wireless Communication Based on Raspberry Pi and Codesys for Mobile Robots Using IoT Technology; EDP Sciences, 2021; Vol. 343 **(BDI indexed article: Proquest).**
5. Vanitha, M.; Selvalakshmi, M.; Selvarasu, R. Monitoring and Controlling of Mobile Robot via Internet through Raspberry Pi Board. *2016 2nd International Conference on Science Technology Engineering and Management, ICONSTEM 2016* **2016**, 462-466, doi:10.1109/ICONSTEM.2016.7560864.
6. Niloy, M.A.K.; Shama, A.; Chakrabortty, R.K.; Ryan, M.J.; Badal, F.R.; Tasneem, Z.; Ahamed, M.H.; Moyeen, S.I.; Das, S.K.; Ali, M.F.; et al. Critical Design and Control Issues of Indoor Autonomous Mobile Robots: A Review. *IEEE Access* **2021**, *9*, 35338-35370, doi:10.1109/ACCESS.2021.3062557.
7. Tzafestas, S.G. Mobile Robot Control and Navigation: A Global Overview. *Journal of Intelligent and Robotic Systems: Theory and Applications* **2018**, *91*, 35-58, doi:10.1007/s10846-018-0805-9.
8. Cronin, C.; Conway, A.; Walsh, J. State-of-the-Art Review of Autonomous Intelligent Vehicles (AIV) Technologies for the Automotive and Manufacturing Industry. *30th Irish Signals and Systems Conference, ISSC 2019* **2019**, 1-6, doi:10.1109/ISSC.2019.8904920.
9. Meystel, A. *Autonomous Mobile Robots: Vehicles with Cognitive Control*; World Scientific: Singapore, 1991;
10. J.C. Latombe *Robot Motion Planning*; Kluwer: Boston, 1991;
11. Leonard, J.J.; Durrant-Whyte, H.F. *Directed Sonar Sensing for Mobile Robot Navigation*; Springer International Publishing: Berlin, 1992;
J.L. Jones, A.M Flynn, B.A. Seiger *Mobile Robots: Inspiration to Implementation*; Peters A.K., Ltd/CRC Press: New York, 1995;
13. Everett, H.R. *Sensors for Mobile Robots*; Peters A.K. Ltd/CRC Press: New York, 1995;
14. Borenstein, J.; Everett, H.R.; Feng, L. *Navigating Mobile Robots*; Peters A.K. Ltd/CRC Press: New York, 1996;
15. R.C. Arkin *Behavior-Based Robotics*; MIT Press: Cambridge, 1998;
16. Canny, J.F. *The Complexity of Robot Motion Planning*; MIT Press: Cambridge, 1988; Vol. Doctoral D;
17. Zhu, X.; Kim, Y.; Minor, M.A.; Qiu, C. *Autonomous Mobile Robots in Unknown*

Outdoor Environments; CRC Press /Taylor and Francis Group: Boca Raton, 2016; ISBN 9781498740562.
18. Nehmzow, U. *Mobile Robotics: A Practical Introduction*; Springer: London, 2003;
19. SIEGWART R. *Introduction to Autonomous Mobile Robots*; 2011; Vol. 49;.
20. Cuesta, F.; Ollero, A. *Intelligent Mobile Robot Navigation*; Springer: Berlin, 2005; Vol. 16; ISBN 3540239561.
21. Berns, K.; von Puttkamer, E. *Autonomous Land Vehicles*; Springer: Berlin, 2009;
22. Dudek, G.; Jenkin, M. *Computational Principles of Mobile Robotics*; Cambridge University Press: Cambridge, 2010;
23. Cook, G. *Mobile Robots: Navigation, Control and Remote Sensing*; Wiley: Hobolen, 2011; ISBN 9780470630211.
24. Berry, C.A. *Mobile Robotics for Multidisciplinary Study*; Morgan & Claypool: San Rafael, 2012; Vol. 3;.
25. Tiwari, R. *Intelligent Planning for Mobile Robotics: Algorithmic Approaches (Premier Reference Source)*; IGI Global: Hershey, 2012; ISBN 1466620749.
26. Kelly, A. *Mobile Robots: Mathematics, Models, and Methods*; Cambridge University Press: Cambridge, 2013;
27. Tzafestas, S.G. *Introduction to Mobile Robot Control*; Elsevier: New York, 2013; ISBN 9780124170490.
Jaulin, L. *Mobile Robotics*; ISTE Press-Elsevier: New York, 2017;
29. Martins, N.A.; Bertol, D.W. *Wheeled Mobile Robot Control*; Studies in Systems, Decision and Control; Springer International Publishing: Cham, 2022; Vol. 380; ISBN 978-3-030-77911-5.
30. Jahn, U.; Heß, D.; Stampa, M.; Sutorma, A.; Röhrig, C.; Schulz, P.; Wolff, C. A Taxonomy for Mobile Robots: Types, Applications, Capabilities, Implementations, Requirements, and Challenges. *Robotics* **2020**, *9*, 109, doi:10.3390/robotics9040109.
Bruzzone, L.; Nodehi, S.E.; Fanghella, P. Tracked Locomotion Systems for Ground Mobile Robots: A Review. *MACHINES* **2022**, *10*, doi:10.3390/machines10080648.
32. Wang, Y.; Li, X.; Zhang, J.; Li, S.; Xu, Z.; Zhou, X. Review of Wheeled Mobile Robot Collision Avoidance under Unknown Environment. *SCIENCE PROGRESS* **2021**, *104*, doi:10.1177/00368504211037771.
33. Taheri, H.; Zhao, C.X. Omnidirectional Mobile Robots, Mechanisms and Navigation Approaches. *Mechanism and Machine Theory* **2020**, *153*, doi:10.1016/j.mechmachtheory.2020.103958.
34. Patle, B.K.; Babu, G.L.; Pandey, A.; Parhi, D.R.K.; Jagadeesh, A. A Review: On Path Planning Strategies for Navigation of Mobile Robot. *DEFENCE TECHNOLOGY* **2019**, *15*, 582-606, doi:10.1016/j.dt.2019.04.011.
35. Crescentini, M.; Syeda, S.F.; Gibiino, G.P. Hall-Effect Current Sensors: Principles of Operation and Implementation Techniques. *IEEE SENSORS JOURNAL* **2022**, *22*, 10137-10151, doi:10.1109/JSEN.2021.3119766.
36. Wang, X.; Sun, X.; Cui, S.; Yang, Q.; Zhai, T.; Zhao, J.; Deng, J.; Ruotolo, A. Physical Investigations on Bias-Free, Photo-Induced Hall Sensors Based on Pt/GaAs and Pt/Si Schottky Junctions. *SENSORS* **2021**, *21*, doi:10.3390/s21093009.
37. Aiello, O. Hall-Effect Current Sensors Susceptibility to EMI: Experimental Study. *ELECTRONICS* **2019**, *8*, doi:10.3390/electronics8111310.
38. Romero-Perigault, J.; Flores-Fuentes, W.; Jo, K.-H.; Caceres Hernandez, D. Wireless Current Monitoring for Autonomous Robot Navigation. In Proceedings of the 2019 IEEE 28TH INTERNATIONAL SYMPOSIUM ON INDUSTRIAL ELECTRONICS (ISIE); IEEE; IEEE Ind Elect Soc, 2019; pp. 1717-1722.
39. Aiello, O.; Fiori, F. A New MagFET-Based Integrated Current Sensor Highly Immune to EMI. *MICROELECTRONICS RELIABILITY* **2013**, *53*, 573-581, doi:10.1016/j.microrel.2012.10.013.

40. Karamipour, E.; Dehkordi, S.F.; Korayem, M.H. Reconfigurable Mobile Robot with Adjustable Width and Length: Conceptual Design, Motion Equations and Simulation. *JOURNAL OF INTELLIGENT \& ROBOTIC SYSTEMS* **2020**, *99*, 797-814, doi:10.1007/s10846-020-01163-7.
41. Luo, R.C.; Lee, S.L.; Wen, Y.C.; Hsu, C.H. Modular ROS Based Autonomous Mobile Industrial Robot System for Automated Intelligent Manufacturing Applications. In Proceedings of the 2020 IEEE/ASME INTERNATIONAL CONFERENCE ON ADVANCED INTELLIGENT MECHATRONICS (AIM); IEEE; ASME, 2020; pp. 1673-1678.
42. Tkacik, M.; Brezina, A.; Jadlovska, S. Design of a Prototype for a Modular Mobile Robotic Platform. *IFAC PAPERSONLINE* **2019**, *52*, 192-197, doi:10.1016/j.ifacol.2019.12.755.
43. Kutzer, M.D.M.; Moses, M.S.; Brown, C.Y.; Scheidt, D.H.; Chirikjian, G.S.; Armand, M. Design of a New Independently-Mobile Reconfigurable Modular Robot. In Proceedings of the 2010 IEEE INTERNATIONAL CONFERENCE ON ROBOTICS AND AUTOMATION (ICRA); IEEE, 2010; pp. 2758-2764.
44. Ryland, G.G.; Cheng, H.H. Design of IMobot, an Intelligent Reconfigurable Mobile Robot with Novel Locomotion. *Proceedings - IEEE International Conference on Robotics and Automation* **2010**, 60-65, doi:10.1109/ROBOT.2010.5509359.
45. Piza, R.; Carbonell, R.; Casanova, V.; Cuenca, A.; Salt Llobregat, J.J. Nonuniform Dual-Rate Extended Kalman-Filter-Based Sensor Fusion for Path-Following Control of a Holonomic Mobile Robot with Four Mecanum Wheels. *APPLIED SCIENCES-BASEL* **2022**, *12*, doi:10.3390/app12073560.
46. Ahmadi, S.M.; Taghadosi, M.B.; Haqshenas, A.M. A State Augmented Adaptive Backstepping Control of Wheeled Mobile Robots. *TRANSACTIONS OF THE INSTITUTE OF MEASUREMENT AND CONTROL* **2021**, *43*, 434-450, doi:10.1177/0142331220961700.
47. Hassan, N.; Saleem, A. Analysis of Trajectory Tracking Control Algorithms for Wheeled Mobile Robots. In Proceedings of the IEACON 2021: 2021 IEEE INDUSTRIAL ELECTRONICS AND APPLICATIONS CONFERENCE (IEACON); IEEE; IEEE Ind Applicat Soc, 2021; pp. 236-241.
48. Ren, Y.; Zheng, L.; Khajepour, A. Integrated Model Predictive and Torque Vectoring Control for Path Tracking of 4-Wheel-Driven Autonomous Vehicles. *IET INTELLIGENT TRANSPORT SYSTEMS* **2019**, *13*, 98-107, doi:10.1049/iet-its.2018.5095.
49. Siwek, M.; Baranowski, L.; Panasiuk, J.; Kaczmarek, W. Modeling and Simulation of Movement of Dispersed Group of Mobile Robots Using Simscape Multibody Software. In Proceedings of the COMPUTATIONAL TECHNOLOGIES IN ENGINEERING (TKI'2018); Military Univ Technol Warsaw, Fac Mech Engn, Dept Mech \& Appl Comp Sci; EC Test Syst; SYMCOM, 2019; Vol. 2078.
50. Stefek, A.; Pham, T. Van; Krivanek, V.; Pham, K.L. Energy Comparison of Controllers Used for a Differential Drive Wheeled Mobile Robot. *IEEE ACCESS* **2020**, *8*, 170915-170927, doi:10.1109/ACCESS.2020.3023345.
51. Jaramillo-Morales, M.F.; Dogru, S.; Gomez-Mendoza, J.B.; Marques, L. Energy Estimation for Differential Drive Mobile Robots on Straight and Rotational Trajectories. *INTERNATIONAL JOURNAL OF ADVANCED ROBOTIC SYSTEMS* **2020**, *17*, doi:10.1177/1729881420909654.
52. Hou, L.; Zhang, L.; Kim, J. Energy Modeling and Power Measurement for Mobile Robots. *Energies* **2019**, *12*, doi:10.3390/en12010027.
53. Canfield, S.L.; Hill, T.W.; Zuccaro, S.G. Prediction and Experimental Validation of Power Consumption of Skid-Steer Mobile Robots in Manufacturing Environments. *Journal of Intelligent and Robotic Systems: Theory and Applications* **2019**, *94*, 825-839, doi:10.1007/s10846-018-0779-7.

54. Valero, F.; Rubio, F.; Llopis-Albert, C. Assessment of the Effect of Energy Consumption on Trajectory Improvement for a Car-like Robot. *ROBOTICA* **2019**, *37*, 1998-2009, doi:10.1017/S0263574719000407.
55. Tătar, M.O.; Petre, B.; Teuțan, E. Design and Development of the Hybrid Mobile Robots. *2018 IEEE International Conference on Automation, Quality and Testing, Robotics, AQTR 2018 - THETA 21st Edition, Proceedings* **2018**, 1-6, doi:10.1109/AQTR.2018.8402729.
56. MathWorks Student Competitions Team. Mobile Robotics Simulation Toolbox, 2022, GitHub. Retrieved August 1, 2022. Https://Github.Com/Mathworks-Robotics/Mobile-Robotics-Simulation-Toolbox.
57. Kim, H.; Kim, B.K. Minimum-Energy Trajectory Planning and Control on a Straight Line with Rotation for Three-Wheeled Omni-Directional Mobile Robots. *IEEE International Conference on Intelligent Robots and Systems* **2012**, 3119-3124, doi:10.1109/IROS.2012.6385568.
58. Kanjanawanishkul, K. Omnidirectional Wheeled Mobile Robots: Wheel Types and Practical Applications. *International Journal of Advanced Mechatronic Systems* **2015**, *6*, 289-302, doi:10.1504/IJAMECHS.2015.074788.
59. Vejlupek, J.; Lamberský, V. Multi-Purpose Mobile Robot Platform Development. *Mechatronics: Recent Technological and Scientific Advances* **2011**, 463-470, doi:10.1007/978-3-642-23244-2_56.
60. Ye, C.; Ma, S. Development of an Omnidirectional Mobile Platform. *2009 IEEE International Conference on Mechatronics and Automation, ICMA* **2009 2009**, 1111-1115, doi:10.1109/ICMA.2009.5246079.
61. Sun, Z.; Hu, S.; He, D.; Zhu, W.; Xie, H.; Zheng, J. Trajectory-Tracking Control of Mecanum-Wheeled Omnidirectional Mobile Robots Using Adaptive Integral Terminal Sliding Mode. *Computers and Electrical Engineering* **2021**, *96*, 107500, doi:10.1016/j.compeleceng.2021.107500.
62. **Marosan, A**.; Constantin, G.; Chicea, A.L.; Crenganis, M.; Morariu, F. DESIGN OF MECHATRONIC MODULES THAT CAN FORM MULTIPLE CONFIGURATIONS OF MOBILE ROBOTS. *Proceedings in Manufacturing Systems* **2022**, *17*, 47-53 **(BDI indexed article: Proquest).**
63. **Marosan, A.**; Constantin, G. Pid Controller Based on a Gyroscope Sensor for an Omnidirectional Mobile Platform. *Proceedings in Manufacturing Systems* **2020**, *15*, 27-34 **(Article indexed in BDI: Proquest, Index Copernicus).**
64. Constantin, G.; **Maroșan, I.-A**.; Crenganiș, M.; Botez, C.; Gîrjob, C.-E.; Biriș, C.-M.; Chicea, A.-L.; Bârsan, A. Monitoring the Current Provided by a Hall Sensor Integrated in a Drive Wheel Module of a Mobile Robot. *Machines* **2023**, *11*, 385 **(Lead author**, **IF = 2,899, Web of Science, Article in Q2 journal, WOS:000874293700001**).
65. Verstraten, T.; Furnemont, R.; Mathijssen, G.; Vanderborght, B.; Lefeber, D. Energy Consumption of Geared DC Motors in Dynamic Applications: Comparing Modeling Approaches. *IEEE Robotics and Automation Letters* **2016**, *1*, 524-530, doi:10.1109/LRA.2016.2517820.
66. Rapalski, A.; Dudzik, S. Energy Consumption Analysis of the Selected Navigation Algorithms for Wheeled Mobile Robots. *Energies* **2023**, *16*, doi:10.3390/en16031532.